



This

"The Development of
on Iron and the
to Predict Their

has been

of

U.S.

Date May 12,

C-169

This is to certify that the

thesis entitled

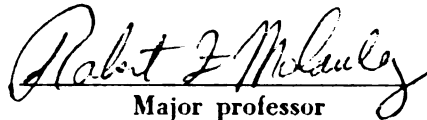
**"The Development of Protective Calcite Coatings
on Iron and the Use of Polarization Measurement
to Predict Their Anti-Corrosion Value"**

presented by

Paul H. Woodruff

**has been accepted towards fulfillment
of the requirements for**

 M.S. **degree in** Civil Engineering


Major professor

Date May 12, 1961

THE DEVELOPMENT OF PRO

THE USE OF POLARIZATION

ANTI-

by F

The purpose of this
ments on the polarization
capacity of calcite coated
corrosion. It was also h
chemical conditions for d
coatings might be better

A review of the lit
knowledge of the effects
calcium carbonate equilib
calcium carbonate supersa
and has been continued he
indicate the tendency of
been considered; of thes
useful because of their

Numerous polarizat
found in the literature,
done in quantitatively c

ABSTRACT

THE DEVELOPMENT OF PROTECTIVE CALCITE COATINGS ON IRON AND THE USE OF POLARIZATION MEASUREMENTS TO PREDICT THEIR ANTI-CORROSION VALUE

by Paul H. Woodruff

The purpose of this research was an evaluation of measurements on the polarization characteristics for predicting the capacity of calcite coated cast iron specimens to resist corrosion. It was also hoped that the optimum physical and chemical conditions for development of highly-protective calcite coatings might be better established by polarization techniques.

A review of the literature revealed a fairly thorough knowledge of the effects of temperature, pH, and salinity on calcium carbonate equilibrium. The effect of polyphosphates on calcium carbonate supersaturations has been under recent study and has been continued here. Several indexes purporting to indicate the tendency of calcium carbonate to form coatings have been considered; of these indexes the DFI and ME were found most useful because of their quantitative nature.

Numerous polarization studies on protective coatings are found in the literature, but little work appears to have been done in quantitatively correlating polarization characteristics

as a coating's resistance
primarily concerned with

Calcite coatings of
developed on sand blasted
six-a-half period of time
scopically and found to c
deposited in a dense regu
translucent, firmly bonde
character. The calcite f
easily scratched.

When other chemical
a linear relationship be
developed and the magnit
force index was found to

Selected coatings
both static and dynamic
provided excellent prot
signs of deterioration.
driving force indexes o
7 to 8 fps. Water vel
inferior coatings. Mi
before and after expos

The exposed coat
for degree of protecti
specimen. The assign
quality of a coating
specimens.

to a coating's resistance to corrosion. This thesis has been primarily concerned with establishing these relationships.

Calcite coatings of superior anti-corrosion value were developed on sand blasted iron specimens in an hour to an hour-and-a-half period of time. The coatings were examined microscopically and found to consist of distorted calcite crystals deposited in a dense regular array. The coatings were translucent, firmly bonded to the metal, and homogeneous in character. The calcite films proved to be hard and were not easily scratched.

When other chemical and physical conditions were constant, a linear relationship between the weight of calcite coating developed and the magnitude of the momentary excess and driving force index was found to exist.

Selected coatings were subjected to 17 days exposure to both static and dynamic rusting conditions. Some coatings provided excellent protection, the metal showing practically no signs of deterioration. The best coatings were developed at driving force indexes of 175 to 450 and flow velocities of 7 to 8 fps. Water velocities of 2.8 and 4.5 fps developed inferior coatings. Microphotographs were taken of the specimens before and after exposure to rusting tests.

The exposed coatings were compared by microscopic methods for degree of protection provided and a rank was assigned to each specimen. The assigned rank indicated the relative protective quality of a coating as compared to that of other exposed specimens.

Polarization tests s
anodic inhibitors. A p
the magnitude in volts of
specimen due to the forma

A comparison study
analysis revealed the pol
measurement of the anti-d

Polarization tests showed the calcite coatings to be cathodic inhibitors. A parameter, ΔZ , was devised to indicate the magnitude in volts of the increased polarization of a cathode specimen due to the formation of a calcite coating.

A comparison study of exposed coatings by correlation analysis revealed the polarization parameter ΔZ to be a reliable measurement of the anti-corrosion value of the coatings.

THE DEVELOPMENT OF PRO

THE USE OF POLARIZATION

ANTI-

Pa

Mich
in partial f

Department of

THE DEVELOPMENT OF PROTECTIVE CALCITE COATINGS ON IRON
AND
THE USE OF POLARIZATION MEASUREMENTS TO PREDICT THEIR
ANTI-CORROSION VALUE

By

Paul H. Woodruff

A THESIS

Submitted to
Michigan State University
in partial fulfillment of the requirements
for the degree of

MASTER OF SCIENCE

Department of Civil and Sanitary Engineering

1961

This thesis is affectionately
dedicated to my daughter
Paula Marie

ACKNOWLEDGMENTS

The author wishes to express his sincere appreciation to: Dr. Robert F. McCauley for his able guidance and advice without which this thesis would not have been possible, to the National Institutes of Health for financial support of the experimental work, and to the U. S. Public Health Service for supporting the author with a traineeship.

The author would also like to thank the following individuals: Kenneth Yerrick and Cordell Johnson for assistance in collection of the data, John Dye for his cooperation in providing test facilities at the Lansing water conditioning plant, my brother Harold for typing the rough draft, my wife Marcia for plotting the polarization data and offering encouragement, and many others who were so generous in providing assistance.

INTRODUCTION

LITERATURE REVIEW . .

- A. Development of
Equilibrium
- B. Development of
Coatings in
- C. Coating Cont.
- D. Influence of
on the Corro
- E. The Mechanis
- F. Polarization

THEORETICAL CONSIDER

- A. The Electro
- B. The Theory
 - 1. Polari
 - 2. Causes
 - a) C
 - b) C
 - c) A
 - d) I
 - e) I
 - 3. Polar
curre
 - a)
 - b)
- C. The Devel
the Surfa
 - a)
 - b)
- D. The Actio
- E. Differen
Equilibr
 - 1. Lan
 - 2. Ryz
 - 3. Sat

TABLE OF CONTENTS

	Page
INTRODUCTION	1
LITERATURE REVIEW	3
A. Development of Calcium Carbonate Equilibrium Parameters	3
B. Development of Protective Calcium Carbonate Coatings in Water Systems	5
C. Coating Control with Polyphosphates	6
D. Influence of Velocity and Oxygen Supply on the Corrosion Process	10
E. The Mechanism of Corrosion	12
F. Polarization Control of the Corrosion Process	14
THEORETICAL CONSIDERATIONS	20
A. The Electrochemical Theory of Corrosion of Iron.	20
B. The Theory of Irreversible Electrode Reactions	25
1. Polarization defined	25
2. Causes of polarization	26
a) Ohmic drop	27
b) Concentration differences	27
c) Activation energy	28
d) Ionic approach-resistance	28
e) Interrelationship of polarization mechanism	29
3. Polarization of electrode related to current density	31
a) Polarization curves from galvanic cells	32
b) Polarization curves from impressed current	34
C. The Development of Local Corrosion Cells on the Surface of Submerged Iron	39
a) Impurities in metal	39
b) Difference in electrolyte concentration	39
D. The Action of Inhibitors	40
E. Different Indexes Used for Calcium Carbonate Equilibrium	44
1. Langelier saturation index	44
2. Ryznar stability index	46
3. Saturation excess	47

4. Momentary ex
5. The driving

EXPERIMENTAL APPARATUS AND

- A. Apparatus for De
Coating on Test S
 1. The dynamic
 2. Test specim
 - a) Cast i
 - b) Black
 3. Test cells
 - a) Primar
 - b) Secon
 - c) Pipe-
- B. Apparatus for M
- C. Apparatus Used
Calcium Carbona
 1. Dynamic ru
 2. Static ru

EXPERIMENTAL PROCEDURE

- A. Dynamic Polari
 1. Preparat
 2. Preparat
 3. Preparat
 - a) Exp
 - b) Exp
 4. Test pr
 - a) Pr
 - b) Te
 5. Polariz
 6. Routine
- B. Evaluation
 1. Micros
 2. Dynami
 3. Static

1.1

- A. Remarks on
- B. Remarks on

TABLE OF CONTENTS (cont.)

	Page
4. Momentary excess	47
5. The driving force index	48
EXPERIMENTAL APPARATUS AND MATERIAL	49
A. Apparatus for Development of Calcium Carbonate Coating on Test Specimens	49
1. The dynamic test unit	49
2. Test specimens	53
a) Cast iron plates	53
b) Black iron pipe nipples	53
3. Test cells	56
a) Primary plate-cell	56
b) Secondary plate-cell	56
c) Pipe-cell	56
B. Apparatus for Making Polarization Measurements .	60
C. Apparatus Used for Evaluating the Quality of Calcium Carbonate Coating on Test Specimens . .	64
1. Dynamic rusting unit	64
2. Static rusting unit	67
EXPERIMENTAL PROCEDURE	69
A. Dynamic Polarization Tests	69
1. Preparation of polyphosphate feed	69
2. Preparation of sodium hydroxide feed . . .	70
3. Preparation of iron specimens	71
a) Experiments with flat plates	72
b) Experiments with pipe sections	72
4. Test procedure	72
a) Procedure for a typical test run . . .	76
b) Tests with the pipe test cell	77
5. Polarization measurements	79
6. Routine chemical water analysis	80
B. Evaluation of the Calcium Carbonate Coatings . .	80
1. Microscopic examination	82
2. Dynamic rusting test	82
3. Static rusting test	84
DATA	86
A. Remarks on Data Notation	86
B. Remarks on Polarization Curve Notation	106

DISCUSSION OF RESULTS

- A. Discussion of
 - 1. Macroscopic coating
 - 2. Microscopic coating
 - a) Velocity
 - b) Efficiency
 - 3. Effect of Momenta Calcite
- B. Inhibitive Action
 - Determined by
 - 1. Iron-Iron
 - 2. Effect of zation
 - a) Calcium
 - b) Phosphorus
 - c) Enzymes
- C. Results of Field Corrosion Qu
 - 1. Rusting of iron sp
 - a) Phosphorus
 - b) Phosphorus
 - 2. Correlation of paramete
 - a) Phosphorus
 - b) Phosphorus
 - c) Calcium
- D. Effect of Excess on the Calcite Coating
- E. Effect of Anti-Corrosion Coatings
- F. Effect of Period on Calcite Coating
- G. Practical Technique of Calcite

CONCLUSIONS

RECOMMENDATIONS . .

BIBLIOGRAPHY

TABLE OF CONTENTS - (cont.)

	page
DISCUSSION OF RESULTS	123
A. Discussion of Calcite Coatings Developed . .	123
1. Macroscopic description of the calcite coatings	123
2. Microscopic description of the calcite coatings	124
a) Velocity effects	124
b) Effects of calcium carbonate supersaturation	124
3. Effect of the Driving Force Index and Momentary Excess on the Weight of Calcite Coating Developed	128
B. Inhibitive Action of Calcite Coatings as Determined by Polarization Tests	131
1. Iron-Iron galvanic cell polarization . .	131
2. Effect of calcite coating on polarization of iron electrodes	133
a) Calcite coatings shown to be cathodic inhibitors	133
b) Probable polarization mechanism . .	136
c) Erratic polarization curves	137
C. Results of Polarization Measurement of Anti-Corrosion Quality	139
1. Rusting tests on calcite coated cast iron specimens	139
a) Plate specimens	140
b) Pipe specimens	149
2. Correlation between polarization potential parameter and anti-corrosion quality of the calcite coatings	153
a) Plate specimens	153
b) Pipe specimens	154
c) Correlation between the dynamic and static rusting tests	154
D. Effect of Driving Force Index and Momentary Excess on the Anti-Corrosion Quality of the Calcite Coatings	157
E. Effect of Development Flow Velocity on the Anti-Corrosion Qualities of the Calcite Coatings	163
F. Effect of Length of Coating Development Period on the Anti-Corrosion Value of the Calcite Coatings	163
G. Practical Application of the Polarization Technique to Measure Anti-Corrosion Quality of Calcite Coatings	166
CONCLUSIONS	167
RECOMMENDATIONS	169
BIBLIOGRAPHY	177

Title

1. Coating Apparatus
2. Test Data . . .
3. Chemical Analysis
4. Analysis of Corrosion
Rusting-Test
5. Results of Statistical
6. Results of Statistical
Specimens .
7. Effect of Coating
Corrosion Quality
8. Effect of Time
Corrosion Quality

LIST OF TABLES

Table		Page
1.	Coating Apparatus Appurtenance Identification . . .	74
2.	Test Data	90
3.	Chemical Analysis of Rusting-Test Water	121
4.	Analysis of Corrosion Equilibrium Parameters for Rusting-Test Water	122
5.	Results of Static and Dynamic Rusting Tests	141
6.	Results of Static Rusting Test on Cathode Pipe Specimens	150
7.	Effect of Coating Development Velocity on Anti- Corrosion Quality of Specimens	164
8.	Effect of Time of Coating Development on Anti- Corrosion Quality of Specimens	165

Figure

1. Polarization
2. Polarization Resistance
3. Effect of Co Potential
4. Polarization Current
5. Types of Con
6. Influence of Cathodic C
7. Deep Well Pum
8. Sodium Hydrox
9. Cast Iron Pla
10. Iron Pipe Spe
11. Primary Plate
12. Primary Plate
13. Pipe Cell . .
14. Pipe Cell Moun
15. Circuit Diagram Measurement
16. Test Cells Moun
17. Dynamic Rusting
18. Construction o
19. Static Rusting
20. Flow Diagram o
21. General View o
22. Coating Evalua
23. Illustration o

LIST OF FIGURES

Figure		Page
1.	Polarization and the Limiting Corrosion Rate . . .	33
2.	Polarization of a Corrosion Cell by Varying the Resistance of the Cell	34
3.	Effect of Corrosion Current on the Electrode Potentials in a Short Circuited Corrosion Cell .	34
4.	Polarization of a Galvanic Cell by an Impressed Current	36
5.	Types of Control in Galvanic Corrosion	38
6.	Influence of Inhibitors on Corrosion Reaction Under Cathodic Control	42
7.	Deep Well Pump and Phosphate Feed	50
8.	Sodium Hydroxide Feed	52
9.	Cast Iron Plate Specimens	54
10.	Iron Pipe Specimens	55
11.	Primary Plate Test Cell	57
12.	Primary Plate Cell Mounted in Apparatus	58
13.	Pipe Cell	59
14.	Pipe Cell Mounted in Apparatus	61
15.	Circuit Diagram of Apparatus for Polarization Measurements	62
16.	Test Cells Mounted in Apparatus	63
17.	Dynamic Rusting Apparatus	65
18.	Construction of Dynamic Rusting Apparatus	66
19.	Static Rusting Test	68
20.	Flow Diagram of Experimental Apparatus	75
21.	General View of Chemical Analysis Equipment	81
22.	Coating Evaluation Check List	83
23.	Illustration of Polarization Curve Notation	108

LIST

Page

4. Polarization Curve
5. Microphotographs
Cast Iron Spec
6. Weight of CaCO_3 at
Equilibrium In
7. Typical Plate Spec
the Development
8. Photographs of C
Exposure to t
9. Microphotographs
Showing the E
Tests . . .
10. Typical Corrosion
11. Photographs of C
and After Exp
12. Anti-Corrosion
Parameter .
13. Anti-Corrosion
to Polarization
14. Cathode--Anode
Compared . .
15. Coating Effectiveness
16. Coating Effectiveness
17. Coating Anti-Corrosion
DFI and Polarization

LIST OF FIGURES - (cont.)

Figure		Page
24.	Polarization Curves	109
25.	Microphotographs (100X) of Calcite Coatings on Cast Iron Specimens	125
26.	Weight of CaCO_3 Coating as a Function of Equilibrium Indexes	130
27.	Typical Plate Specimen Polarization Curves During the Development of a Good Coating	132
28.	Photographs of Coated Plate Specimens (2X) After Exposure to the Rusting Tests	142
29.	Microphotographs (100X) of Coated Iron Plates Showing the Effect of Exposure to the Rusting Tests	147
30.	Typical Corrosion Cell	148
31.	Photographs of Coated Pipe Specimens (2X) Before and After Exposure to Static Rusting Test . . .	151
32.	Anti-Corrosion Quality Related to Polarization Parameter	155
33.	Anti-Corrosion Quality of Pipe Specimens Related to Polarization Parameter	156
34.	Cathode--Anode Anti-Corrosion Quality Ratings Compared	158
35.	Coating Effectiveness as a Function of the DFI . .	159
36.	Coating Effectiveness as a Function of the ME . . .	160
37.	Coating Anti-Corrosion Quality as a Function of DFI and Polarization Parameter ΔZ	162

Appendix

- A. Some Calculations
Hydraulic
Apparatus
- B. Calculation of
Momentary
- C. Rank Correlation
Rusting Test
Parameter
- D. Calculation of
Test Ratio

LIST OF APPENDICES

Appendix		Page
A.	Some Calculations of Chemical Feed and Hydraulic Conditions of Rusting Apparatus	170
B.	Calculation of the Driving Force Index and Momentary Excess	172
C.	Rank Correlation Coefficient for Static Rusting Test Rating vs Polarization Parameter (ΔZ) Rating	173
D.	Calculation of Regression Line for Static Test Rating vs ΔZ	175

INTRODUCTION

The only form of iron that can be completely free of corrosive attack is a single pure crystal. Iron used in water main service is always subject to attack. One of man's eternal struggles has been to find methods of reducing this enormous loss of investment. Uhlig (47) estimated the loss due to corrosion in the United States in 1949 to be 5.5 billion dollars of which some 600 million dollars was due to replacement and maintenance of underground piping. Not included in this estimate would be the cost of over-design in anticipation of corrosion. The water works industry in particular suffers from the direct and indirect effects of corrosion. Tuberculation which often occurs in cast iron pipe can lead to loss of carrying capacity and an outbreak of "red water."

For these reasons much work has been done in developing inhibitors and other means of reducing the amount and severity of metal loss from cast iron water distribution systems. The corrosive medium, being potable water, limits the possible alternatives that might otherwise prove effective.

One of the oldest inhibitors is provided by nature in the form of coatings of rust and other materials obtained from the water such as calcium carbonate. However it is only within the past twenty-five years that much has been known about the conditions that must exist in a water to obtain these "natural coatings." During the last ten years workers have begun to

develop more sophisticated controls of the "natural coating" process through the use of polyphosphates.

About four years ago, McCauley successfully started work on the development of calcite (crystalline calcium carbonate) coatings which could be deposited in a few hours time through adjustment of the alkalinity -- calcium makeup of the water. His work has been directed at determining the physical and chemical conditions which must be established to produce calcite coatings of high anti-corrosion value. Until now, the degree of corrosion protection obtained with calcite coatings was measured by exposure and then physical examination to determine if corrosion had been inhibited. This system could not be used in a distribution system. Successful corrosion control would therefore be made easier by an instantaneous measurement of the anti-corrosion quality of the calcite coating as it is deposited.

It has been the object of this thesis to assist in establishing the optimum conditions for developing calcite coatings of maximum corrosion resistance. Primarily, this work has been directed toward the use of polarization measurements for determining those physical and chemical conditions which produce the most useful coatings.

In order to accomplish these objectives experiments were conducted with cast iron specimens under various conditions of calcium carbonate supersaturation, water velocity, and length of coating period. The effect of each variable on the quality of coating was studied. Polarization measurements were made on the specimens periodically during the coating period, then correlated with the anti-corrosion quality of the coating.

LITERATURE REVIEW

A. Development of Calcium Carbonate Equilibrium Parameters

Sixty years ago Whitney (49) first stated the electrochemical nature of corrosion. Since then, much progress has been made in learning to control this ravage of nature. For instance, in water treatment practice, techniques which have been developed to arrest corrosion in distribution systems now include: (1) addition of silicates, (2) oxygen removal by deaeration, (3) coal tar and concrete pipe linings, (4) chlorination to control bacterial slimes which indirectly initiate corrosion, (5) addition of polyphosphates, and (6) adjustment of the pH—carbon dioxide--calcium carbonate equilibrium. These control procedures have been used separately and in combination with varying degrees of success.

One of the most promising methods of corrosion control has been the controlled deposition of calcium carbonate coatings on the pipe walls of water distribution systems. During the past twenty-five years much has been done to formulate the equilibrium relationships of calcium carbonate in water. The first practical test for degree of CaCO_3 supersaturation or under-saturation of a water was developed in 1932 by Tillman and coworkers (45). Prediction of the tendency of a water to deposit or remove scale was further simplified in 1936 by

Langelier's formulation of his (17) "saturation index." This index was based on principles of physical chemistry and provided an indication of the direction of equilibrium driving force. A positive index indicated a tendency for the water to be scale forming and a negative index to be scale dissolving. Moore (30) has described how a water may be adjusted to give a positive scale forming index by adding lime and/or sodium carbonate.

In 1946 Langelier (19), (20) made further refinements in the computation of his "saturation index" by considering temperature effects on the pH of the water. Further progress resulted from the work of Larson and Buswell (22) who determined the effect of salinity on ionization constants at different temperatures.

To further separate scale forming waters from scale dissolving waters, Ryznar (38) in 1942 proposed an empirical "stability index." The index, was devised with the view of estimating the degree of scaling to be expected from a water under specified alkalinity, calcium and hydrogen ion concentration.

Dye (6) has recently suggested use of the concentration of calcium carbonate which is in excess of the solubility product constant as an index of the scale forming tendency of a water. Dye termed this index the "momentary excess" of calcium carbonate. McCauley (25) has proposed a new parameter, the "driving force index," defined as the ratio of the product of the calcium and carbonate concentrations over the solubility product of calcium carbonate, all expressed as calcium carbonate. McCauley has believed his index to be indicative of the magnitude of the equilibrium force causing deposition of calcium carbonate.

As a result of the work just described, a good understanding has been reached on the effect of pH, temperature, and salinity upon the equilibrium of calcium carbonate in water. However much remains to be known concerning optimum conditions for the development and maintenance of calcium carbonate coatings.

B. Development of Protective Calcium Carbonate Coatings in Water Systems

The early use of protective coatings in water mains depended on the long term development of calcite--iron oxide deposits. Many workers have discussed mixed scale of calcium carbonate and corrosion products. Tillman and coworkers were among the first to report the value of the mixed scale in reducing corrosion (45). Evans (11) reported that a heterogeneous layer of rust and calcium carbonate gave better protection from corrosive attack than either material alone.

McCauley (24) summarized the limitations of uncontrolled calcium carbonate--corrosion product coatings in 1958, stating that no reliable procedure for obtaining good anti-corrosion protection had been devised for normal water works operating conditions. McCauley believed that the role of dissolved oxygen in the formation of protective coatings was in doubt and that the conditions of calcium carbonate supersaturation for insuring the development of a protective coating were not certain.

Experimental work by McCauley and Abdullah (28) with mixed coatings of calcium carbonate and corrosion products resulted in several important findings. Using cast iron specimens which had been machined and thoroughly cleaned, protective coatings were deposited using only lime and carbon dioxide additives to a

deionized water which was saturated with dissolved oxygen. The resulting coatings on cast iron were mixtures of calcium carbonate, (5 to 40 percent), ferrous carbonate, and ferric oxide. With stainless steel specimens, only calcium carbonate deposits were found. The coatings which resulted from static conditions were soft and loosely bonded to layers of rust. Further experimental work showed that better bonded, harder coatings could be established in solutions containing colloidal calcium carbonate than from solutions of the same pH and hardness with no colloids present. However, calcium carbonate crystals of greater than colloidal size did not have as favorable an effect on the coating formation as did the colloidal form. Coatings developed in one to five days under dynamic conditions with flow velocity of 2 fps were harder and more durable than the coating formed in the same length of time under static conditions. The formation of the protective coating, it was postulated, depended on the development of an initial deposit of dense material that was well bonded to the metal. The best coatings were obtained in one day's time at a pH of 8.3 and a momentary CaCO_3 excess of 4.0 ppm. At high pH values and high momentary excess (35-45 ppm), the coatings were mostly soft, loose grained, chalky calcite.

C. Coating Control with Polyphosphates

On the basis of previously cited experimental work, control of calcium carbonate deposition is needed if adequate protection of water distribution systems is to be provided. Much work has been done on the unusual ability of metaphosphates to hold and prevent deposition of calcium carbonate from a supersaturated

solution. Rosenstein (37) discovered that a concentration of 1 ppm of molecularly dehydrated phosphate would effectively inhibit the formation of calcium carbonate scale when ammonia was added to irrigation waters. Reitemeier and Buehrer (34) investigating the inhibiting action of trace amounts of sodium hexametaphosphate found that a certain "threshold level" of metaphosphate (about 1.5 ppm) prevented deposition of calcium carbonate. The presence of metaphosphate in concentrations below the threshold level interfered with the crystallization process of calcium carbonate producing large, grossly distorted crystals. The precipitating calcium carbonate was found to adsorb the metaphosphate. From this finding, they postulated that the adsorption of metaphosphate on the crystal faces caused restricted and distorted crystallization.

Rice and Hatch (35) were among the first to report on the advantages of threshold treatment of water supplies. Rice and Hatch defined the threshold level as the concentration of hexametaphosphate which must be added to a water to remove crystal nuclei from contact with the solution on the threshold of the crystallization process. Several workers have stated that threshold treatment tends to slowly remove old deposits of calcium carbonate chalk and corrosion products from metal pipe walls. However, Larson (21) has shown that metaphosphate will not remove magnesium hydroxide scale which may also be present in a water distribution system.

Because the carbon dioxide--calcium carbonate equilibrium tends to shift to the right at high temperatures, scale formation has often been a serious problem in hot water service. Illig (16),

experimenting with metaphosphate to determine its effect on the stability of calcium carbonate supersaturations, found 2.0 ppm was sufficient to hold 600 ppm calcium carbonate in solution at 40° C and that the same metaphosphate concentration could hold only 200 ppm calcium carbonate at 100° C.

Rice and Hatch (35) reported hexametaphosphate to also be an effective corrosion inhibitor. This inhibitory action was attributed to the formation of an adsorbed film of metaphosphate on the metal surface. However, McCauley (25) pointed out that high velocity and continuous feed of polyphosphates were essential to the development and maintenance of a protective metaphosphate film, thereby eliminating the possibility of corrosion protection by metaphosphates in sections of low flow and in dead ends.

Lamb and Eliassen (8), (9) as a result of their experimental work on the inhibitive mechanism of metaphosphates conclude the following:

1. When present in sufficient quantity, metaphosphate will remove the products of corrosion from the anodes of corrosion cells and some of the corrosion products removed will be deposited on the cathodes.
2. Positively charged colloidal particles of hydrous ferric oxide and metaphosphate will be formed in the vicinity of the anodes and some of these particles will be deposited on the cathodes.
3. The rate of deposition of metaphosphate on the cathodes, and its inhibitory affect, is increased by the presence of corrosion products or iron in solution.

4. The protective film is deposited on the cathode through a process of electrodeposition.

Partly because of the aforementioned limitations on calcium carbonate--corrosion product and metaphosphate--corrosion product coatings, McCauley (25) experimented to determine the optimum conditions for the development of pure calcite coatings when using polyphosphate to control coating development. It was found that the addition of .02 to 3.2 ppm metaphosphate to a ground water, similar in chemical analysis to that used in the experimental work which is reported here, permitted use of large supersaturation of calcium carbonate with a resulting dense deposition of calcite in a few hours time. Good coatings of pure calcite were obtained on sand blasted cast iron specimens in 2-7 hours at a momentary excess (ME) of 23-31 ppm and a driving force index (DFI) of 40-250 at a flow velocity of 1.5 fps with the pH ranging from 8.8-9.7. Superior coatings were found on specimens which were coated at higher velocities up to the maximum tested, 13.5 fps. At a flow velocity of 3.0 fps and a metaphosphate level of 0.5 ppm good coatings were obtained in two hours at a ME of 80-145 and a DFI of 135-245 with the pH varying from 9.4-9.7.

McCauley (27) reported that a six inch cast iron water line 1200 feet in length has been successfully coated with a dense glass like calcite coating on several occasions using the techniques established in the laboratory when using 1 x 3 inch cast iron plates. McCauley outlined a step by step procedure for laying down calcite coatings on cast iron water distribution piping in two hours time. However, there was still some doubt as to the optimum DFI, ME, and polyphosphate level for maintaining the coating.

The calcite coatings from this work were described as translucent bluish tinged and glass like. Microscopic examination of coatings developed in two-hour experiments with 3 fps velocity revealed a dense crystalline structure on small cast iron test plates with practically no rust, but with some pin holes. It was evident that the coatings developed in these experimental tests were of a different type than the common uncontrolled coatings previously reported. For instance, McCauley (25) stated that almost no rusting occurred on a test nipple with a good coating developed at 8 fps velocity after six months exposure to oxygen saturated water.

D. Influence of Velocity and Oxygen Supply on the Corrosion Process

It is evident from the literature (9), (10), (12), (25), (36), (43), and (46), that in cast iron water mains carrying water which is supersaturated with calcium carbonate two mechanisms are competing: (1) deposition and formation of a protective coating, and (2) formation of galvanic cells and corrosion of the pipe. The velocity of flow affects the rate of both mechanisms. Romeo, Skrinde, and Eliassen (36) using Fick's law of diffusion showed by mathematical analysis that for hydraulically smooth pipe in turbulent flow: (1) The rate of oxygen supply from the flowing water to the corroding metal of the pipe wall varied as the 0.875th power of the velocity in pipes of the same diameter, (2) The rate of oxygen supply to the pipe wall varied as the 0.125th power of the pipe diameters in flows of equal velocity. However with disruption of the laminar layer by increased velocity or pipe roughness, i.e. a

hydraulically rough pipe, the rate of oxygen supply depended on velocity distribution and the mixing length. The rate of oxygen transfer was thus increased by increased turbulence.

McCauley (25) felt that a similar mechanism governed the rate and uniformity of calcite coating development. He has postulated that deposition takes place from the laminar film developed in turbulent flow and transfer of calcium and carbonate ions from the main flow must be established by the turbulent mixing action.

Mathematical analysis by McCauley (25) showed that a velocity of 3-6 fps should be sufficient to develop hydraulic roughness in cast iron water mains. McCauley's experimental work has shown that better coatings could be developed at velocities of 3-13.5 fps than at 0-1.5 fps. Also, at the lower velocity, a much higher momentary excess of 60 ppm was necessary to develop a coating similar to that developed at the higher velocities with a momentary excess of only 5 ppm. Because of these facts McCauley suggested that increased kinetic energy of highly turbulent flow may contribute to the total energy requirements in the formation of calcite coatings.

It is generally concluded that corrosion of bare iron increases with velocity, since a larger velocity results in increased oxygen supply to the corroding metal. For instance, Romeo, Skrinde, and Eliassen (36), and Uhlig (46) have stated that (1) when a corrosion product film is formed, the reactions leading to continued corrosion take place within the film, where the conditions may be far different from those established in the main flow and (2) flow velocity within a boundary film is near

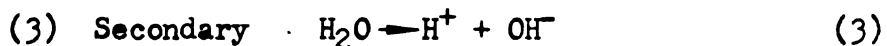
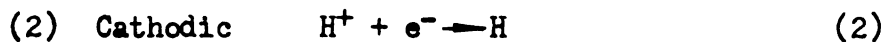
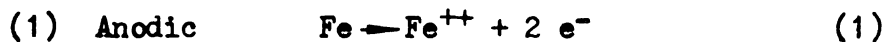
zero so that transfer of chemicals and dissolved gases must depend mainly on diffusion.

McCauley (25) has pointed out that because both corrosion rate and rate of coating development appear to increase with velocity, the chemical equilibrium driving force for calcium carbonate deposition must be large enough to move the coating reaction more rapidly than the corrosion reactions. Once corrosion has started at a point on the metal, that point becomes difficult to coat with calcite.

The effect of pore holes on protective coatings was discussed by Rabald (33), who stated that the number and size of holes were reduced by the formation of corrosion products. Rabald believed that the resulting reduction in pore area caused a decrease in diffusion into the narrow pores, that the local galvanic cells became more polarized and the corrosion rate was reduced.

E. The Mechanism of Corrosion

Early writers speculated that the primary means of electron transfer from the cathode was by the development of a galvanic cell on the corroding metal surface. Proposed reactions were:



More recent work by Camp (2), Evans (12), and Speller (40) has shown the cathodic mechanism to be of significance only at very low pH levels and in the absence of dissolved oxygen.

Potter (31) pointed out that hydrogen of the water molecule played an important role in electron transfer in the absence of appreciable concentrations of hydrogen ion. According to Speller (40), in neutral or slightly alkaline water hydrogen evolution at the cathode accounted for less than three per cent of the total electron transfer mechanism. Gatty and Spooner (13), summing up the work of many others, showed graphically the affect of pH on the rate of corrosion. These workers found the rate will be greatest at low pH, decreasing rapidly as the pH increased from 2 to 4. At pH 4, hydrogen evolution became the minor and oxygen reduction the major electron transfer mechanism.

From thermodynamics, Camp (2) has shown that a great variety of electrode reactions are theoretically possible. Reactions depend largely on the ionic make-up of a water. Camp has reported a technique for computing the most probable electrode reaction using the Nernst equation and the chemical analysis of a water. However the predicted electrode reactions coincide with the true reactions only if polarization of the electrode is absent. Since polarization is almost always present, Camp's techniques are severely limited.

Whatever the true electrode reactions may be, corrosion of iron in aqueous solutions has been found to be under cathodic control if the pH is less than 11. Many workers (7), (12), (13), (17), (33), (36), (40), (44), (46) have discussed the importance of oxygen depolarization. Most of the above authors have thought dissolved oxygen to be the most important mechanism of removing hydrogen from the cathode, thereby decreasing the hydrogen over-potential, (polarization) and thus increasing the rate of corrosion.

Many authors have postulated that if a metal is under cathodic control the corrosion rate may be slowed down by removing oxygen or by covering cathodic areas with protective coatings to reduce contact between these areas and the dissolved oxygen.

F. Polarization Control of the Corrosion Process

The literature contains much discussion of polarization. The polarization or overvoltage, (the terms are used interchangeably in the literature) of an electrode can be due to any of four mechanisms or combinations thereof. Evans (12) listed the mechanisms as: (1) ohmic drop, (2) concentration, (3) activation, and (4) approach--resistance polarization. Discussion and explanation of polarization types will be found in the Theoretical Considerations section of this thesis.

Because hydrogen overpotential has been found to be very high as compared to other types of electrode reactions, much effort has been made to understand its properties. Potter (31) and Kartüm and Bockris (17) have summarized: (1) Hydrogen overpotential varies with the current density, the electrode metal, and surface conditions; (2) At current densities below about $100\text{ma}/\text{dm}^2$ visible evolution of hydrogen does not usually take place, but the liberated gas immediately dissolves in the electrolyte (water) and diffuses away from the electrode; (3) Hydrogen overpotentials usually decrease with temperature; (4) Hydrogen overvoltage is established almost immediately upon the passage of current. Establishment is on the order of 10^{-2} seconds, and varies slowly, sometimes over a period of hours or days.

The overpotential of an electrode has been found to be due to several types of polarization. According to Evans (12) each type is a different function of the current density, and a mechanism may predominate at a low current density but not at a high current density. Thus, polarization curves can take on an endless variety of shapes depending on the electrode and the type or types of polarization taking place.

The measurement of electrode polarization is a technique that has been used in the past by many workers to study properties of corroding metals and the influence of coatings on the corrosion process. Evans (11), (12) described polarization measurements on corroding iron, showing that in aqueous solutions the corrosion of iron tended to be under cathodic control. For cathodic control of an iron--iron galvanic cell, the polarization of the cathode is greater than that of the anode and the cathodic reaction limits the corrosion current. Rabald (33), Uhlig (46), Eliassen and Lamb (7) and Gatty and Spooner (13) reported similar findings. Evans (12) and Uhlig (46) have reported that films of oxides and corrosion products tended to increase the polarization of the cathode and to decrease the corrosion rate.

Skold and Larson (39), using polarization measurements to measure the instantaneous corrosion rate of cast iron in tap water, reported that the polarization potential was a straight line function of the applied cathodic and anodic currents at low current density.

Eliassen and coworkers (10) have reported polarization data for iron specimens exposed to a synthetic water under various pH and velocity conditions. The corrosion reaction was found to be under mixed control with the formation of a mixed

calcium carbonate coating at a pH of 10 and with velocities of 1 and 2 fps. With the passing of time up to the 30 day test limit, the cathode and anode curves did not change slope but shifted, the anode in the more noble (negative) direction and the cathode in the more active direction. The low alkalinity at this high pH level caused rapid precipitation of corrosion products at the anode, with a resulting increased tendency for the iron to go into solution. The cathodes of the galvanic couples were found to be completely covered with calcium carbonate. In the pH range 7 to 9 the polarization curves showed primarily cathodic control. Again a film of calcium carbonate was formed on the cathodes. Data suggested that cast iron pipe in a system containing a supersaturation of calcium carbonate tended to form a calcium carbonate--corrosion product coating which produced cathodic control of the corrosion reaction up to a pH of about 9, mixed control from pH 9 to 11, and anodic control at a pH above 11. According to Eliassen and coworkers (10) corrosion control reversal occurred because of the effect of pH on the solubility of iron and corrosion products.

Eliassen and Lamb (8), in other studies, showed that when metaphosphate alone was deposited on the cathodes of galvanic cells no effect on the polarization curve was exhibited. However in a later publication (9), polarization tests showed that the formation of mixed corrosion product--metaphosphate coatings increased the cathodic polarization and decreased the corrosion reaction rate. Rabald (33) stated that the corrosion current, i.e. reaction, was reduced with the formation of a mixed calcium carbonate--corrosion product coating. Rabald showed the reduction in corrosion current to be much greater with antadhesive, sealing

film than with a loose amorphous coating.

McCauley and Abdullah (28) have reported the results of polarization measurements which were made to determine the change in the polarization characteristics of the electrodes as a protective coating of calcium carbonate and corrosion products built up during a five day period. A current density of 1.65 ma/dm^2 was applied during the coating period. Potential versus applied current density measurements were made at intervals throughout the five day coating period. The cathode EMF at zero applied current density shifted in the active (positive) direction about 0.23 volts and the slope of the curves increased with the passing of time, indicating increased polarization with coating build up. The open circuit anode EMF shifted about 0.13 volts in the more noble (negative) direction, but the slope of the curves remained almost constant with the passage of time, indicating no change in the polarization of the anodes. From these measurements it was concluded that the coating acted as a cathodic inhibitor.

Sudrabin and Marks (44) have reported similar polarization data. The polarization curve of a bare clean piece of steel was compared to that of a similar piece of steel covered with a thin calcium carbonate film. The EMF of the clean steel at 0.01 ma/dm^2 current density was 0.40 volts and 0.52 volts at 1.0 ma/dm^2 current density. The EMF of the coated metal at 0.01 ma/dm^2 current density was 0.55 volts and 1.00 volts at 1.0 ma/dm^2 . Thus increased polarization due to the CaCO_3 coating was evident.

According to Gatty and Spooner (13), the potential of pure bare iron in tap water containing dissolved oxygen was found to vary. Variations were found to depend upon: (1) The roughness of the surface -- The coarser the surface, the more noble the potential, (2) The time of exposure -- The longer the exposure, the more noble the potential, (3) The ionic strength and make-up of the solute -- In general, the more concentrated the solute, the more noble the potential, (4) The degree of prewetting -- The greater the degree of prewetting, the more active the potential, (5) The degree of oxygen saturation -- The greater the amount of oxygen in contact with the electrode; the more noble the potential.

Potter (31) and Evans (12) have shown Pourbaix diagrams which related the potential of iron in pure water to pH levels between 0 and 14. From the Pourbaix diagrams, it was possible to predict corrosion, passivity, or immunity tendencies of pure iron with a given potential in a water of known pH level. The diagrams predicted iron in water of pH 9 to 10 to be immune or cathodic when its potential was about 0.7 volts or greater on the hydrogen scale or 0.95 on the saturated calomel electrode scale.

Stumm (39) recently reported findings which were not in general agreement with those of other workers. Stumm stated that, with the passing of time, corrosion in iron pipe carrying a supersaturation of calcium carbonate tended to come under anodic control. The deposited calcium carbonate--corrosion product coating acted as an anodic inhibitor by limiting the anodic area. Corrosion was then reduced due to (1) hindering the diffusion

of the anodic products into the solution or (2) creating conditions at the interface which decelerated the electron transfer or inhibited chemical reactions.

THEORETICAL CONSIDERATIONS

A. The Electrochemical Theory of Corrosion of Iron

Corrosion is that process in which a metal returns to its natural oxidized condition. As will be shown, corrosion is a spontaneous reaction whereby the metal goes from a higher to a lower energy state. As used in this paper, corrosion describes the destruction of a metal or alloy as it passes from the elementary to the combined state by electrochemical change.

Whitney (49), in 1903, was the first to report the mechanism of corrosion to be electrochemical in nature. Camp (2), Eliassen and Lamb (7), Evans (11), (12), Gatty and Spooner (13), Potter (31), Speller (40) and many other workers have further developed the theory. It is now accepted that the corrosion process depends on the development of galvanic cell action. By some mechanism the pure metal is oxidized at the anode of the corrosion cell. Electrons released due to the anode oxidation travel to the cathodic area where they must be removed by reduction if the reaction is to continue. The reaction at each electrode is called a half-cell or single electrode reaction.

Camp (2) has listed six types of electrode reactions which are common to the corrosion process, the first three apply to the anode of the corrosion cell as written proceeding from left to right.

Type 1 Metallic element $\xrightleftharpoons[\text{Red}]{\text{Ox}}$ cations + electrons



Type 2 Anions + metal $\xrightleftharpoons[\text{Red}]{\text{Ox}}$ compound + electrons

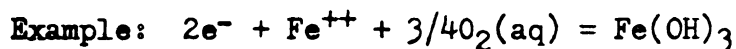


Type 3 Reductant + metal $\xrightleftharpoons[\text{Red}]{\text{Ox}}$ compound + cations + electrons



The above reactions going from right to left could occur at the cathode also. The following three types proceeding from left to right are cathodic reactions.

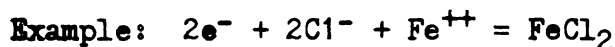
Type 4 Electrons + cations + oxidant $\xrightleftharpoons[\text{Ox}]{\text{Red}}$ compound



Type 5 Electrons + oxidant $\xrightleftharpoons[\text{Ox}]{\text{Red}}$ anions



Type 6 Electrons + anions + cations $\xrightleftharpoons[\text{Ox}]{\text{Red}}$ compound



If a cathodic and anodic reaction can occur simultaneously on a section of submerged iron, galvanic cell action causes current to flow. By convention, the movement of cations (positive electricity) in the solution is taken as the direction of current flow, i.e. from anode to cathode. In actual fact, the flow of electrons (negative electricity) is in the opposite direction.

Faraday's law states that the amount of a substance deposited or liberated at an electrode is directly proportional to the electrical charge passed through the solution. In other words, the amount of iron oxidized in a corrosion cell is directly proportional to the corrosion current.

The corrosion current depends on the difference in potential of the electrodes and on the resistance of the cell in accordance to Ohm's law. The EMF of a cell is defined as the work done per unit charge passed through the solution. The maximum work available at constant temperature and pressure is the change in free energy ΔF , of the net reaction. Under conditions of a reversible cell then,

$$\Delta F = - nFE \quad (5)$$

where ΔF is the free energy change in calories per mole for n equivalents reacting and E is the reversible potential of the reaction taking place in volts. The minus sign is chosen so that reactions proceeding spontaneously are those with positive E (EMF). The proportionality constant F' is 96,500, which is the number of coulomb's per Faraday of current. If the reactants are in their standard states, with activity equal to unity at a temperature of 25°C, the free energy change is equal to ΔF° , the standard free energy change for the reaction. The change in free energy for a reaction at a temperature other than 25°C with reactants of activity not equal to unity can be related to the standard free energy change thus:

$$\Delta F = \Delta F^\circ + 2.303RT \log Q \quad (6)$$

where ΔF° is the standard free energy change, R is the universal gas constant, T is the temperature in degrees Kelvin and Q is the

ratio of (the product of the activities of the corrosion products) to (the product of the activities of the reactants). For this ratio, both the corrosion product activities and the reactant activities must be raised to a power equal to the coefficient of the electrode reaction.

As an example, for the anode reaction: $\text{Fe} = \text{Fe}^{++} + 2\text{e}^-$,

$$Q_{\text{Ox}} = a_{\text{Fe}^{++}}/a_{\text{Fe}}$$

The solid iron, by definition, has unit activity; therefore the above reaction would reduce to

$$Q_{\text{Ox}} = a_{\text{Fe}^{++}}$$

The change in free energy for the example anode reaction can then be written:

$$\Delta F_{\text{anode}} = \Delta F^{\circ}_{\text{anode}} + 2.303RT \log a_{\text{Fe}^{++}} \quad (7)$$

The classical Nernst equation from physical chemistry can be obtained by combining equations (5) and (6) in the following manner:

$$\begin{aligned} \frac{-\Delta F}{nF'} &= \frac{-\Delta F^{\circ}}{nF'} - \frac{2.303RT}{nF'} \log Q \\ E &= E^{\circ} - \frac{2.303RT}{nF'} \log Q \end{aligned} \quad (8)$$

The Nernst equation given above makes it possible to calculate the reversible potential, E , for any possible electrode reaction under all circumstances, if the electrode reacting quantity (Q) and the standard potential (E°) for the electrode reaction is known. If the example iron--iron anode reaction is considered again, equation (7) may be given in the form of the Nernst equation thus:

$$E_{\text{anode}} = E_{\text{Ox}} = E^{\circ}_{\text{Ox}} - \frac{2.303RT}{nF'} \log Q_{\text{Ox}} \quad (9)$$

Where iron is passing into solution as positively charged divalent ions the potential of the anode relative to a standard reference hydrogen electrode of assumed zero potential, is then given by

$$E_{\text{anode}} = E^{\circ}_{\text{anode}} - \frac{2.303RT}{2F} \log a_{\text{Fe}^{++}}, \quad (10)$$

where E° is the so-called standard potential of the $\text{Fe}|\text{Fe}^{++}$ electrode relative to a standard hydrogen electrode.

The development of the equation giving the half-cell potential of the cathode is exactly analogous to the preceding argument for the anode potential. The potential of the cathode half-cell is written:

$$E_{\text{cathode}} = E_{\text{Red}} = E^{\circ}_{\text{Red}} - \frac{2.303RT}{nF} \log Q_{\text{Red}}. \quad (11)$$

The total EMF of the corrosion cell is equal to the sum of the half-cell potentials:

$$E_{\text{cell}} = E_{\text{anode}} + E_{\text{cathode}} = E_{\text{Ox}} + E_{\text{Red}}. \quad (12)$$

If the oxidation and reduction reactions have been so written that $n_{\text{Ox}} = n_{\text{Red}} = n$, the reversible cell EMF will be given by

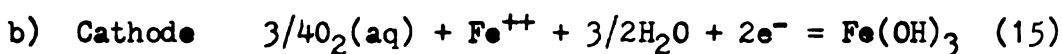
$$E_{\text{cell}} = E^{\circ}_{\text{Ox}} + E^{\circ}_{\text{Red}} - \frac{2.303RT}{nF} \log Q_{\text{Ox}} Q_{\text{Red}}. \quad (13)$$

Recall that oxidation reactions occur at the anode and reduction reactions at the cathode.

It is seen from the previous development that the reversible EMF of corrosion cells can be predicted from the standard half-cell potentials which have been computed and published in reference texts. Camp (2) has reported some 267 standard half-cell electrode potentials for corrosion reactions likely to take place in metal piping carrying water. If the composition of the water is known, it is possible to determine the most likely electrode reactions on

the basis of an examination of pairs of all possible anodic reactions. The most anodic reaction is then most likely to take place. Similarly, it is necessary to examine all possible cathodic reactions to determine which is the most cathodic. The flow of electricity will begin with the half-cell reactions which have the greatest difference in potential.

By the preceding thermodynamic considerations Camp (2) has shown the following corrosion reactions to take place for iron in pure water containing some dissolved oxygen at 25°C:



assuming reversible electrode behavior.

However, once current starts to flow in the corrosion cell, the previously developed equations will not predict the actual electrode potentials, since the electrode reactions are no longer reversible in nature. (The phenomenon of irreversible electrode behavior will be considered later under the theory of polarization).

Polarization of the electrodes, which occurs with current flow in the corrosion cell, effectively reduces the potential difference between the electrodes. Other electrode reactions of lower potential difference then become possible and prediction of the correct mechanism becomes hazardous.

B. The Theory of Irreversible Electrode Reactions

1. Polarization Defined.

Potter (31) has stated that, theoretically, no electrode equilibrium could be shown by observation to be thermodynamically reversible (no net reaction taking place). Moreover, no electrode

reaction could proceed reversibly throughout its course from reactants to product.

In any real electrode system, thermodynamic reversibility is a state which may be attained only by observing working conditions which are impracticable to satisfy. Therefore when a reaction proceeds in a corrosion cell at some net rate, the reaction is thermodynamically irreversible and, in order to sustain the reaction current flow, the potential of the electrodes must shift in such a manner as to increase the EMF of the cell. The greater the current flow per unit area (current density), the greater the irreversibility of the electrode process and the greater the shift in electrode potentials.

Potter (31) defined polarization as the degree of irreversibility of an electrode as measured by the departure of the electrode potential from the reversible value. For given conditions of pressure, temperature, and ionic concentration, the reversible value of an electrode is the potential when no current is flowing. Thus, an irreversible electrode is said to be polarized or to exhibit overpotential which is equal in magnitude to the departure of the electrode potential from the reversible value.

2. Causes of Polarization

As previously mentioned, Evans (12) has stated that overpotential may be due to any or all of the following energy consuming phenomena:

1. An ohmic drop through a coating on the electrodes.
2. Electrolyte concentration differences.

3. Energy required for activation.
4. Electrolyte approach -- resistance.

a) Ohmic Drop

If a film is present on an electrode surface, the ohmic drop depends on the resistance of the coating. In any case, the polarization potential is equal to the IR drop through the film and is a straight line function of the current density.

b) Concentration Differences

Concentration polarization is due to a decrease in concentration of the electrolyte in the immediate vicinity of the electrode because of a rapid discharge of ions at the electrode and a slow migration of ions which replace them (14). Any action which helps to bring the discharging ions to the electrode at an increased rate tends to decrease the concentration polarization. Thus, increased turbulence with the resulting more rapid mixing decreases the magnitude of the concentration polarization.

The electrode potential increase due to concentration polarization can be estimated using the Nernst equation (8):

$$E_{\text{polar}} = \frac{2.303RT}{nF} \log Q \quad (16)$$

for water at 25°C

$$E_{\text{polar}} = \frac{.0592}{n} \log Q. \quad (17)$$

For a thousand fold decrease in electrolyte concentration the increase in electrode potential is

$$E_{\text{polar}} = 3 \times \frac{.0592}{n} = \frac{0.18}{n} \text{ volts,} \quad (18)$$

where n is the valence change of the discharging ion.

From the above, it is seen that concentration polarization values are usually not large (14).

c) Activation Energy

Activation polarization is due to a "slow step" in the actual process of discharging the ion on the electrode. This "slow step" may be due to the limited rate at which the discharging ion can be adsorbed and then removed during discharge. The large hydrogen and oxygen overpotentials which are sometimes experienced are probably due to activation polarization. Glasstone and Lewis (14) reported the magnitude of the hydrogen overpotential on an iron electrode in 1 N hydrochloric acid at 100 ma/dm² current density to be 0.40 volts. A similar value of 0.37 volts was reported for the oxygen overpotential on an iron electrode in 1 N potassium hydroxide at 10 ma/dm² current density.

It has been found (12), (13), (14), (17), (31), (33) that when polarization of an electrode is due almost exclusively to hydrogen activation polarization the increase in overpotential is logarithmically related to the current density by Tafel's equation:

$$w = a + b \log I \quad (19)$$

where w is the overvoltage in volts at the current density I , and for a given electrode under specified conditions a and b are constants. This situation seldom if ever occurs with cast iron in neutral or alkaline water, due in part to the low concentration of hydrogen ions.

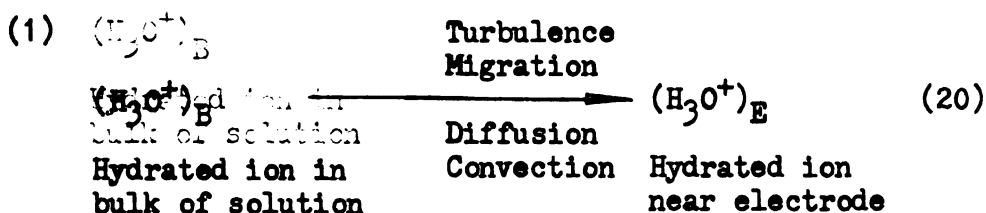
d) Ionic Approach - Resistance

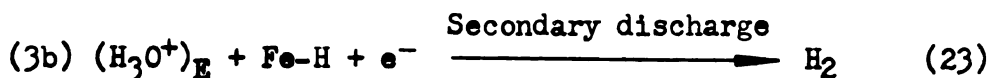
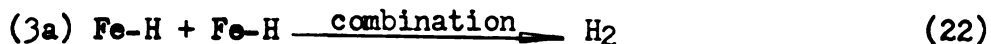
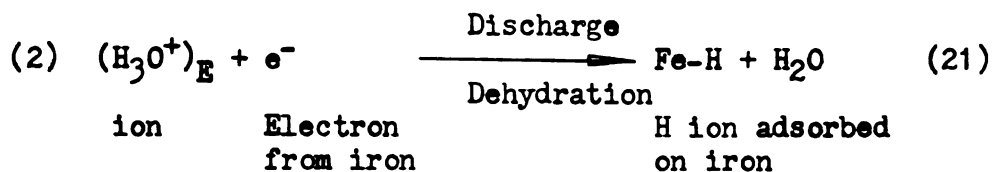
Approach -- resistance polarization is usually considered as part of the ohmic drop (12) but is actually due to special

circumstances at the electrode. This special circumstance can be illustrated by considering an electrode which has developed a limited number of protruding crystals where ionic discharge preferentially takes place. In this case, the resistance of the bottleneck approach is much higher than that can be accounted for by the normal ohmic resistance of the solution or coating. Evans (12) suggested that the linear relationship between the polarized electrode potentials and current density, which often exists when polarization measurements of a corrosion cell are made at low current density, is probably due to approach -- resistance polarization. From this presumption, it was postulated that activation polarization and concentration polarization were overwhelmed by the much larger approach-resistance polarization at very low current densities. This explanation would account for the linearity of relationship, since approach--resistance polarization is ohmic in character and therefore directly proportional to the current flow.

e) Interrelationship of Polarization Mechanisms

To illustrate the interrelationship of the mechanisms of polarization, consider a cathodic electrode reaction which depends on hydrogen ions for removal of electrons. Potter (31) has summarized the various steps involved by the following scheme:

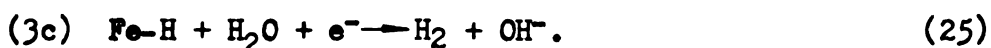




However in alkaline solution the discharge step cannot reasonably involve a hydrogen ion because of the small concentration of this ion under alkaline conditions. Potter (31) stated that the discharge appeared to take place from a water molecule itself, i.e.,



The secondary discharge (3b above) must also involve a water molecule in alkaline solution, i.e.,



The observed rate of the cathodic evolution of hydrogen is the rate of the overall reaction, i.e.,



It follows, however, that each separate step in the overall reaction proceeds at this same rate. One of these steps therefore determines the overall rate, and may be "coaxed" to maintain this rate only by an additional supply of energy (i.e., by a greater potential). The additional energy for the sluggish step of the process is provided by the overpotential.

It is apparent that if step one is the rate-determining-step, concentration polarization is involved. Activation polarization would be involved if any of steps 2, 2a, 3a, 3b, or 3c were rate determining. Ohmic drop or approach resistance polarization might also play a part if there were film formation on the cathode. In this case the slow step would be movement of the electron through the film to meet the hydrogen ion.

3. Polarization of Electrode Related to Current Density.

The result of polarization can be seen by considering the conditions at steady state. Steady state implies a condition in which the energy decrease in the corrosion process is equal to the sum of the energies dissipated in the various parts of the electrochemical corrosion cell (23). If the energy decrease in the corrosion reaction and the various energies dissipated in the process are converted into potentials by the earlier relationship of this section:

$$\Delta F = -nFE \quad (5)$$

where the symbols have the same meaning as before, the equation for the steady state corrosion rate may be written

$$E_R = E_A + E_C + E_{IRi} + E_{IRe} \quad (27)$$

where

E_R = The reversible (maximum) EMF of the corrosion cell.

E_A = Total polarization of the anode, or sum of the anodic polarization due to all the aforementioned mechanisms

E_C = Total polarization of the cathode, or sum of the cathodic polarization due to all the aforementioned mechanisms.

$E_{IRi} = IRi$ = Product of current flowing and resistance of electrolyte between cathode and anode areas.

$E_{IRe} = IRe$ = Product of current flowing and resistance of the metal between cathode and anode areas.

This resistance, R_e , for the usual short circuited corrosion cell is very small; hence

E_{IRe} may be neglected in most cases.

All the dissipative terms making up the right-hand side of the above equation are functions of the current density. Therefore their relationship to the total available energy, E_R , the current density and the limiting corrosion rate may be shown graphically as in Figure 1.

a) Polarization Curves from Galvanic Cells

If the anodic and cathodic areas of a corroding iron specimen can be separated, the classical polarization curve of Figure 2 results. By varying an external resistance in the metal circuit between the cathode and anode from infinity to zero, it is possible to observe the shift in potential of the electrodes which results from increased current density. When R is infinite, no current flows, and $E_C - E_A$ is the open circuit EMF (i.e. reversible EMF) of the galvanic cell. As R is made smaller, I increases and $E_C - E_A$ grows smaller as each electrode experiences its characteristic polarization. Finally, as R approaches zero, (the minimum short circuit resistance) I approaches its maximum value which is the limiting corrosion current. Because R is generally very small in a short circuited galvanic couple, a very small value of $E_C - E_A$ is sufficient to drive the maximum current.

Where the cell circuit is externally varied, Figure 2 is an instantaneous picture of electrode potentials at certain current densities. The points on the curve are obtained by taking measurements during short periods of closed circuit. It is important to recognize that Figure 2 portrays the polarization characteristics of the electrodes but does not describe the electrode potential -- current density picture of a short circuited corrosion cell with the passage of time when under no external control.

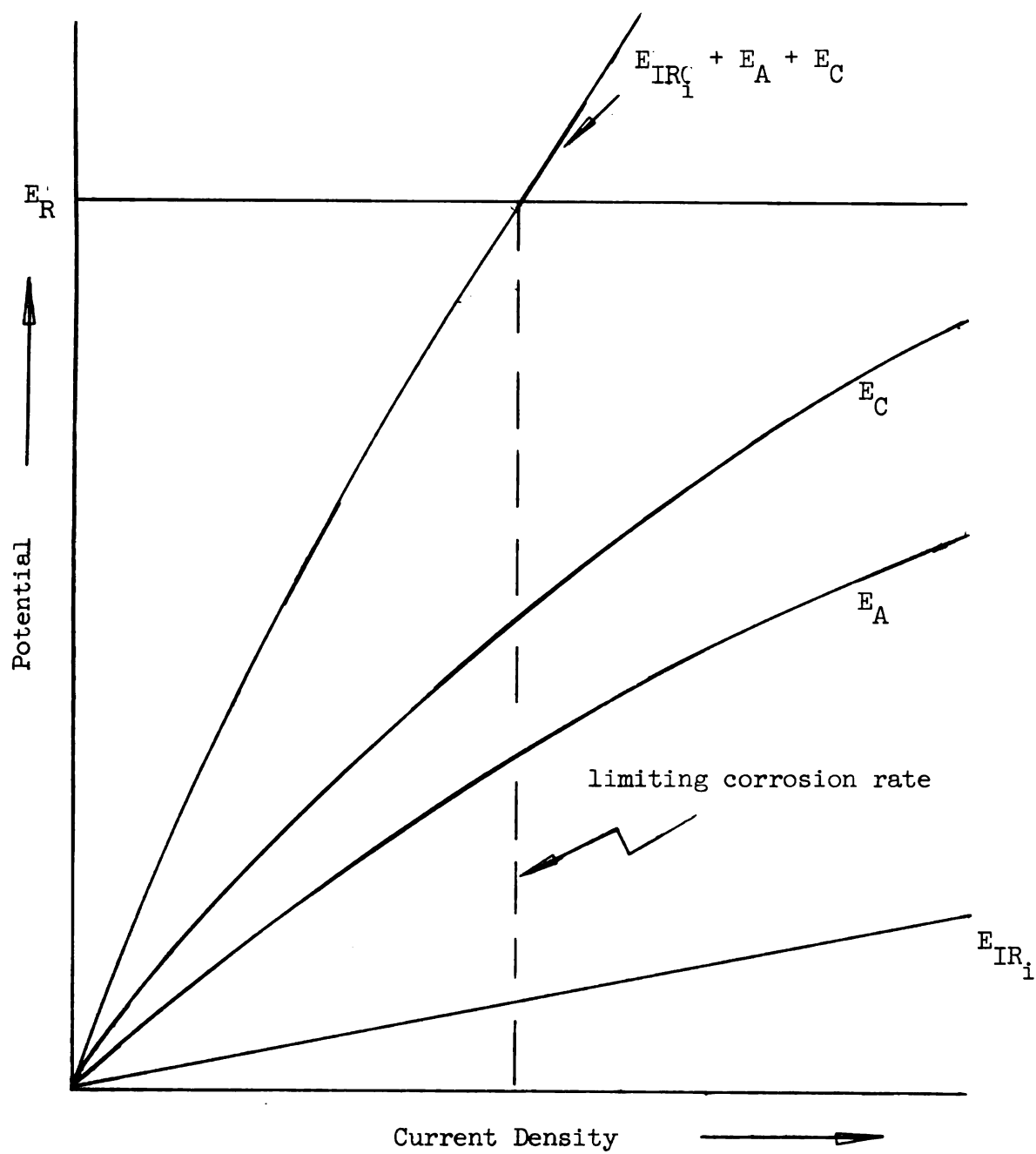


Figure 1. Polarization and the Limiting Corrosion Rate.

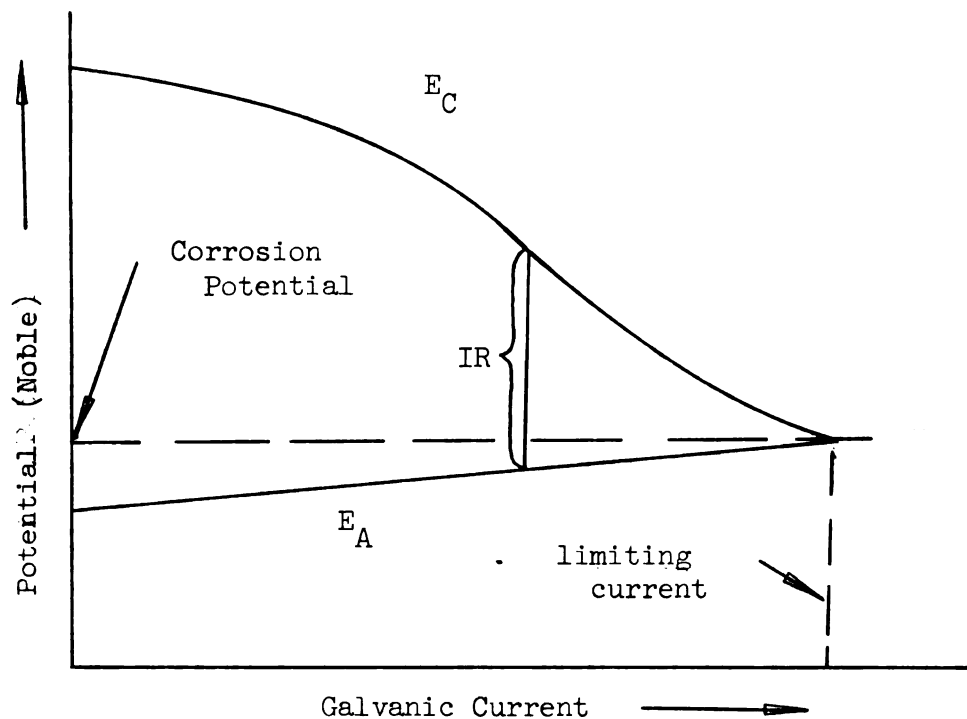


Figure 2. Polarization of a Galvanic Cell by Varying the Resistance of the Cell.

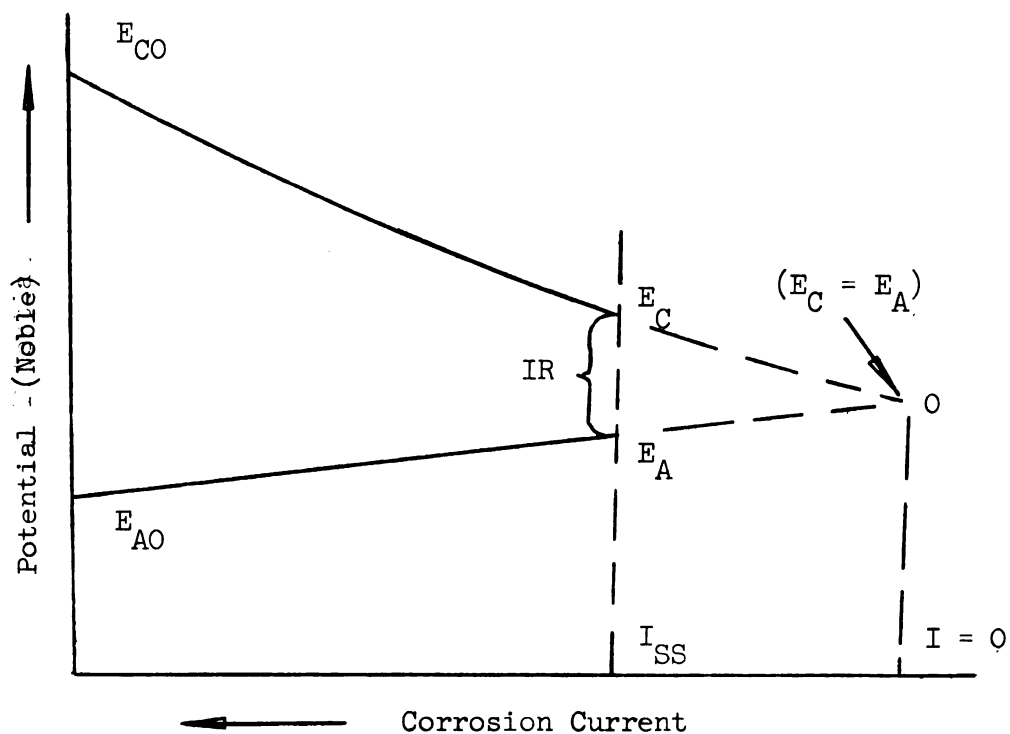


Figure 3. Effect of Corrosion Current on the Electrode Potentials in a Short Circuited Corrosion Cell.

Figure 3 shows a condition in which the ohmic resistance of the circuit remains constant and current is allowed to flow in the corrosion cell (1). With no mechanical or electrical changes in the circuit, the anode open circuit potential E_{AO} and the cathode open circuit potential E_{CO} approach the values E_A and E_C due to polarization of the electrodes. The polarization reduces the effective EMF of the cell, as $E_C - E_A$ becomes smaller, and thus the corrosion current must decrease. At some point the polarization reaches a steady state and the corrosion current becomes I_{ss} . However the dotted lines E_{AO} and E_{CO} indicate that if complete polarization of the electrodes were possible, E_A and E_C would become equal, thereby eliminating the potential difference and thus reducing the corrosion current to zero.

b) Polarization Curves from Impressed Current

Figure 4 illustrates polarization curves obtained by impressing a current through a galvanic cell and measuring the polarization (or shift in potential) with increased current density. The greater the magnitude of the dissipative, irreversible effects of the electrode reaction, the greater the polarization of the electrode.

When polarization measurements are made in this way, the anode and cathode are separate specimens arbitrarily chosen by the direction of the impressed current flow. As the current density is increased, the difference in potential $E_C - E_A$ of the electrodes must increase to provide for the dissipative effects that take place. This technique (47) provides another method of determining

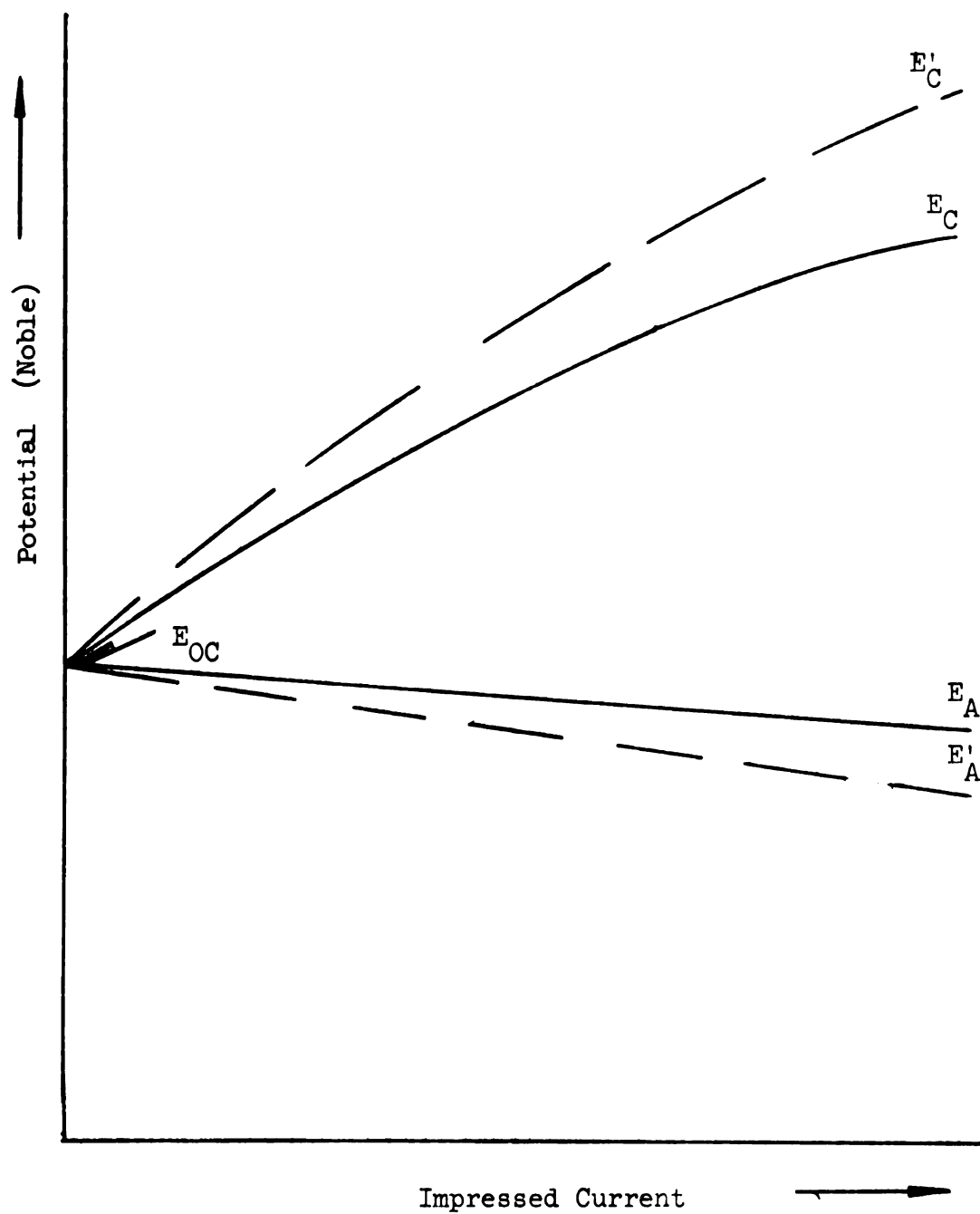


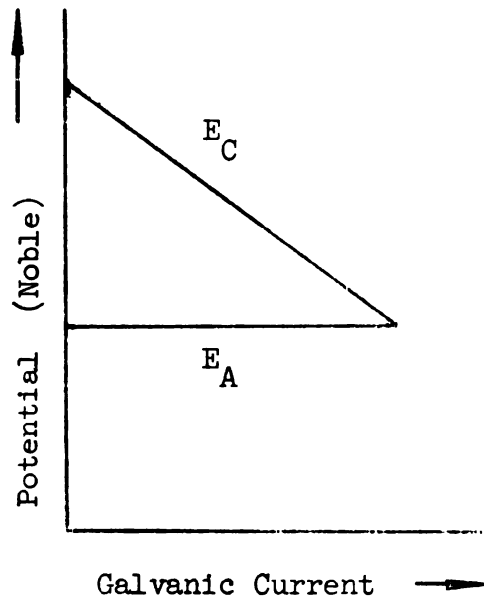
Figure 4. Polarization of a Galvanic Cell by an Impressed Current.

the polarization characteristics of a galvanic cell which should agree with the results of the resistance method used in Figure 2.

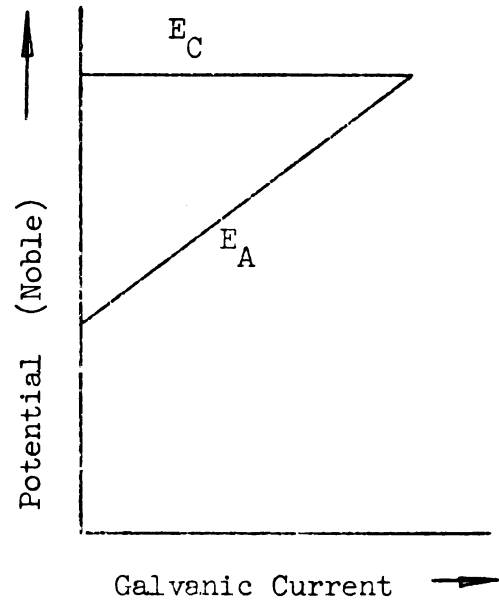
As discussed previously, the degree of polarization depends on: (1) The characteristics of the electrode metal, (2) The metallic surface condition, (3) The strength and kind of electrolyte, (4) Reactions which are occurring at the electrode, and (5) Whether an electrode film is or is not formed.

Because of the variation of polarization characteristics, it is helpful to classify corrosion cells by the type of polarization produced on each electrode. Considering Figure 1, if E_C is the major dissipative term, the corrosion process is said to be under cathodic control. Likewise if E_A is the major dissipative term, the process is said to be under anodic control. Figure 2 and Figure 3 illustrate cathodic control of a corrosion cell. In these figures, it is apparent the cathode potential has been polarized to a much greater extent than the anode.

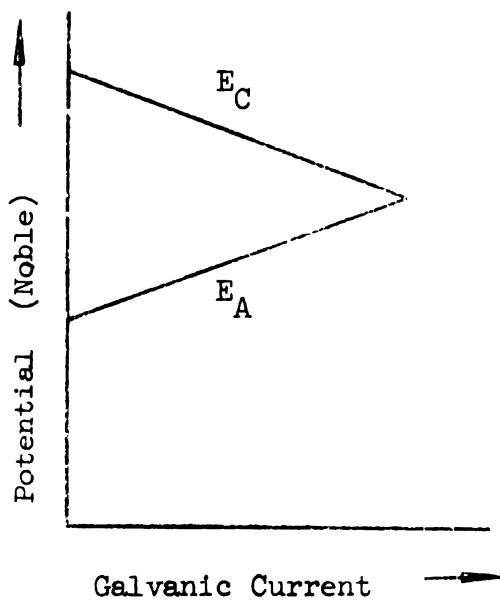
Figure 5 illustrates the four types of control: (1) cathodic, (2) anodic, (3) mixed, and (4) resistance. When a process is under cathodic control a slight shift in the cathode polarization curve may produce a large change in the corrosion current. Likewise if a process is under anodic control, a slight shift in the anode polarization curve may produce a significant change in the corrosion current. However, from Figure 5 it is apparent that the inverse is not true, i.e. a slight shift in the anode polarization curve when the process is under cathodic control does not significantly change the corrosion current. The case where resistance in the circuit controls is of little interest, since it rarely occurs in the field.



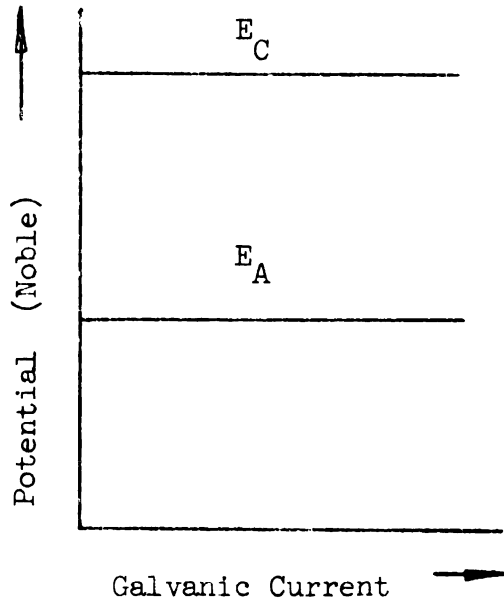
a) Cathodic Control



b) Anodic Control



c) Mixed Control



d) Resistance Control

Figure 5. Types of Control in Galvanic Corrosion.

C. The Development of Local Corrosion Cells on the Surface of Submerged Iron.

A difference in potential between two points on an iron surface are necessary for corrosion to be initiated. There are basically four ways (7), (11), and (48) in which this potential difference and resulting local corrosion cells can develop:

- (1) Impurities in the metal.
- (2) A difference in concentration.
- (3) A difference in temperature.
- (4) A difference in stress.

The first two of the above methods are very common in occurrence and deserve further explanation.

a) Impurities in Metal

Cast iron for water main use always contains traces of impurities. If the iron is submerged in water containing substances which react with the impurities of the metal with a resulting potential which is more negative or noble than the potential which iron could develop with any possible reaction, current will flow and oxidation of the iron will occur.

b) Difference in Electrolyte Concentration

It is to be recalled that the activity of ions in solution is equal to the product of their concentration and their activity coefficient. Therefore a difference in activity is proportional to a difference in concentration. Because the potential which an electrode develops depends on the activity or concentration of the reacting substances, a difference in ionic activity between two points of an iron section causes a difference in potential. Current then flows between the two points and corrosion is experienced.

A concentration difference develops because of unequal mixing, which may be due to several factors such as:

- (1) Uneven surface: Deep depressions may remain stagnant with mixing dependent on diffusion, whereas mixing may readily occur at peaks which protrude into the flow of water.
- (2) Sediment accumulations.
- (3) Film development; inorganic, organic, and biological.

Some bacterial slimes act both as a shield preventing mixing and as a source of acid production. High concentration build ups are possible under the semiporous films and metallic attack is usually experienced.

A very important special type of concentration or "differential aeration" cell results from the shielding of some points on the surface of iron with a resulting difference in concentration of dissolved oxygen. If two points of a metallic surface experience different levels of contact with dissolved oxygen, the point receiving the greater amount will tend to be cathodic to the other point.

Oxygen-metal contact is also of importance because of the role oxygen plays in depolarizing cathodic areas, thus increasing the corrosion rate.

D. The Action of Inhibitors

Inhibitors have been defined (47) as substances which effectively decrease the corrosion rate when added in small amounts to the corrosive environment of a metal or alloy. Potter (31) has added that an inhibitor should be capable of renewing itself.

Thus, according to Potter, methods such as plating and painting should be thought of as attempts to prevent, rather than inhibit corrosion, by separating the metal from the corrosive environment. There is some overlap however, since some film forming inhibitors act in much the same way as a coating of paint.

Corrosion inhibitors may be classified as inorganic, and organic, soluble and insoluble, basic and neutral, volatile and nonvolatile, etc. A more general classification is by designating inhibitors according to whether their action is on the cathodic or the anodic reactions in the corrosion process.

An inhibitor which forms an impermeable film over the total exposed surface area, inhibits both anode and cathode reactions by making contact with the electrolyte impossible. However, it is possible for a permeable film to also inhibit one or both electrode reactions if the film is effective in making the electrode reactions more difficult due to increased polarization of the electrode. A substance which increases E_A in Figure 1 is an anodic inhibitor (47). For this same figure, cathodic inhibitors are those which increase the magnitude of E_C . Mixed inhibitors obviously increase both E_A and E_C .

The relative effectiveness of cathodic and anodic inhibitors on a process under primarily cathodic control is shown by the polarization curves in Figure 6. The points on these curves were obtained in the same manner as for Figure 2, that is by varying the resistance of the galvanic cell. It is obvious that the corrosion current I_0 of Figure 6 is affected to a greater extent by cathodic than by anodic inhibitors.

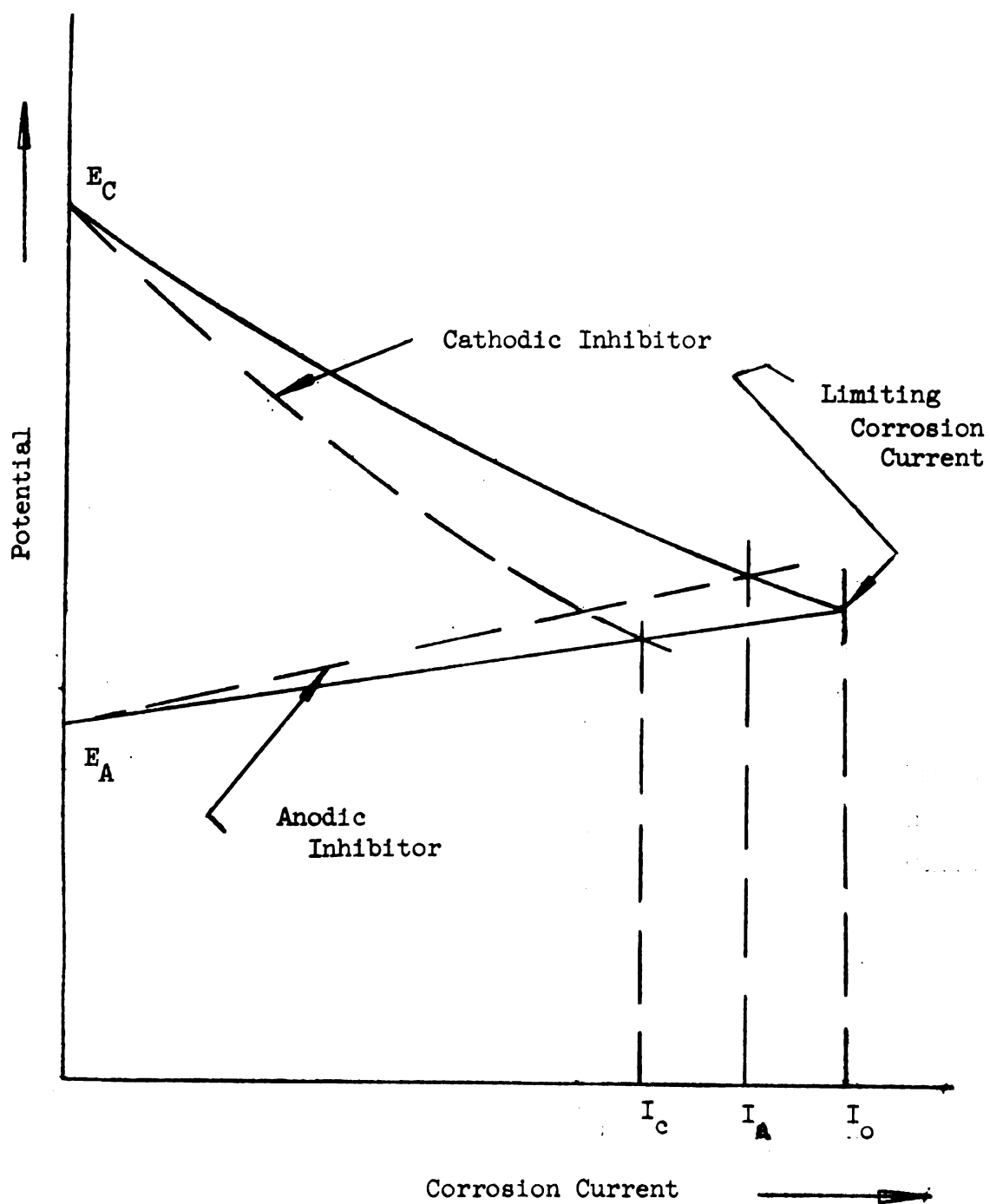


Figure 6. Influence of Inhibitors on Corrosion Reaction Under Cathodic Control.

The results of adding cathodic and/or anodic inhibitors can also be shown by the dashed curves of Figure 4 which shows the potential shift, E'_C , when a cathodic inhibitor is added and the shift, E'_A for an anodic inhibitor. The increased polarization due to the action of the inhibitors is responsible for the above described potential shifts.

Evans (12), Potter (31), Uhlig (46) have discussed the consequences of using different types of inhibitors to reduce the corrosion of iron in water. An inhibitor may act in such a way as to reduce the rate of corrosion while increasing the intensity of attack. As pointed out previously, the corrosion of iron in water is under cathodic control and is limited by the cathodic reaction rate. Thus, if an anodic inhibitor is used in insufficient quantities to inhibit all anodic areas, the corrosion rate will be affected only slightly but the attack will be intensified on the remaining uninhibited anodic areas. Severe pitting may result and local failure is possible. For this reason Evans (12) has classified anodic inhibitors as dangerous.

On the other hand, cathodic inhibitors are usually safe since they do not cause intensified attack when their supply is inadequate at the cathodic areas. Partial effectiveness will reduce the rate of corrosion and because the anodic area is not affected the intensity of attack must decrease.

Some inhibitors are capable of causing both cathode and anode reactions to polarize to a greater degree. In cast iron water systems these inhibitors, if not used in sufficient quantities, may also cause pitting.

The film forming properties must be considered in deciding the safety of an inhibitor. A cathodic inhibitor which forms a dense, semi-impermeable film over the total exposed surface may also prevent the anodic reaction from occurring due to the separation of the metal and the electrolyte. With a film of this type, local faults in the film may develop into points of intensified anodic attack. Thus, in those instances where pitting may cause failure, certain types of film forming cathodic inhibitors may also be classified as dangerous.

Film formation may occur preferentially at either the anodes or cathodes of corrosion cells. Or, as discussed previously, films may be adsorbed generally over the entire surface of the metal. Films may be formed through (1) electrodeposition of charged ions or colloidal particles on the electrode, (2) adsorption of appropriate chemicals on the metal surface, or (3) through the production of insoluble precipitates of the corrosion reaction.

Eliassen and Lamb (7) have stated that a preferential protective cathodic film may be inefficient due to the tendency of the shielded cathodic areas to become anodic to the exposed anodes. This condition would result from the differential aeration set up by the protective film, with a resulting continual change in the location of cathodes and anodes. Even with differential aeration cells, however, the corrosion rate would still be reduced.

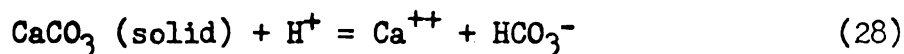
E. Different Indexes Used for Calcium Carbonate Equilibrium.

1. Langelier Saturation Index.

The Langelier Saturation Index was the first to have wide spread use and represented an early step in quantifying the

stability of bicarbonate waters. Limitations of this index are widely known and reported (12), (22), (26), (38); however, the index is still in general use.

The Langelier Index is based on the equilibrium of the reversible pipe scaling reaction:



The equilibrium constant K can be expressed as

$$K = \frac{(\text{Ca}^{++})(\text{HCO}_3^-)}{(\text{H}^+)} \quad (29)$$

where the terms in brackets are expressed as molal concentrations. If each term of the above equation is written as a negative logarithm, the equation can be expressed for the pH at equilibrium thus:

$$\text{pH}_{\text{eq.}} = \text{pCa}^{++} + \text{pHCO}_3^- - \text{pK} \quad (30)$$

Langelier (18) showed that pK was the difference between pK_s (the solubility product constant of calcium carbonate) and pK_2 (the second ionization constant of carbonic acid). By relating pHCO_3^- to the total alkalinity, Langelier developed the following expression for $\text{pH}_{\text{eq.}}$:

$$\text{pH}_s = (\text{pK}_2 - \text{pK}_s) + \text{pCa}^{++} + \text{pAlk.} + \log\left(1 + \frac{2\text{K}_2}{\text{H}_s}\right) \quad (31)$$

where pH_s was the hypothetical pH of the water when the calcium content and alkalinity were in equilibrium if no changes occurred. All concentration were molar except alkalinity, which was expressed as titrable equivalents of base per liter.

Langelier's "saturation index" is the algebraic difference in the actual pH of a water and the calculated pH_s from equation 31:

$$\text{Saturation index} = \text{pH actual} - \text{pH saturation} \quad (32)$$

positive index indicates oversaturation and a tendency for the water

to deposit calcium carbonate and a minus index value indicates under-saturation and a tendency for the water to dissolve calcium carbonate.

The constants K_2 and K_3 in equation 31 are temperature dependent and also vary with the ionic strength of the water. Larson and Buswell (22) have discussed the variation in the ionization constant with changes in salinity. Langelier (20), as a result of further studies, also reported the effect of temperature on the equilibrium constants.

It should be noted that the pH of the water in equation 32 must be the actual pH at the temperature of the water at the point of concern. Langelier (19) and Dye (5) have reported the effect of temperature on the pH of a water.

Calcium carbonate has a strong tendency to remain in super-saturated solution and in the absence of crystallization nuclei oversaturated solutions of calcium carbonate have been preserved for years (28). Therefore the amount of calcium carbonate deposited cannot be predicted from equilibrium data alone. Because of this fact, the "saturation index" is an indication of directional tendency only and is not a measure of capacity.

2. Ryznar Stability Index

Ryznar's (38) "stability index" is similar in character to Langelier's "saturation index" in that it is related to the difference in the pH at saturation and the actual pH of a water, thus:

$$\text{Stability index} = 2\text{pH saturation} - \text{pH actual} \quad (33)$$

This index is positive for all water. Ryznar has claimed his

index to be quantitative in nature as a result of experimental work with the formation of calcium carbonate scale on glass coils at temperatures of 120-200°F. At a stability index of 7.5 and above Ryznar found no scale to be formed; at an index value of 6 and below scaling took place within a five hour test period.

3. Saturation Excess

The "saturation excess" is a direct measurement of the tendency of a water to deposit or dissolve calcium carbonate. Values are determined by the "marble test", in which the water is passed over finely ground calcium carbonate (48). The change in alkalinity is then a measure of the "saturation excess" or "deficiency." Langelier (20) and Dye (6) have also reported graphical methods for determining the "saturation excess."

4. Momentary Excess

The "momentary excess" has been defined by Dye (6) as the moles per liter of calcium carbonate which are in excess of the solubility product constant of calcium carbonate. The derivation of the expression for momentary excess, usually referred to as ME, is as follows:

$$(Ca^{++} - ME)(CO_3^{=} - ME) = K_s^i \quad (34)$$

with the concentrations expressed as moles per liter. Solving for ME by the quadratic equation yields:

$$ME = Ca^{++} + CO_3^{=} \pm \sqrt{\frac{(Ca^{++} + CO_3^{=})^2 - 4(Ca^{++} \times CO_3^{=} - K_s^i)}{2}} \quad (35)$$

If both the solubility product constant K_s^i (corrected for temperature and salinity) and the $CaCO_3$ concentrations are expressed as ppm calcium carbonate, equation 35 becomes:

$$ME = Ca^{++} + CO_3^{--} - \sqrt{\frac{(Ca^{++} + CO_3^{--})^2 - (Ca^{++})(CO_3^{--}) - K_s^!(10)^{10}}{2}} \quad (36)$$

Equation 36 was used extensively in the work reported in this thesis since it was believed to be more quantitative than the preceeding indexes.

5. The Driving Force Index

McCauley (22) has developed the "driving force index" which he refers to as the DFI. On the basis of his experimental work in determining the optimum conditions for the controlled development of calcium carbonate coatings, McCauley reported the index to be more quantitative in nature than the older indexes, since it indicates the magnitude of the deposition driving force.

The DFI is expressed as the ratio of the product of the calcium and carbonate concentrations to the solubility product constant for calcium carbonate corrected for temperature and salinity. Thus if the concentrations of calcium and carbonate in the water, and the solubility product constant are expressed as ppm calcium carbonate, the "driving force index" is given by:

$$DFI = \frac{(Ca^{++}) (CO_3^{--})}{K_s^!(10)^{10}} \quad (37)$$

The DFI was also used throughout the work reported in this thesis because the index was believed to be based on the law of mass action, and was therefore indicative of the magnitude of the chemical force acting to cause deposition.

EXPERIMENTAL APPARATUS AND MATERIALS

A. Apparatus for Development of Calcium Carbonate Coating on Test Specimens

1. The Dynamic Test Unit

The dynamic test unit was constructed of 3/4 inch plastic pipe and fittings as shown in Figure 7. Water was withdrawn through a 3/4 inch nipple which was tapped into the 6 inch discharge pipe of a Michigan State University deep well. The well, shown in Figure 7, was pumped continuously at a uniform rate of 350 gpm. The 25 psi pressure in the well discharge line was sufficient to provide a velocity of up to eight feet-per-second through the test cells. Flow through the experimental apparatus was regulated with a globe valve on the 3/4 inch test water bypass line and measured with a Brooks Rotometer Company 0-25 gpm rotometer installed in the test line.

The cast iron specimens were the only metal in the test water bypass system. All piping was of 5/8 inch ID Tygon tubing and Van-Cor or Koroseal (unplasticized polyvinyl chloride) 3/4 inch ID plastic pipe. Fittings were of the same material as the plastic pipe. Hills-McCanna Company Model 500 A metal valves with hard rubber linings and Fisher Scientific Company Castaloy jumbo hosecocks were used for flow control through the test apparatus.

Calgon,* a glassy polyphosphate, and sodium hydroxide, commercial grade, were fed to the test water in predetermined

* A product of Hagan Laboratories.

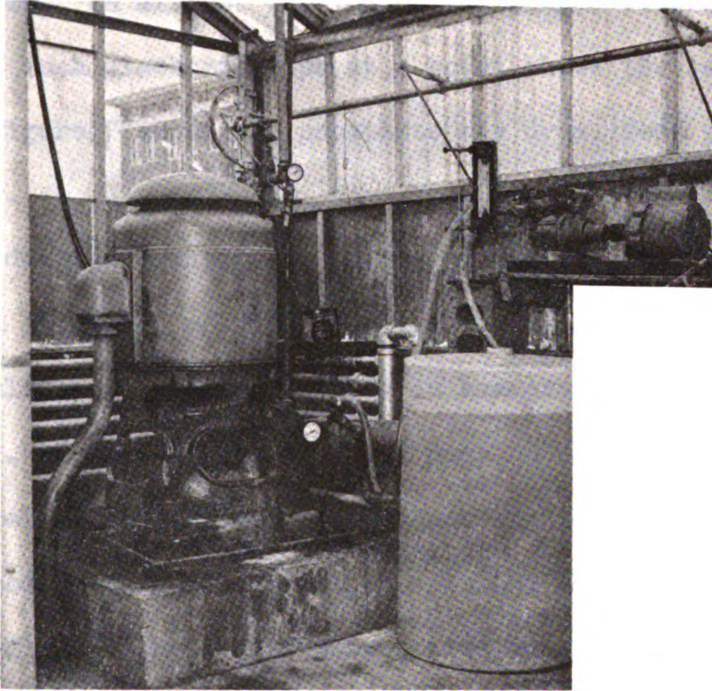


Figure 7. Deep Well Pump and Phosphate Feed.

amounts as described in the Procedure Section of this report. During each experiment, Calgon solution was stored in a 54 gallon polyethylene drum, and mixed continuously by recirculating most of the solution with a Continental Pump Company pump, model EC 44C. This pump consisted of a stainless steel rotor turning within a flexible rubber stator to produce a screw type uniform flow. An aliquot portion of the pumped flow was fed into the 6 inch discharge pipe at a point above the test water outlet. Figure 7 shows the phosphate mix drum, feed pump, and flow meter.

The desired quantity of sodium hydroxide was dissolved daily in a 54 gallon polyethylene drum. Mixing was accomplished by recirculating the solution with an Eastern Industries pump model VW 1. This small centrifugal pump, consisting of a hard rubber impeller and stainless steel housing was also used to feed the sodium hydroxide solution into the test water line.

The flows of both sodium hydroxide and phosphate feed solutions were measured with Brooks Rotometer Company 0-13 gph rotometers.

A small 5 gallon polyethylene lined pressure drum was installed in the piping apparatus at a point just beyond the sodium hydroxide feed. This arrangement allowed further mixing to take place, in order to stabilize the pH of the test water.

The upper middle part of Figure 8 shows the large 0-25 gpm rotometer used for metering test water flow. The sodium hydroxide mixing drum, feed pump, flow meter, and stabilization drum are shown in the lower center of the photograph.

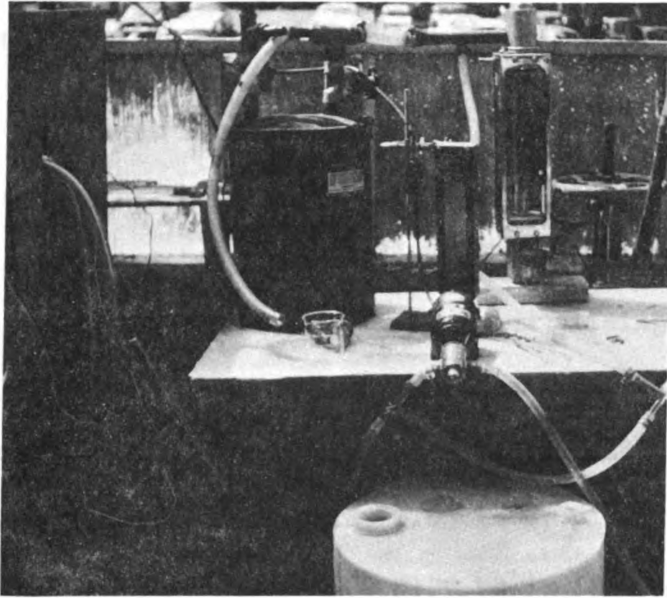


Figure 8. Sodium Hydroxide Feed.

2. Test Specimens

a) Cast Iron Plates

Cast iron plate specimens shown in Figure 9 were 3.0 x 1.0 x 0.09 inch wafers sliced from cast iron bars and finished by surface grinding with a 40-grit diamond dressed wheel. The plates were cleaned by sand blasting before use. In order to eliminate any corrosion due to moisture, the plates were stored in a desiccator before use. The backs of the plates were coated with fingernail polish as explained in the experimental procedure.

b) Black Iron Pipe Nipples

Pipe specimens shown in Figure 10 were made by cutting 3/4 inch ID, standard weight, butt weld, black iron pipe into six inch lengths, machining the ends square, and slicing each specimen longitudinally into two equal halves. As explained in the Procedure Section, the pipe halves were electrically insulated from one another by gluing a thin, 0.03 inch, piece of rubber stripping of the same width as the pipe wall, to both longitudinal edges.

Pipe electrode contacts were 0.125 inch round brass welding rod inserted into holes drilled in the centers of the outside surfaces of the pipe-halves. Each brass contact was approximately one inch long, held in place perpendicular to the pipe wall by a tight friction fit.

The pipe specimens were cleaned by sand blasting and stored in a desiccator until ready for use.

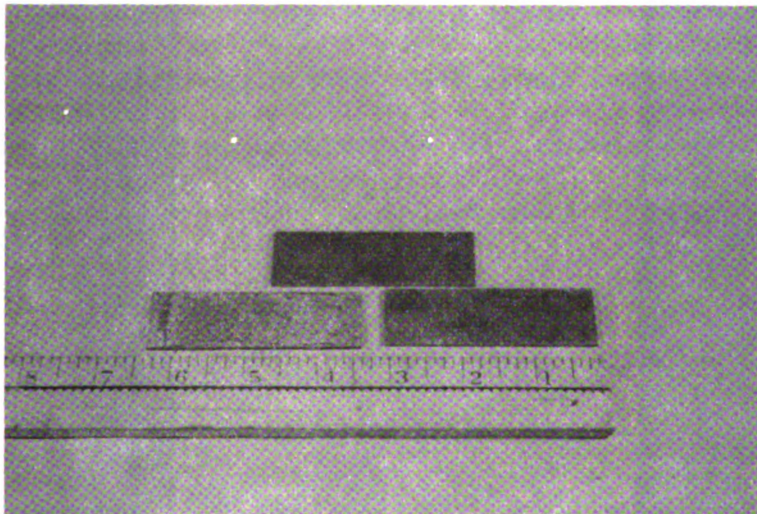


Figure 9. Cast Iron Plate Specimens.

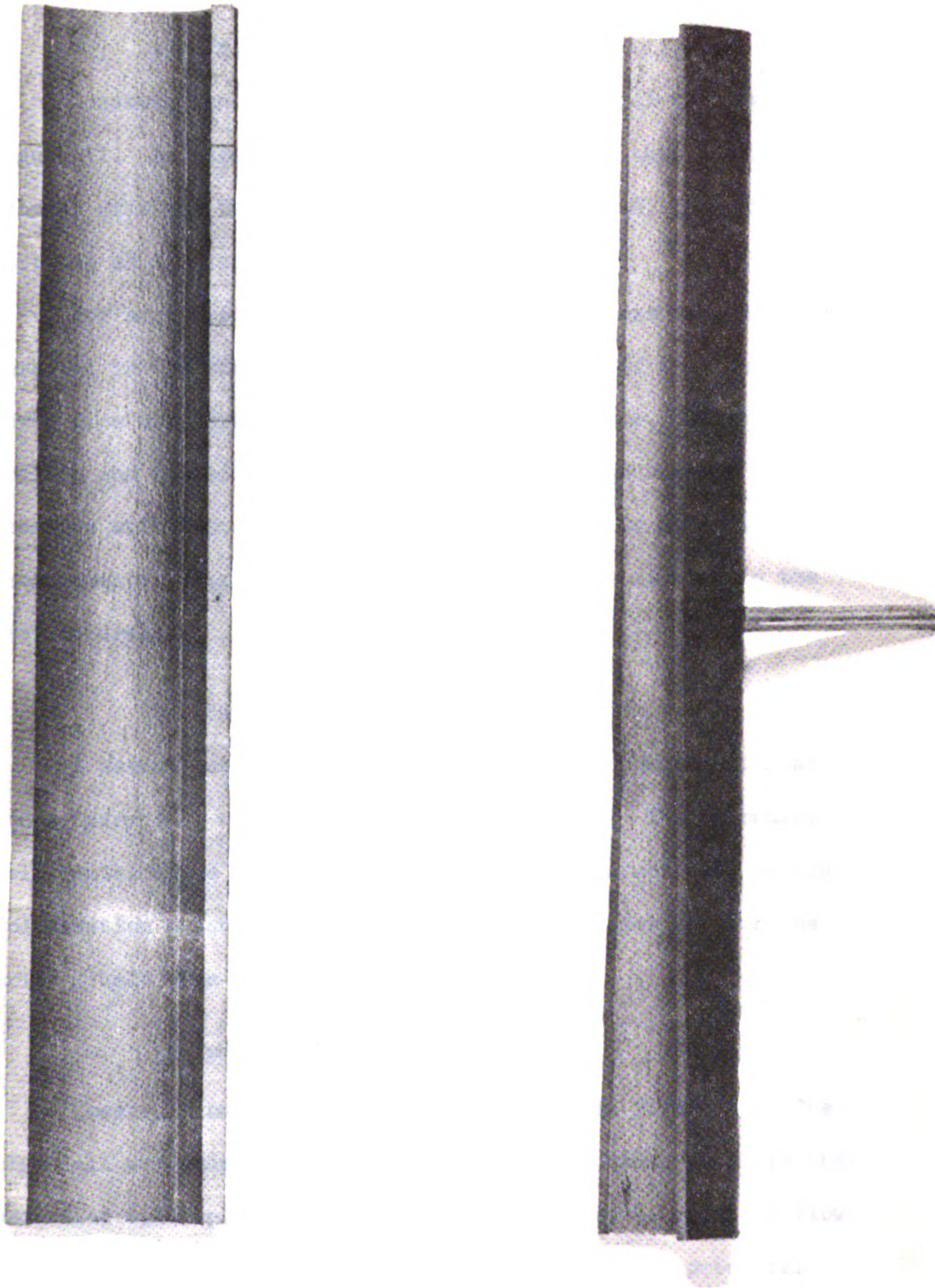


Figure 10. Iron Pipe Specimens.

3. Test Cells

a) Primary Plate Cell

Construction of the Lucite plastic test cell is shown in Figure 11. As shown, a $3/4$ inch hole was bored through the central axis and two parallel slots were machined, each at a distance of $1/4$ inch from the center.

For each experiment, two cast iron specimens were mounted parallel in the slots, separated by a distance of $1/2$ inch. Water flow was parallel to the specimen's surface. Holes were drilled and tapped on either side of the cell to connect each specimen with a stainless steel contact screw for potential measurements. Figure 12 shows the primary cell mounted in the test apparatus.

b) Secondary Plate Cell

A second Lucite plastic cell of the same construction as the primary cell was used in six experiments. The secondary cell contained no electrode contact screws, was not used to make polarization measurements and was connected in series with the primary unit when in use.

c) Pipe Cell

Construction of the pipe-cell is shown in Figure 13. The pipe-cell was made of plastic pipe and Tygon tubing to house the assembled split-pipe specimens in such a way as to maintain flow continuity and to allow measurement of pipe-section potential. Two pieces of $3/4$ inch ID plastic pipe were cut into 16 and 4 inch lengths respectively and one end face of each piece was

Figure 11. Primary Plate Test Cell.

Figure 11. Primary Plate Test Cell.

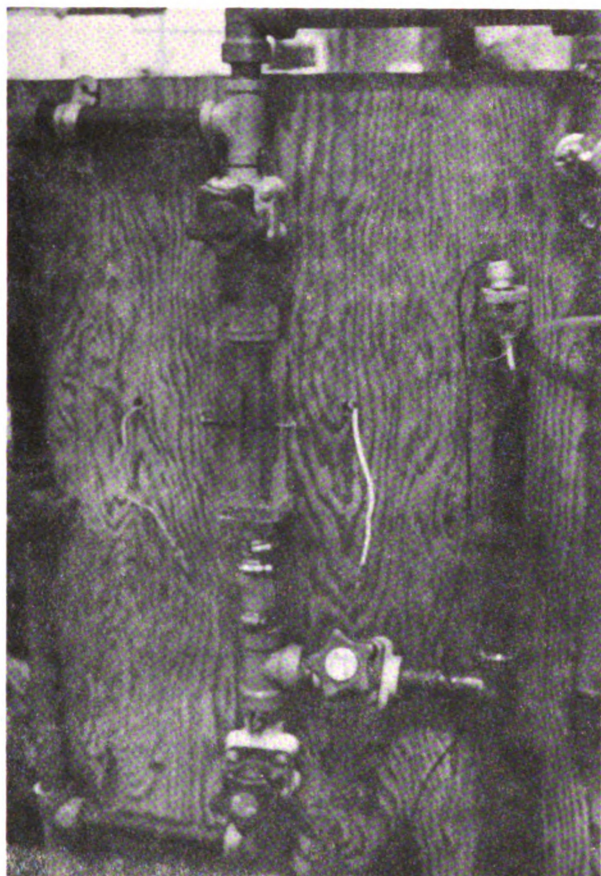
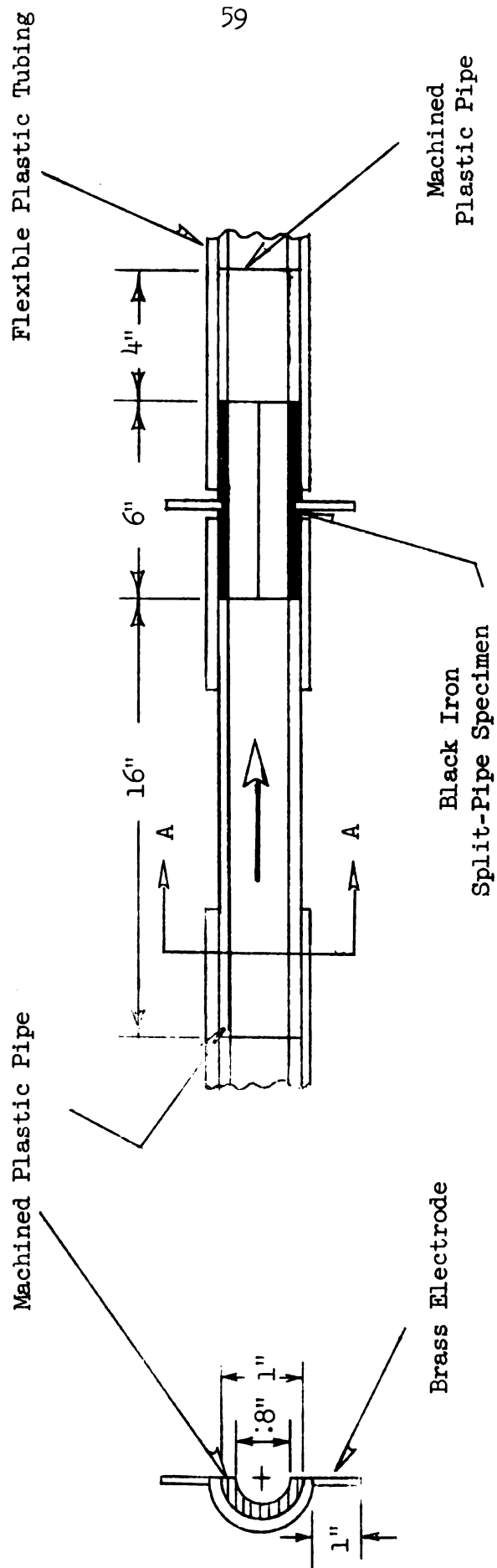


Figure 12. Primary Plate Cell Mounted in Apparatus.



(NTS)

Figure 13. Pipe Cell.

squared with a cutting tool. The pipe was then reamed to 0.815 ID in order to match the pipe-cell diameter. About half of a six inch piece of 1 inch Tygon tubing was slipped over the squared off end of each plastic pipe section. The remaining three inches of Tygon tubing was slid over an end of the assembled pipe specimen.

Joints between the plastic pipe and pipe specimen were made tight by holding them flush together, then binding the Tygon tubing to the pipe sections with hose clamps. A tight flush fit was thus assured between the matched ends of the pipe cell mounted in the test apparatus which is shown in Figure 14.

B. Apparatus for Making Polarization Measurements

The electrical apparatus used in making polarization measurements was assembled as shown in the circuit diagram in Figure 15. One circuit included the direct current power supply,* a General Radio model 1432M resistance box set at 100,000 ohms, a W. M. Welch Scientific Company 0-5 milliammeter, and the terminals of a standard single-pole double throw switch. Connected to the terminals of the switch were two leads with attached alligator clips. During polarization measurements, the clips were fastened to metal screws or rods to contact the anode and cathode specimens, as required.

* Conventional rectifier unit with a maximum output of 400 volts at 2 amps built by the Electrical Engineering Department of Michigan State University.



Figure 14. Pipe Cell Mounted in Apparatus.

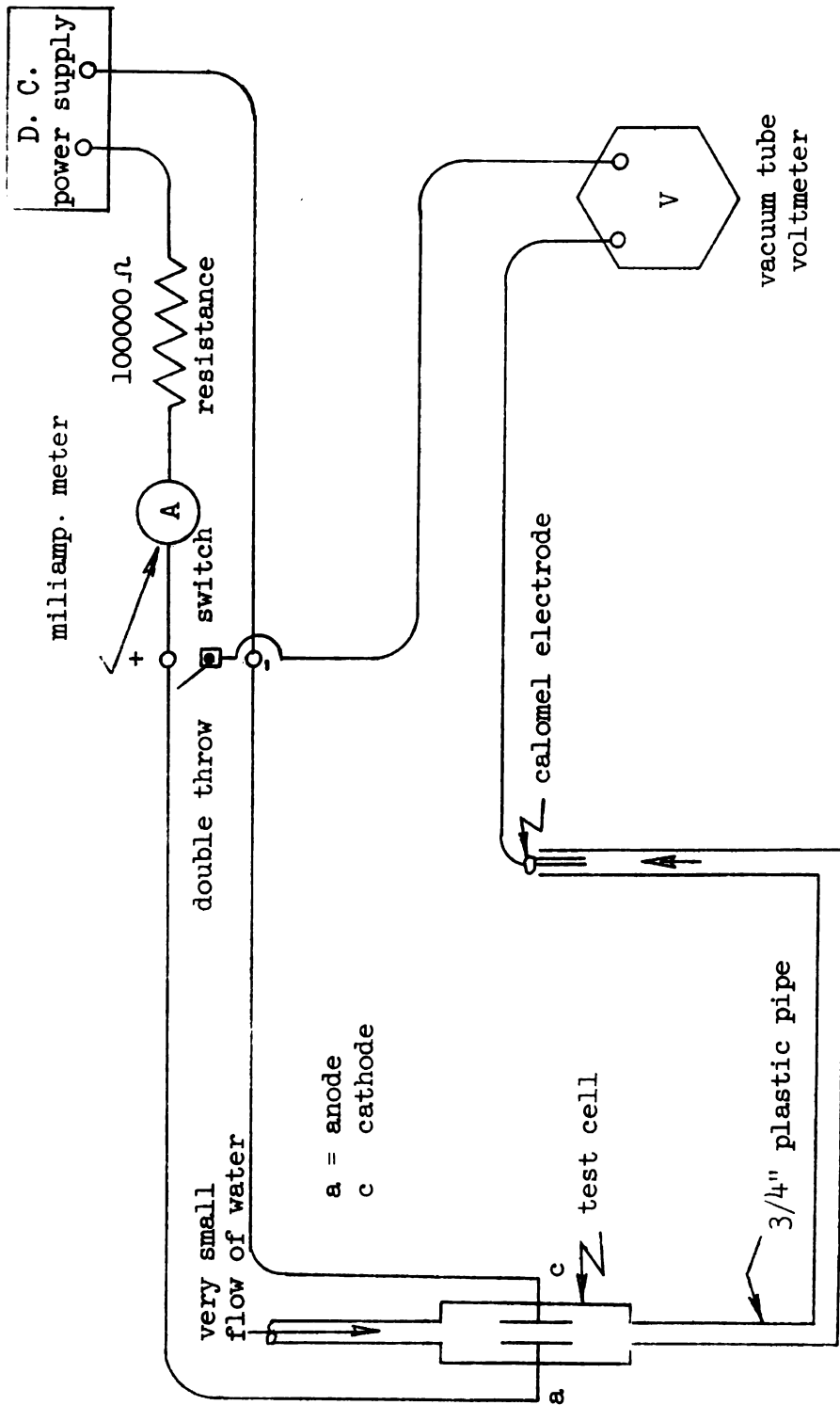


Figure 15. Circuit Diagram of Apparatus for Polarization Measurements.

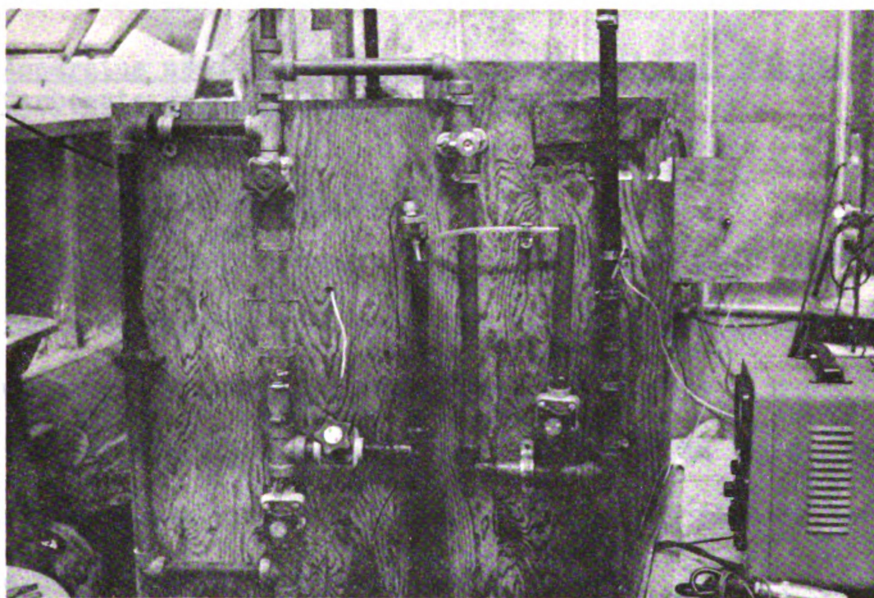


Figure 16. Test Cells Mounted in Apparatus.

The second circuit was connected to the first through a lead to the pole of the double throw switch. This circuit included the following: Hewlett-Packard model 410B vacuum tube voltmeter; a Beckman Instruments, Inc. saturated calomel reference electrode; the anode or cathode specimen (depending on which terminal the double throw switch was closed on) and the water in the cell and connecting calomel electrode standpipe. Figure 16 shows some of the electrical equipment and the test cells as they were set up during most of the testing program.

C. Apparatus used for Evaluating the Quality of Calcium Carbonate Coating on Test Specimens

1. Dynamic Rusting Unit

The apparatus shown in Figure 17 was built in order to provide a controlled flow test for rusting under dynamic conditions. The water box was constructed of 3/4 inch marine plywood fastened together with metal screws and bolts as shown in Figure 18 and made water tight with Pittsburg Plate Glass Company plastic roof cement. All exposed screws were painted with enamel.

Water was admitted to the box through a plastic pipe and floor flange. The box was connected to a 20 foot section of rubber hose and flow through the apparatus was recorded with a conventional 3/4 inch water meter. Tables 3 and 4 in the Data Section show the analysis of the lime softened water used for the test.

The vertical section of the water box was built in such a way as to hold the coated cast iron plates with their longitudinal axes vertical and parallel with a spacing of 3/8 of an inch between plates. Glass plates of the same dimensions as the specimens were

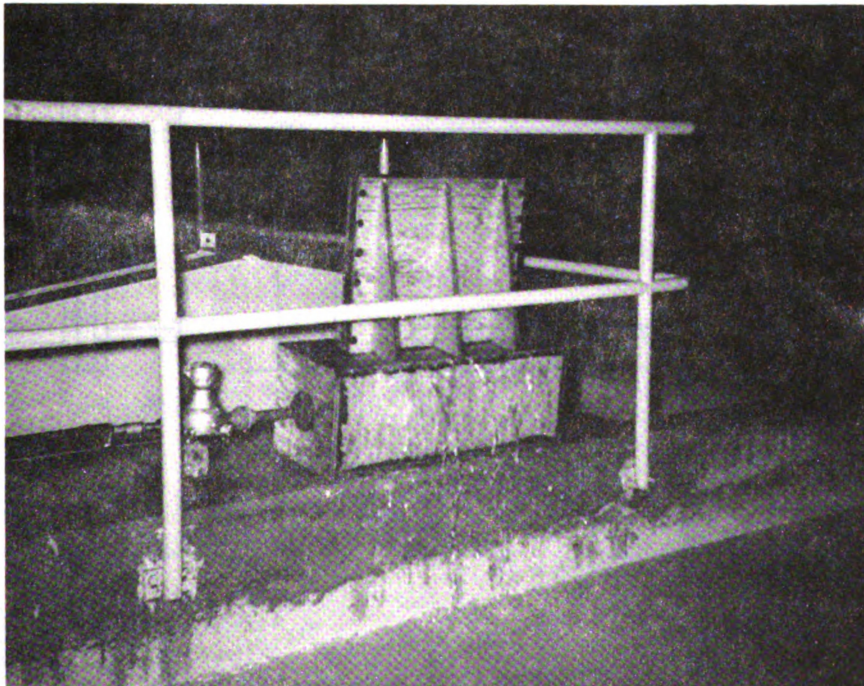
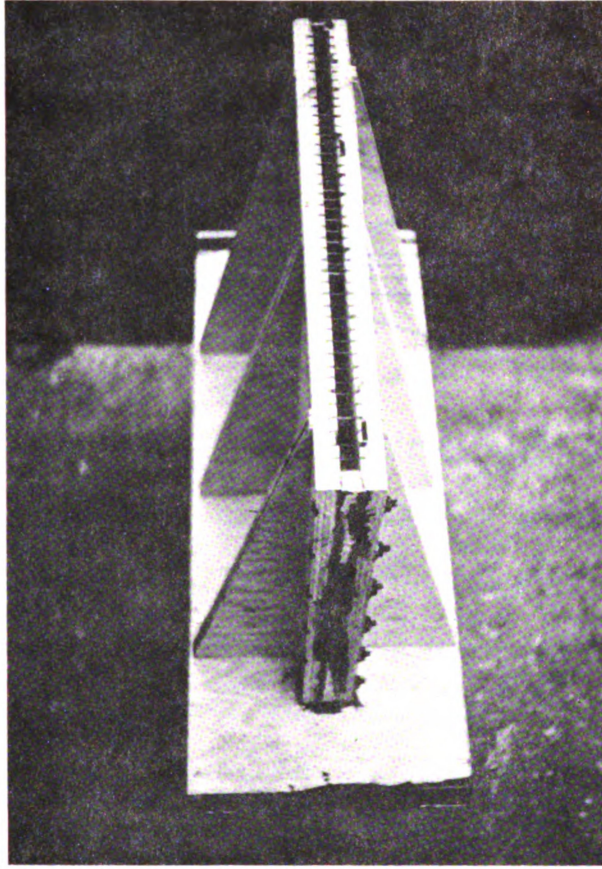


Figure 17. Dynamic Rusting Apparatus.

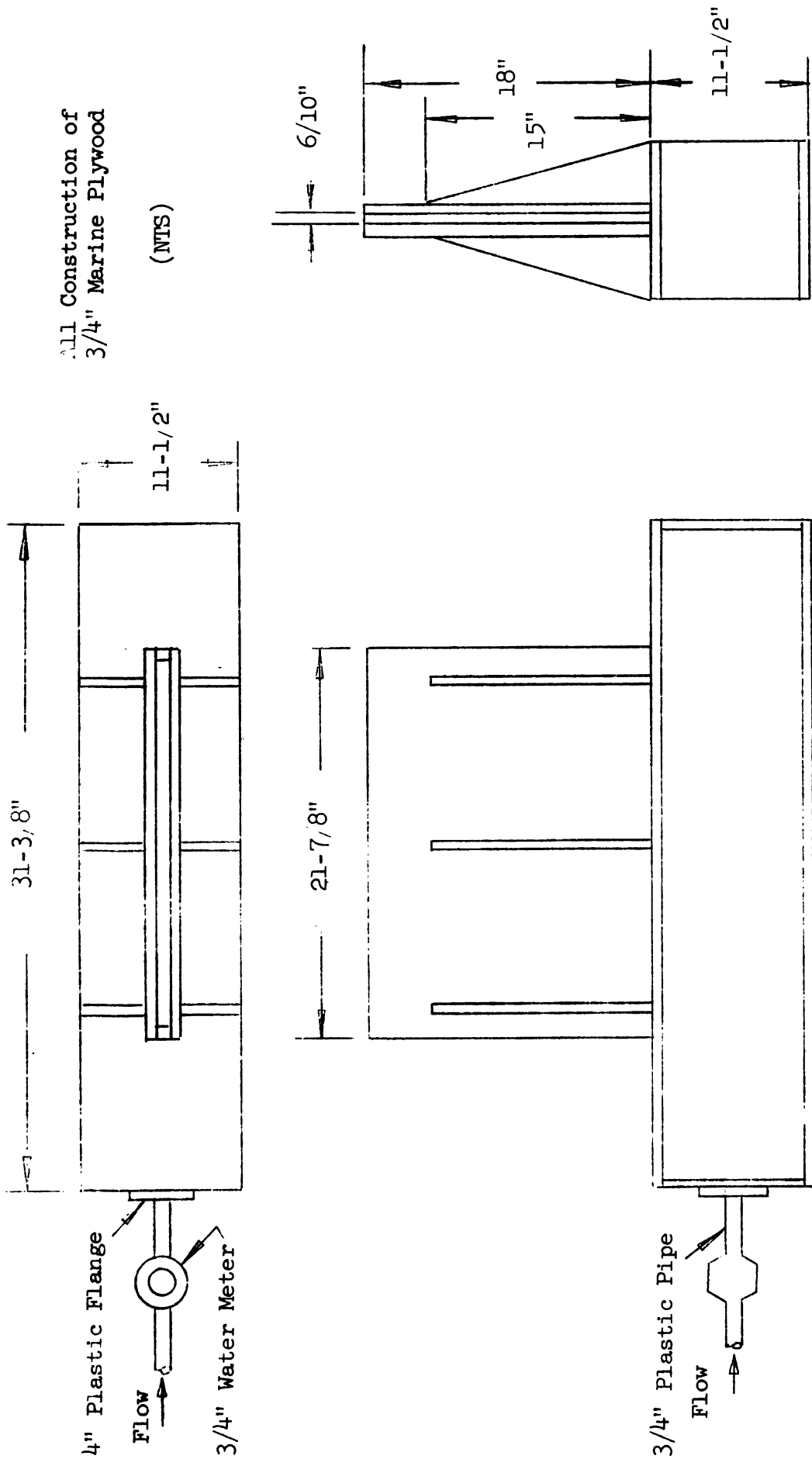


Figure 18. Construction of Dynamic Rusting Apparatus.

placed immediately below the plates in the vertical section of the test apparatus to establish laminar flow. Thus, water was forced at a uniform rate through the stilling box, then through the vertical section and overflowed to waste. In this way, water flowed parallel to the exposed faces of the plates at a constant rate throughout the test.

2. Static Rusting Unit.

Using chemically identical water to that for dynamic tests, coated specimens were tested for ability to withstand corrosion under static conditions. For this study, specimens were placed in twenty-three 260 ml and six 1000 ml glass bottles, such as are shown in Figure 19. Bottles were stored in a dark room at nearly constant temperature. The water was changed daily as described in the Experimental Procedures Section.

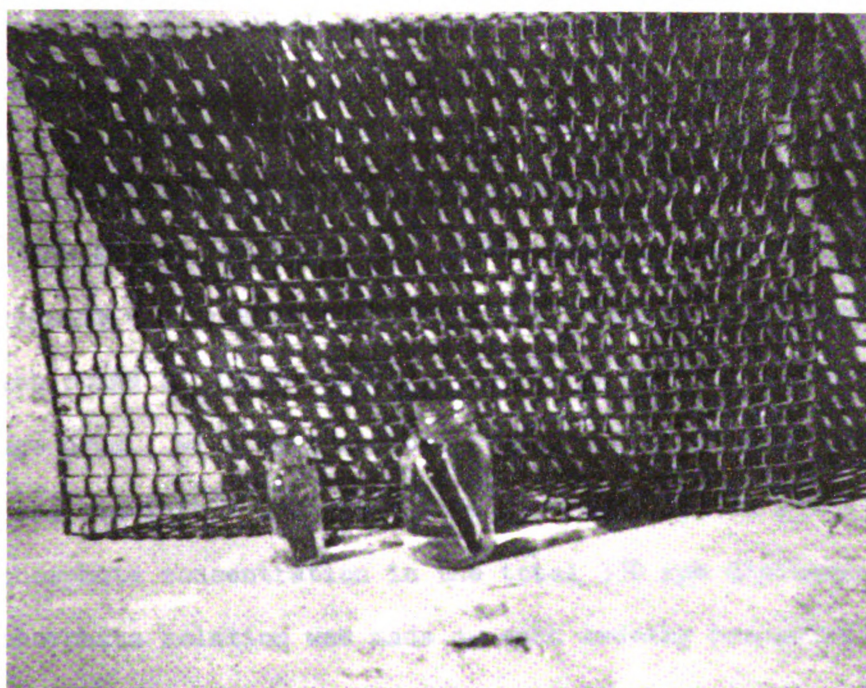


Figure 19. Static Rusting Test.

EXPERIMENTAL PROCEDURE

A. Dynamic Polarization Tests

Water from a Michigan State University deep well was chemically treated and pumped through the experimental apparatus to provide dynamic conditions. Calcium carbonate coatings were developed on cast iron specimens during a two hour test period. Polarization measurements were made at intervals during the coating development.

1. Preparation of Polyphosphate Feed

The glassy polyphosphate* feed solution used in these experiments was prepared by adding 0.012 pounds of the chemical to each pound of water contained in the 54 gallon polyethylene storage drum. With this concentration, a feed rate of 8.7 gph into the six inch** well discharge pipe resulted in a 0.5 mg/l metaphosphate concentration in the total 350 gpm discharge. The polyphosphate solution was made up each evening preceding a test run. During the run, the phosphate solution was continuously mixed by recirculating a large part of the flow passing through the feed pump.

The same phosphate concentration was fed to the well discharge pipe throughout the entire three month experimental

* Calgon, a product of Hagan Laboratories.

** See Appendix A.

period. This continuous feed was necessary to keep the polyphosphate demand of the well discharge pipe satisfied at all times, thus ensuring a constant 0.5 mg/l concentration of polyphosphate in the test water.

Early in the experimental work, it was found necessary to insure complete mixing of the polyphosphate with the test water before adding any additional chemicals. In order to insure the required complete mixing, the phosphate solution was introduced near the discharge outlet of the 350 gpm deep well pump. Intimate mixing then took place as the water passed through an elbow, check valve, and propeller type water meter before reaching the test water outlet point.

2. Preparation of Sodium Hydroxide Feed

Sodium hydroxide solution was made up in varying concentrations for the different test runs. Crystalline sodium hydroxide, commercial grade, was added to thirty gallons of de-ionized water and mixed in a 54 gallon polyethylene drum shortly before each run. During an experiment, the contents of the drum were mixed by returning most of the pumped solution to the storage drum. Only a small portion of the solution was bled off for pH adjustment of the test water.

The pH of the test water was controlled by varying the concentration and the feed rate of sodium hydroxide solution. During a test run, sodium hydroxide passed thru a 0-13 gph rotometer and was forced into the test water line by pressure from the feed pump. The test water then flowed into a five gallon polyethylene pressure-type container where final mixing and stabilization was accomplished.

In all tests sodium hydroxide was fed to the test water only and the larger 350 gpm flow passed from the pump to a reservoir without pH adjustment.

3. Preparation of Iron Specimens

a) Experiments with Flat Plates

Small, 1 x 3 x .09 inch, gray cast iron plates shown in Figure 9 were used as test specimens throughout the experimental program. The plates were cleaned by sand blasting all surfaces. After cleaning, the plates were handled only by the edges and were stored in a desiccator until ready for use.

Preliminary tests were made to determine the effect of leaving all or part of the back side of the plates uncoated and exposed. This testing was accomplished by comparing polarization tests of bare metal plates that had been covered with varying amounts of fingernail polish. From the test it was evident that a very small current did flow from the backs of the bare plates.

The back sides of the test plates were, therefore, coated with protective materials. A black nonelectrolytic paint, EPOXY X - 1365 from the Dearborn Chemical Company was used for five experiments. However, this material proved difficult to dry, hard to apply, and was often sloughed off by the flow of water in the test cell. Therefore, red fingernail polish was adopted for all subsequent experiments. The back side of the plates, except for a small spot where the electrode screw made contact, was coated with fingernail polish and dried shortly before each experiment.

b) Experiments with Pipe Sections

In some experiments, pipe halves were used to make comparisons between calcite coatings deposited on flat and on cylindrical surfaces. For these tests, 3/4 inch black iron pipe nipples were cut longitudinally.

The pipe halves were cleaned by sand blasting, then stored in a desiccator until needed. Pipe halves were electrically insulated from each other in the pipe cell by a thin, 0.03 inch rubber strip. The rubber was fastened with Ply Bond glue and trimmed with shears after drying so that the width of the rubber matched the thickness of the pipe wall, leaving no protrusions on the inside of the pipe.

Experimental runs were then conducted by clamping the pipe sections into their original positions with a jacket of Tygon tubing. A flow condition resulted which was almost identical to that existing in uncut pipe nipples. The two insulated pipe sections served as cathode and anode respectively for the required polarization tests.

4. Test Procedure

With the exception of the last few test runs, all experiments were two hours in length. No more than two runs were made in a single day.

Before starting each run, a chemical analysis of the raw well water was made for determination of calcium hardness, total alkalinity, phosphate (meta and ortho), and pH. The D.C. power supply and vacuum tube voltmeter were then turned on and allowed to warm up.

The sodium hydroxide solution for the test was made up and allowed to mix for at least half an hour before each experiment. The phosphate pump (1) was in continuous operation to maintain a constant polyphosphate feed to the well discharge pipe. Adjustment of the phosphate concentration in the raw well water to exactly 0.5 ppm was accomplished an hour previous to the experiment by adjusting valve (1) (see flow diagram of Figure 20 and Table 1) to increase or decrease the flow from the polyphosphate mix barrel. No further phosphate adjustment was required during a test run.

Previous to starting a test run, valve (5) was opened, valve (4) opened and pump (2) started in order to initiate a sodium hydroxide feed into the test water. Valves (2), (3), (8), and (10) were opened and valves (13), (6), (9), (14), and (11) closed. Water then flowed from the six inch well line through a 0-25 gpm rotometer, was adjusted in pH by addition of NaOH, and discharged to waste.

The sodium hydroxide flow was adjusted to the desired pH level for each test by manipulating valve (5). The small five gallon stabilization drum was initially bypassed during the pH adjustment so that the effect of changes in the NaOH feed could be observed without delay. Once the desired pH range had been achieved, valves (6) and (7) were opened, valve (3) closed, and fine adjustment of valve (5) was made until the pH was at the correct level.

The flow velocity in the test lines could be varied between 1.5 to 8.3 fps by adjusting the position of valve (2). For most tests the velocity over the specimens was seven fps, as previous work (25) had shown the higher velocity produced better quality coatings.

Table 1

Coating Apparatus Appurtenance Identification

A. Phosphate Feed

Feed pump: pump (1)

Flow measurement with 0-13 gph rotometer

Flow control valve: valve (1)

B. Sodium Hydroxide Feed

Feed pump: pump (2)

Flow measurement with 0-13 gph rotometer

Flow control valves: valves (4) and (5) - recirculation and
feed control

valves (3), (6), and (7) - five gallon
stabilization drum
flow control

C. Test Water - Main Stream

Flow measurement with 0-25 gpm rotometer

Flow control valves: valve (2) - flow regulation

valve (8) - pipe cell diversion

D. Test Water - Primary Plate Test Cell

Flow control valves: valves (9), and (11) - test cell shut off

valve (10) - test cell bypass

valve (12) - electrode standpipe flow
control

E. Test Water - Pipe Test Cell

Flow control valves: valves (13), and (14) - test cell shut off

valve (15) - electrode standpipe flow
control

To Reservoir

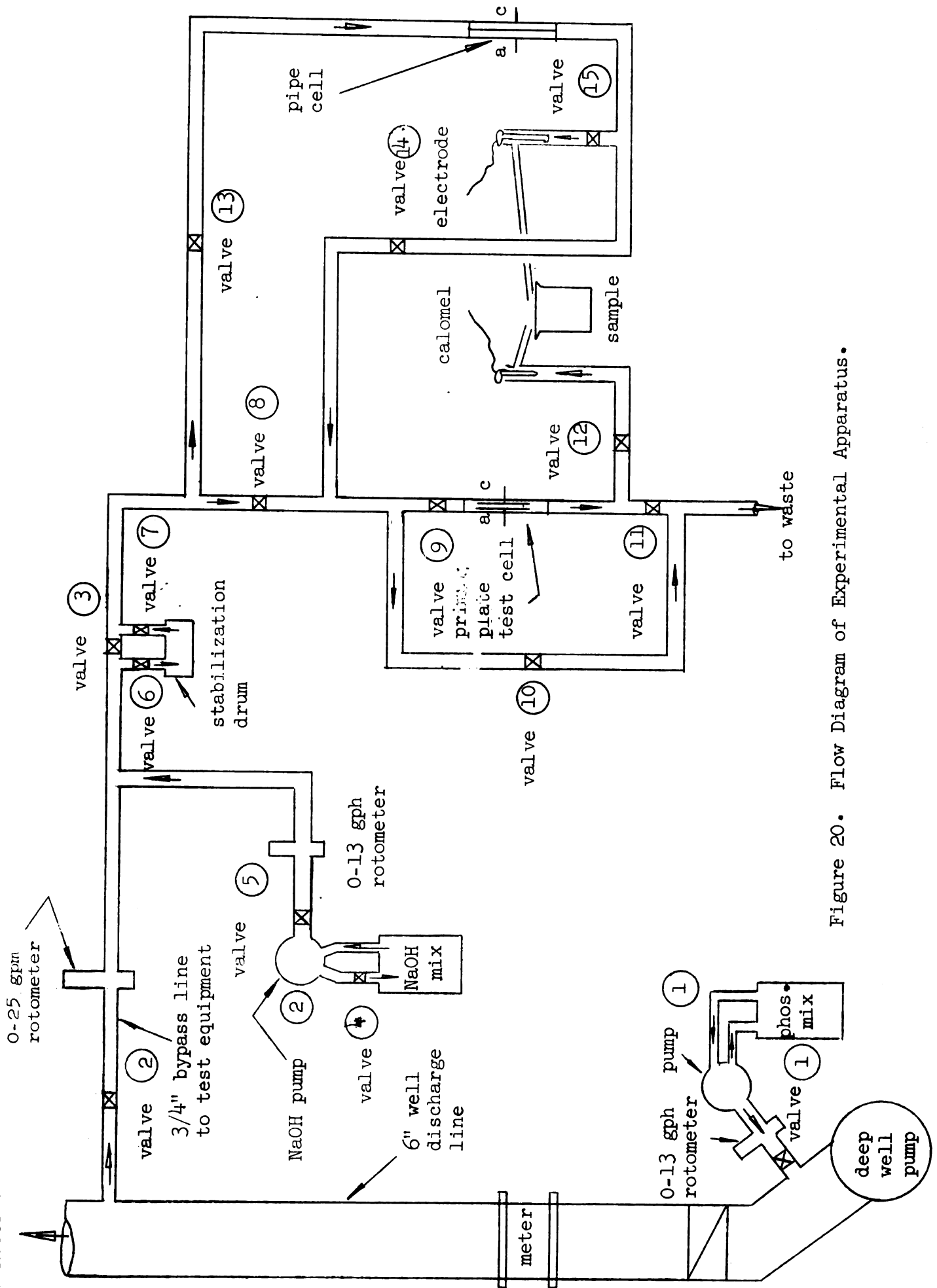


Figure 20. Flow Diagram of Experimental Apparatus.

a) Procedure for a Typical Test Run

At least one day previous to each test, the back sides of the cast iron specimen plates were coated with fingernail polish or other protective material and the plates dried and stored in a desiccator. The plates were removed from the desiccator and placed in the plastic test cell just before beginning the test. When the plates were in place, valve (9) was opened just enough to allow water to fill the test cell and valve (12) was opened until a small overflow was observed in the electrode standpipe. The initial polarization measurements were quickly taken. Valves (9) and (11) were then opened, and valve (10) closed to route the flow through the test cell.

Each half-hour, the flow of water through the test cell was bypassed by opening valve (10). Valves (1) and (9) were closed almost completely, but cracked just enough to keep the test cell and the electrode standpipe full and flowing slightly. The electrode wires were connected to the stainless steel contact screws which held the test plates in the plastic cell with a metal to metal contact. Polarization measurements were quickly made, and the full flow of water returned to the test cell.

The pH and calcium hardness of the water were checked each fifteen minutes and alkalinity was checked every thirty minutes during the test. The phosphate level was checked after an hour of operation and again at the end of the test run. Adjustments in sodium hydroxide flow were made as required to maintain a constant pH value.

On several test runs, a second plastic cell with cast iron plate specimens was placed in the line in series with the primary

cell below valve (11). This cell had no electrical connections and all water passing through it discharged to waste. By placing specimens in both test cells it was possible to determine whether the electric current which was impressed during polarization measurements had any effect on the coating developed in the primary cell.

At the end of each test the sodium hydroxide feed was discontinued by closing valve (5) and the water was shut off by closing valve (2). Specimens were removed from the test cell, dried, and marked with red pencil to identify the cathode, anode and test run number, then stored in a desiccator.

The empty test cells were remounted in the apparatus and all of the piping was cleaned by running muriatic acid through the lines to dissolve deposited calcium carbonate. The equipment was then flushed with clear well water and drained.

b) Tests with the Pipe Test Cell

In tests made with the pipe test cell, the pipe was connected in series with and preceding the primary plate cell. As previously mentioned, the pipe cell duplicated hydraulic conditions in an ordinary 3/4 inch ID cast iron pipe. Therefore, by comparing the coating and the polarization measurements of this cell with those for the plate-cell it was possible to determine whether differences in hydraulic conditions of the two test cells affected coating development.

Use of the pipe-cell required changes in the operating procedure. For these tests, it was necessary that each of the two cells have its own electrode standpipe. The same calomel

electrode was used, however, as a reference for both cells.

Therefore, this procedure was established:

After the desired pH level had been reached, but previous to beginning a run, water was bypassed long enough to permit the prepared pipe-cell to be connected into the piping. Water was admitted to the pipe-cell by cracking valve (13) sufficiently to completely cover the pipe specimens. Valve (15) was opened just enough to maintain a small overflow in the electrode standpipe. Valve (14) was then opened full and valve (8) closed, permitting the water to pass through the pipe-cell and to discharge to waste through the pipe-cell bypass.

The prepared plates were inserted in the primary cell and initial polarization measurements made as described previously. Finally, valves (9) and (11) were opened and valve (10) closed. The water now passed first through the pipe-cell, then through the plate-cell and was discharged to waste.

Polarization measurements were made each half-hour for both cells. The measurements were alternated at fifteen minute intervals between the two test units.

While polarization measurements were being made on the pipe-cell, valve (8) was opened and valve (14) closed. In this way the pipe cell was kept full, the electrode standpipe overflowing, and all of the water running through the plate cell. When measurements were completed on the pipe-cell, valve (14) was opened and valve (8) closed. Polarization measurements on the primary cell required the same operations as when the cell was used alone.

5. Polarization Measurements

Polarization measurements were made at half-hour intervals during all test runs. While measurements were being made, the flow in the test cells was so low as to provide near-static conditions. When these conditions were established, the alligator clips from the direct current power supply were attached to the specimen contact points. Another alligator clip was used to connect the calomel electrode to the vacuum tube voltmeter. The current between the plates was turned up in steps and the potential of the cathode and of the anode relative to the calomel electrode was read for each current density. A double throw switch permitted the vacuum tube voltmeter to be connected to the cathode or to the anode as desired. Figure 15 shows the circuit diagram.

Voltage readings were usually taken at six milliamp intervals; 0.0, 0.3, 0.5, 1.0, 1.5, and 2.0. Additional voltage measurements were made at 3.0 and 4.0 milliamps for a few of the tests.

In the preliminary test it was found that the current impressed during the polarization measurements tended to affect the coating. Therefore, the readings were taken quickly; usually the current was on less than a minute and a half for each of four readings. Thus, during a 2-hour test period, current was impressed for a total time of between 4 and 6 minutes.

It was also observed early in the testing program that the polarization curves showed the calcium carbonate coatings to be a definite cathodic control, making it unnecessary to take anodic measurements.

6. Routine Chemical Water Analysis

As previously discussed, the raw well water from the 350 gpm pump was fed Calgon, a glassy polyphosphate. Sodium hydroxide was fed to the bypass flow of test water only. Determinations for phosphate, total and calcium hardness, total alkalinity, and pH were made on the raw and test water using standard techniques.

The pH was determined using a Beckman Zeromatic Glass Electrode pH Meter. Analysis for ortho and total phosphate, total alkalinity, total hardness and calcium hardness, and total dissolved solids were by methods described in the 10th edition of Standard Methods (41). However, in the latter part of the experimental work, cyclohexendecametetraacetate (CDTA), a product of Hach Chemical Company, Ames, Iowa, was substituted for EDTA in the calcium and total hardness determinations (15).

Determination of hydroxide and carbonate alkalinities was by nomograph as described in the 10th edition of Standard Methods. Some of the analytical apparatus can be seen in Figure 21.

B. Evaluation of the Calcium Carbonate Coatings

A correlation has been made in the Discussion Section between the results of the polarization measurements and the ability of the coating to withstand corrosion. Microscopic examination revealed certain qualities of the coating which were thought to be the controlling factors affecting the ability to resist corrosion. In order to ascertain whether the controlling qualities had been correctly identified, dynamic and static rusting tests were made. The samples selected for testing represented a broad range of quality as determined from microscopic examination and included specimens developed under

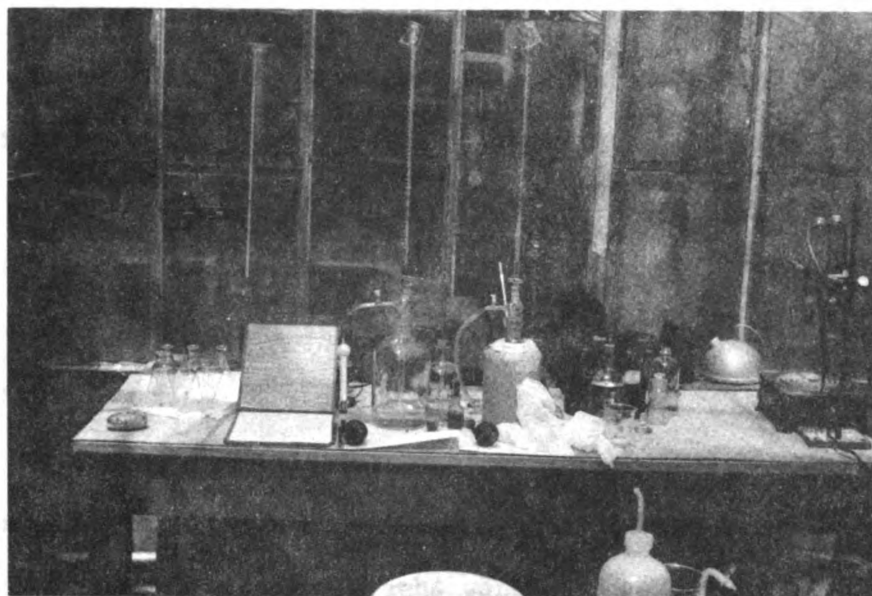


Figure 21. General View of Chemical Analysis Equipment.

various chemical and physical conditions. The rusting tests also served as an indication of how well the coatings stood up under normal flow conditions.

1. Microscopic Examination

After each test run, the specimens were dried with clean cheesecloth, given identifying marks, and stored in a desiccator. Initial microscopic examination was usually made within twenty-four hours after the test run was completed.

A check list as shown in Figure 22 was made up and a card was filled out for each set of specimens. Six items; (1) color of coating, (2) overall quality of coating, (3) amount of rust, (4) grain size, (5) frequency and magnitude of holes in the coating, and (6) structure of the coating were noted for each specimen. All microscopic examination was with a 100 power binocular microscope.

For latter comparison, microphotographs of the coatings were taken of all the cast iron plate specimens subjected to the rusting test. Microphotographs were also made of some of the plates after being subjected to rusting conditions.

2. Dynamic Rusting Test

As an indication of the quality of the coating developed on the specimens, 23 coated cast iron plates were exposed for 17 days to a uniform flow of lime-softened water in the apparatus shown in Figure 17. All uncoated areas on the plates were covered with fingernail polish and dried before the specimens were subjected to this test.

Run No. _____
 Length of Run _____

Date of Run _____
 Date Exam. _____

Plate Mat'l: _____
 CI _____
 Vel. of Flow _____
 M.E. _____

Back Painted: _____
 Mat'l. _____ %
 Alk. _____ pH _____
 DFI _____

COATING Anode = X

Cathode = 0 2nd Cell = 1

1. Color _____

5. Holes:

2. Coating:
 Nil
 Very Poor
 Poor
 Fair
 Good
 Excell.

Nil
 Pin, few
 Pin, some
 Pin, many
 Med.
 Large

3. Rust:
 Nil
 Little
 Moder.
 Consid.
 Complete

6. Type:
 Dense
 Loose
 Glassy
 Sugary
 Thin

4. Grain:
 Fine
 Med.
 Large

Figure 22. Coating Evaluation Check List.

For dynamic testing, the plates were taken to the Lansing water treatment plant where a continuous supply of lime-softened water was available. During the test, the plates were continuously covered with a uniform flow of water. An analysis of the test water is shown in Tables 3 and 4 in the Data Section.

The plates selected for this test represented a cross section in quality ratings as determined from the microscopic examination. In each case the anode plate was used in the dynamic test and the cathode was used in the static test to be described in the next section.

In order to evaluate flow conditions, water was passed through a 3/4 inch water meter before entering the test apparatus. A daily check of the flow in gallons-per-minute and of the total flow to date was made and recorded. Throughout testing, the flow was kept at a constant 12.0 gpm, representing a velocity of 0.419 fps over the plates. For this flow the Reynolds number was 1140.*

At the end of the 17 day period the plates were removed from the test apparatus, dried in an oven at 66° C. for 44 hours, and stored in a desiccator. Examination was then made to evaluate the capacity of the various coatings to withstand corrosion.

3. Static Rusting Test

The cathode of the 23 selected specimens were also exposed for 17 days to lime-softened Lansing water which was chemically identical to that used for testing the cathodes in the dynamic

* See Appendix A.

test. Each plate was immersed in a full 260 ml bottle. All uncoated areas on the plates were covered with fingernail polish and dried before starting the test.

In addition, six coated cathode pipe-halves were also tested by immersion in full 1000 ml bottles. The uncoated areas of the pipe halves were covered with aluminum paint and dried before exposure. As will be noted from Figure 19 the bottles had small throats and were kept filled to minimize atmosphere-liquid interaction. The specimens were completely submerged during the 17 day test.

The water in each bottle was changed once each day by holding a rubber tube connected to a water faucet under the surface and allowing the bottle to overflow at a moderate rate for about twenty seconds. Care was taken not to disturb the specimens. The temperature of the water before and after changing was recorded. The room air temperature was nearly constant at 19° C. Usually, the water temperature had increased from an initial 13 degree level to room temperature at the end of each 24 hour period.

After the specimens were removed from the bottles, they were air dried over a hot plate for 36 hours and stored in a desiccator. Examination of the coatings was then made to evaluate its corrosion resistance.

DATA

A. Remarks on Data Notation

1. Test Number

An * indicates specimens were not subjected to polarization measurements.

2. Chemical Analysis

It is to be remembered that the values given in this section are the average for the test period. The dissolved oxygen in the well water used was about 2 ppm.

3. Equilibrium Constants

Because of the variations inherent in the chemical analysis, the values given in this section should be regarded as ± 5 percent. The values represent the average for the test run and may actually have varied somewhat during the test.

Example calculations are shown in Appendix B.

4. Microscopic Description of the Calcium Carbonate Coating.

a) Color

Description	Notation
Metallic gray	M
Light metallic gray	LM
Green metallic gray	GM
Rust streaked metallic gray	RSM
Tan-gray	TM
Rust-gray	RM
Rust	R

b) Amount of Rust

Description	Notation
Nil	N
Little	L
Moderate	M
Considerable	C
Covered	Cv

c) Type of Holes

Description	Notation
Nil	N
Few pin	FP
Some pin	SP
Many pin	MP
Medium	M
Too thin	TT

The variation in hole size ranging from less than 30μ (pin) to 75μ (large).

d) Description of the Crystal Structure

Description	Notation
Fine, $< 30 \mu$	F
Medium, $30 - 75 \mu$	M
Large, $> 75 \mu$	L
Dense	D
Loose-knit	LK
Glassy	G
Sugary	S
Thin	T

e) General Quality Rating

Description	Notation
Excellent	E
Good	G
Fair	F
Poor	P
Very Poor	VP
Nil Coating	NC

5. Rusting Test Rating

The 23 pairs of plate specimens which were exposed to rusting conditions were compared for ability to resist corrosion. The anode specimens, which were tested dynamically, were rated separately from the cathode samples which were used in the static test. The results of the comparison of specimens was a rating of 1 to 23 showing the relative resistance to corrosion of each individual specimen when compared to the other specimens in the test. The rating 1 represents the best coating or the specimen which corroded the least; and the rating 23 represents the specimen which had the poorest coating, i.e. corroded the most.

6. Results from Polarization Tests

The parameter used was derived in the following way.

$$\Delta Z = (\Delta E)_{cc} - (\Delta E)_{oc}$$

Taken from the cathode polarization curves where cc indicates at 10 ma/dm² applied current density and oc indicates zero applied current density.

Where $\Delta E = EMF_t = MAX - EMF_t = 0$ at the respective current densities.

As an example consider test No. 18.

$$\Delta E_{oc} = EMF_{t=120} - EMF_{t=0} \quad \text{at zero applied current density}$$

$$\Delta E_{oc} = 0.66 - 0.53 = 0.13 \text{ volts}$$

$$\Delta E_{cc} = EMF_{t=120} - EMF_{t=0} \quad \text{at } 10 \text{ ma/dm}^2 \text{ applied current density}$$

$$\Delta E_{cc} = 1.24 - 0.87 = 0.37 \text{ volts}$$

$$\Delta Z = (\Delta E)_{cc} - (\Delta E)_{oc}$$

$$\Delta Z = 0.37 - 0.13 = 0.24 \text{ volts}$$

Table 2
Test Data

	Test No.	1	2	3				
	Specimen	C.I.Plates	C.I.Plates	C.I.Plates				
	Run Time Hrs.	2	2	2				
	Water Vel. fps	8.1	7.6	7.7				
	Water Temp oC	14	14	14				
C H E M I C A L I S	pH	9.36	9.39	9.37				
	Tot. Alk. ppm CaCO ₃	420	416	424				
	Ca ⁺⁺ ppm CaCO ₃	230	228	232				
	CO ₃ ⁼ ppm CaCO ₃	79	80	81				
	T.D. Solids ppm	435	437	433				
	EQUILI- BRIUM CALCUL- LATIONS	k _s ¹ x 10 ¹⁰	125	125	125			
ME ppm CaCO ₃		78	79	80				
DFI		145	146	150				
M D I E O C S F R C O R C S I O C P A T T P I I O N C N G		Anode	Cath.	Anode	Cath.	Anode	Cath.	
	Color	R	M	R	M	RM	M	
	Amount Rust	Cv	N	Cv	L	M	N	
	Type Holes		FP		MP,M	TT	SP,M	
	Desc. of Crystal		FD		FL,ML	LLS	FD	
	General Quality	NC	G	NC	G ⁻	VP	F ⁺	
RUSTING TEST	Test Rating							
POLAR. TESTS	ΔZ	-0.15	-0.16	-0.04				

Table 2 - Cont.

	Test No.	4		4*		5		5*	
	Specimen	C.I.Plates		C.I.Plates		C.I.Plates		C.I.Plates	
	Run Time Hrs.	2		2		1.9		1.9	
	Water Vel. fps	7.7		7.7		7.7		7.7	
C H E N M A I L C Y A S I S	Water Temp oC	14		14		14		14	
	pH	9.39		9.39		9.40		9.40	
	Tot. Alk. ppm CaCO ₃	412		412		417		417	
	Ca ⁺⁺ ppm CaCO ₃	228		228		238		238	
	CO ₃ ⁼ ppm CaCO ₃	81		81		82		82	
	T.D. Solids ppm	433		433		430		430	
EQUILI- BRIUM CALCUL- LATIONS	k _s x 10 ¹⁰	125		125		124		124	
	ME ppm CaCO ₃	80		80		81		81	
	DFI	148		148		157		157	
M D I E O C S F R C O R C S I O C P A O T T P I I I O N C N G		Anode	Cath.		Anode	Cath.			
	Color	RM	M	M	LRM	M	M		
	Amount Rust	L ⁺	L	L	M	L	L		
	Type Holes	MP,L	SP,M	FP, M	SP, M,L	MP,M	SP, M		
	Desc. of Crystal	MLS	FDG	FDG	MD	FL, LL	FD		
	General Quality	P	F ⁺	G	F	F	G ⁻		
RUSTING TEST	Test Rating								
POLAR. TESTS	ΔZ	-0.25				-0.05			

Table 2 - Cont.

	Test No.	6	6*	7	7*		
	Specimen	C.I.Plates	C.I.Plates	C.I.Plates	C.I.Plates		
	Run Time Hrs.	2	2	2	2		
	Water Vel. fps	7.7	7.7	7.5	7.5		
C H E N M A I L C Y A S L I S	Water Temp oC	14	14	14	14		
	pH	9.45	9.45	9.35	9.35		
	Tot. Alk. ppm CaCO ₃	428	428	410	410		
	Ca ⁺⁺ ppm CaCO ₃	230	230	234	234		
	CO ₃ ⁼ ppm CaCO ₃	95	95	74	74		
	T.D. Solids ppm	449	449	427	427		
EQUILI- BRIUM CALCUL- LATIONS	k _s x 10 ¹⁰	126	126	124	124		
	ME ppm CaCO ₃	94	94	73	73		
	DFI	174	174	134	134		
M D I E O C S F R C O R C S I O C P A O T T P I I O N C N G		Anode	Cath.		Anode	Cath.	
	Color	TM	M	M	M	M	M
	Amount Rust	M	L	M	L ⁺	L ⁺	M
	Type Holes	FP,M	FP,M	FP,L	FP	FP	SP
	Desc. of Crystal	MDG	FD	FDG	FD	FD	MLS
	General Quality	F ⁻	G	G	G	G	F ⁺
RUSTING TEST	Test Rating						
POLAR. TESTS	ΔZ	+0.100		+0.21			

Table 2 - Cont.

	Test No.	8		8*		9		9*	
	Specimen	C.I.Plates		C.I.Plates		C.I.Plates		C.I.Plates	
	Run Time Hrs.	2		2		2		2	
	Water Vel. fps	8.0		8.0		7.5		7.5	
C H E M I C A L I S	Water Temp °C	14		14		14		14	
	pH	9.42		9.42		9.40		9.40	
	Tot. Alk. ppm CaCO ₃	419		419		414		414	
	Ca ⁺⁺ ppm CaCO ₃	235		235		225		225	
	CO ₃ ⁼ ppm CaCO ₃	90		90		81		81	
	T.D. Solids ppm	436		436		435		435	
EQUILI- BRIUM CALCUL- ATIONS	k _s x 10 ¹⁰	125		125		125		125	
	ME ppm CaCO ₃	89		89		80		80	
	DFI	169		169		146		146	
M I C R O S C O P I O N C N G		Anode	Cath.		Anode	Cath.			
	Color	M	M	M	M	M	M		
	Amount Rust	L	L ⁺	L	L ⁺	L ⁺	L		
	Type Holes	SP	SP	FP,M	FP,M	FP,M	FP		
	Desc. of Crystal	FDG	FDG	FD	FD,L	FDG	FDG		
	General Quality	G	G	G	G ⁻	G	G ⁺		
RUSTING TEST	Test Rating	16	15						
POLAR. TESTS	ΔZ	+0.22			+0.14				

Table 2 - Cont.

	Test No.	10		11		12		13	
	Specimen	C.I.Plates		C.I.Plates		C.I.Plates		C.I.Plates	
	Run Time Hrs.	2		2		2		2	
	Water Vel. fps	7.5		7.6		7.8		7.6	
C H E M I C A L I S	Water Temp oC	14		14		14		14	
	pH	9.43		9.43		9.42		9.41	
	Tot. Alk. ppm CaCO ₃	426		430		426		421	
	Ca ⁺⁺ ppm CaCO ₃	231		224		227		226	
	CO ₃ ⁼ ppm CaCO ₃	88		93		92		86	
	T.D. Solids ppm	443		451		447		438	
EQUILI- BRIUM CALCUL- LATIONS	k _s x 10 ¹⁰	126		126		120		125	
	ME ppm CaCO ₃	87		92		91		85	
	DFI	162		165		166		156	
M D I E O C S F R C O R C I O C P A T T I O N G		Anode	Cath.	Anode	Cath.	Anode	Cath.	Anode	Cath.
	Color	M	RSM	M	RM	M	RM	M	RM
	Amount Rust	N +	N Z	N	L	L	M ⁻	M	L
	Type Holes	FP	M	FP,M	FP,M	FP,M	MP	SP,M	FP
	Desc. of Crystal	FDG	M- FLS	FDG	ML	FDG	FDG	FDG	FDG
	General Quality	G	F	G	F	G ⁺	G	G	G
RUSTING TEST	Test Rating					8	11	15	12
POLAR. TESTS	ΔZ	+0.16		+0.02		+0.20		+0.17	

Table 2 - Cont.

	Test No.	14		15		16		17	
	Specimen	C.I.Plates		C.I.Plates		C.I.Plates		C.I.Plates	
	Run Time Hrs.	2		2		2		2	
	Water Vel. fps	7.6		7.6		7.6		7.6	
C H E M I C A L I S	Water Temp oC	14		14		14		14	
	pH	9.41		9.52		9.50		9.52	
	Tot. Alk. ppm CaCO ₃	424		431		434		441	
	Ca ⁺⁺ ppm CaCO ₃	226		227		220		244	
	CO ₃ ⁼ ppm CaCO ₃	88		108		106		111	
	T.D. Solids ppm	441		452		457		464	
EQUILI- BRIUM CALCUL- LATIONS	k _s x 10 ¹⁰	125		126		126		127	
	ME ppm CaCO ₃	87		107		105		110	
	DFI	159		195		185		212	
M D I E O C S F R C O R C S I O C P A O T T P I I I O N C N G		Anode	Cath.	Anode	Cath.	Anode	Cath.	Anode	Cath.
	Color	LM	RM	M	M	M	M	M	M
	Amount Rust	M ⁻	M ⁻	L	N	M	M	L ⁻	L
	Type Holes	FP,M	SP, M,L	FP	FP	SP,M	SP,M	FP	SP
	Desc. of Crystal	FDG	FL	FDG	FDG	FDG	FDG	FDG	FDG
	General Quality	F ⁺	F ⁺	G ⁺	E	G	G ⁺	E	G ⁺
RUSTING TEST	Test Rating			14	3	11	8	2	2
POLAR. TESTS	ΔZ	-0.06		+0.14		+0.16		+0.16	

Table 2 - Cont.

	Test No.	18		19		20		21	
	Specimen	C.I.Plates		C.I.Plates		C.I.Plates		C.I.Plates	
	Run Time Hrs.	2		2		2		2	
	Water Vel. fps	7.5		7.5		7.5		7.5	
C H E M I C A L I S	Water Temp oC	14		14		14		14	
	pH	9.60		9.80		9.81		10.19	
	Tot. Alk. ppm CaCO ₃	446		482		478		559	
	Ca ⁺⁺ ppm CaCO ₃	234		221		208		214	
	CO ₃ ⁼ ppm CaCO ₃	128		190		189		340	
	T.D. Solids ppm	463		499		501		574	
EQUILI- BRIUM CALCUL- ATIONS	k _s x 10 ¹⁰	127		129		129		132	
	ME ppm CaCO ₃	127		186		181		213	
	DFI	235		326		305		550	
M I C R O S C O P I C O N G		Anode	Cath.	Anode	Cath.	Anode	Cath.	Anode	Cath.
	Color	M	M	M	RM	M	RM	M	RM
	Amount Rust	L	M	L	L ⁺	L	L	N	L
	Type Holes	FP	MP,M	FP,M	SP, M,L	M,L	MP,M	MP, M,L	MP, M,L
	Desc. of Crystal	FDG	FDG	FDG	F- LDG	F- LDG	F- LDG	MDG	MLS
	General Quality	E ⁻	G	G ⁻	F ⁺	G	G	F ⁺	F
RUSTING TEST	Test Rating	1	1			7	5	12	17
POLAR. TESTS	ΔZ	+0.24		+0.17		+0.16		+0.06	

Table 2 - Cont.

	Test No.	22	23	24	25				
	Specimen	C.I.Plates	C.I.Plates	C.I.Plates	C.I.Plates				
	Run Time Hrs.	2	2	2	2				
	Water Vel. fps	7.6	7.6	7.5	7.5				
C H E M I C A L I S	Water Temp °C	14	14	14	14				
	pH	10.20	10.00	10.00	10.30				
	Tot. Alk. ppm CaCO ₃	558	516 v	495	573				
	Ca ⁺⁺ ppm CaCO ₃	220	214	224	215				
	CO ₃ ⁼ ppm CaCO ₃	340	250	245	375				
	T.D. Solids ppm	579	537	512	578				
EQUILI- BRIUM CALCUL- ATIONS	k _g x 10 ¹⁰	132	130	129	132				
	ME ppm CaCO ₃	219	211	219	214				
	DFI	567	412	425	611				
M I C R O S C O P I C O F C O R R O S I O N G		Anode	Cath.	Anode	Cath.	Anode	Cath.	Anode	Cath.
	Color	M	M	M	RM	M	RM	M	M
	Amount Rust	L	N	N	M ⁻	L	M	L	M
	Type Holes	MP, M.L	FP,M	SP,M	SP, M.L	SP,M	SP,M	SP, M.L	MP, M.L
	Desc. of Crystal	LLS	M- LDG	FDG	M- LDG	FDG	F- MDG	M- LLS	M- LLS
	General Quality	VP	F ⁺	E	G	E	G ⁻	F	F
CRUSTING TEST	Test Rating			3	4				
POLAR. TESTS	ΔZ	+0.06	+0.14	+0.09	+0.09				

Table 2 - Cont.

	Test No.	26	27	28	29				
	Specimen	C.I.Plates	C.I.Plates	C.I.Plates	C.I.Plates				
	Run Time Hrs.	2	2	2	2				
	Water Vel. fps	7.6	7.6	7.7	8.3				
C H E M I C A L I S	Water Temp °C	14	14	14	13				
	pH	10.29	10.41	9.02	9.00				
	Tot. Alk. ppm CaCO ₃	574	591	393	359				
	Ca ⁺⁺ ppm CaCO ₃	235	216	225	231				
	CO ₃ ⁼ ppm CaCO ₃	380	423	37	32				
	T.D. Solids ppm	587	604	410	364				
EQUILI- BRIUM CALCUL- LATIONS	k _g x 10 ¹⁰	132	134	124	125				
	ME ppm CaCO ₃	234	215	36	31				
	DFI	677	681	67	59				
M I C R O S C O P I O N G		Anode	Cath.	Anode	Cath.	Anode	Cath.	Anode	Cath.
	Color	M	M	M	RM	RM	TM	TM	TM
	Amount Rust	N	L	N	L	C	C ⁺	C	C
	Type Holes	MP, M.L	SP,M	MP, ML	MP, M.L				
	Desc. of Crystal	M- LLS	FLS	MLS	LLS				
	General Quality	F ⁺	F ⁺	F	F	NC	NC	NC	NC
RUSTING TEST	Test Rating			13	14	23	23		
POLAR. TESTS	ΔZ	+0.04	+0.05	+0.04	-0.12				

Table 2 - Cont.

	Test No.	30		31		32		33	
	Specimen	C.I.Plates		C.I.Plates		C.I.Plates		C.I.Plates	
	Run Time Hrs.	2		2		2		2	
	Water Vel. fps	8.3		8.0		7.9		1.6	
C H E M I C A L	Water Temp °C	13		13		13		13	
	pH	9.20		9.31		9.42		9.69	
	Tot. Alk. ppm CaCO ₃	402		410		419		413	
	Ca ⁺⁺ ppm CaCO ₃	236		232		232		157	
	CO ₃ ⁼ ppm CaCO ₃	53		68		86		133	
	T.D. Solids ppm	407		415		440		434	
EQUILI- BRIUM CALCUL- ATIONS	kg x 10 ¹⁰	128		128		129		129	
	ME ppm CaCO ₃	52		67		85		132	
	DFI	98		123		155		162	
M I C R O S C O P I O N C N G		Anode	Cath.	Anode	Cath.	Anode	Cath.	Anode	Cath.
	Color	RM	RM	M	TM	M	TM	M	RM
	Amount Rust	C ⁺	C ⁺	TM	C	M	MM	FL ⁺	M ⁺
	Type Holes			TT		MP	MP	TT	TT
	Desc. of Crystal			F		FD ⁺	FD ⁺	FL ⁺	FL
	General Quality	NC	NC	VP	NC	F ⁺	F ⁺	P ⁺	P
RUSTING TEST	Test Rating					18	18		
POLAR. TESTS	ΔZ	-0.11		-0.12		+0.16		+0.08	

Table 2 - Cont.

	Test No.	34		35		36		36		
	Specimen	G.I.Plates		C.I.Plates		C.I.Plates		Pipe Nipple		
	Run Time Hrs.	2		2		2		2		
	Water Vel. fps	2.8		4.5		4.5		5.5		
	Water Temp °C	13		13		13		13		
CHEMICAL ANALYSIS	pH	9.60		9.60		9.40		9.40		
	Tot. Alk. ppm CaCO ₃	386		428		390		390		
	Ca ⁺⁺ ppm CaCO ₃	166		195		194		194		
	CO ₃ ⁼ ppm CaCO ₃	108		119		76		76		
	T.D. Solids ppm	391		433		405		405		
	EQUILIBRIUM CALCULATIONS	k _s x 10 ¹⁰	127		129		128		128	
		ME ppm CaCO ₃	107		118		75		75	
DFI		141		180		115		115		
MICROSCOPIC NOTING		Anode	Cath.	Anode	Cath.	Anode	Cath.	Anode	Cath.	
	Color	TM	RM	GM	GM	RM	RM	RM	RM	
	Amount Rust	M ⁺	M	L	M ⁺	C	C ⁺	C ⁺	C ⁺	
	Type Holes	MP, M.L	MP, M.L	MP, M.L	MP, M.L	MP, M.L	MP, M.L	TT	TT	
	Desc. of Crystal	FL	FLT	F-ML	FLT	FLST	FLST	FLS	F-MLS	
	General Quality	P	P ⁺	F	F ⁻	P	P	VP	VP	
RUSTING TEST	Test Rating	22	22	20	20	21	21			
POLAR. TESTS	ΔZ	+0.02		+0.06		+0.05		0.00		

Table 2 - Cont.

		Test No.	37		37		38		38	
		Specimen	C.I.Plates		Pipe Nipple		C.I.Plates		Pipe Nipple	
		Run Time Hrs.	2		2		2		2	
		Water Vel. fps	7.0		5.5		4.5		3.5	
CHEMICAL ANALYSIS		Water Temp °C	13		13		13		13	
		pH	9.70		9.70		9.70		9.70	
		Tot. Alk. ppm CaCO ₃	456		456		472		472	
		Ca ⁺⁺ ppm CaCO ₃	208		208		206		206	
		CO ₃ ⁼ ppm CaCO ₃	148		148		157		157	
		T.D. Solids ppm	463		463		477		477	
EQUILIBRIUM CALCULATIONS		k _s x 10 ¹⁰	132		132		130		130	
		ME ppm CaCO ₃	147		147		156		156	
		DFI	233		233		249		249	
DESIGN CONDITIONS			Anode	Cath.	Anode	Cath.	Anode	Cath.	Anode	Cath.
		Color	M	M	M	M	LM	LM	M	M
		Amount Rust	L	L	L	L	L ⁻	L ⁻	M	L
		Type Holes	FP	FP	FP,M	FP,M	SP,M	SP,M	SP	SP
		Desc. of Crystal	FDG	FDG	FDG	FDG	FDT	FDT	FD	FD
		General Quality	E	E	G	G	G ⁻	G ⁻	G	G
TESTING TEST	Test Rating					17	16		4**	
OLAR. ESTS	ΔZ	+0.17		+0.09		+0.10		+0.01		

Table 2 - Cont.

	Test No.	39		39		40		40	
	Specimen	C.I.Plates		Pipe Nipple		C.I.Plates		Pipe Nipple	
	Run Time Hrs.	2		2		0.5		0.5	
	Water Vel. fps	3.3		2.6		7.1		5.6	
C H E M I C A L I S	Water Temp °C	13		13		13		13	
	pH	9.70		9.70		9.73		9.73	
	Tot. Alk. ppm CaCO ₃	470		470		471		471	
	Ca ⁺⁺ ppm CaCO ₃	203		203		207		207	
	CO ₃ ⁼ ppm CaCO ₃	155		155		161		161	
	T.D. Solids ppm	470		470		480		480	
EQUILI- BRIUM CALCUL- ATIONS	k _s x 10 ¹⁰	130		130		130		130	
	ME ppm CaCO ₃	152		152		158		158	
	DFI	242		242		250		250	
M I C R O S C O P I O N G		Anode	Cath.	Anode	Cath.	Anode	Cath.	Anode	Cath.
	Color	M	M	M	M	M	M	M	M
	Amount Rust	L	L	M	M	L ⁻	M	L	L
	Type Holes	FP,M	MP,M	MP,M	MP,M	M	M		
	Desc. of Crystal	FD	FD	FL	FD	FDT	FDT	FD	FD
	General Quality	G ⁻	F ⁺	F	F	G	G ⁻	G	G
RUSTING TEST	Test Rating					10	13		1**
POLAR. TESTS	ΔZ	+0.28		+0.06		+0.08		+0.04	

** Static rusting test rating on the basis of comparison between 6 pipe specimen made in the same manner as the plate specimen ratings.

Table 2 - Cont.

	Test No.	41		41		42		42	
	Specimen	C.I.Plates		Pipe Nipple		C.I.Plates		Pipe Nipple	
	Run Time Hrs.	1.0		1.0		1.5		1.5	
	Water Vel. fps	7.1		5.6		7.1		5.6	
C H E M I C A L I S	Water Temp °C	13		13		13		13	
	pH	9.66		9.66		9.71		9.71	
	Tot. Alk. ppm CaCO ₃	447		447		485		485	
	Ca ⁺⁺ ppm CaCO ₃	210		210		219		219	
	CO ₃ ⁼ ppm CaCO ₃	139		139		164		164	
	T.D. Solids ppm	454		454		490		490	
EQUILI- BRIUM CALCUL- LATIONS	k _s x 10 ¹⁰	129		129		131		131	
	ME ppm CaCO ₃	137		137		162		162	
	DFI	226		226		274		274	
M I C R O S C O P I O N C N G		Anode	Cath.	Anode	Cath.	Anode	Cath.	Anode	Cath.
	Color	M	M	M	M	M	M	M	M
	Amount Rust	L	L	L	M	L ⁻	L ⁻	L	L
	Type Holes	SP,M	SP,M			FP, M,L	SP, M,L	FP	FP
	Desc. of Crystal	FDG	FD	FD	FD	FDG	FDG	FDG	FDG
	General Quality	G	G	G ⁻	F ⁺	G ⁺	G	E	E
RUSTING TEST	Test Rating	5	9		3**	9	10		
POLAR. TESTS	ΔZ	+0.11		+0.02		+0.11		+0.07	

Table 2 - Cont.

	Test No.	43		43		44		44	
	Specimen	C.I. Plates		Pipe Nipple		C.I. Plates		Pipe Nipple	
	Run Time Hrs.	2.5		2.5		0.5		0.5	
	Water Vel. fps	7.1		5.6		7.1		5.6	
C H E M I C A L I S	Water Temp °C	13		13		13		13	
	pH	9.71		9.71		9.70		9.70	
	Tot. Alk. ppm CaCO_3	480		480		447		447	
	Ca^{++} ppm CaCO_3	210		210		216		216	
	$\text{CO}_3^{=}$ ppm CaCO_3	164		164		149		149	
	T.D. Solids ppm	485		485		452		452	
EQUILI- BRIUM CALCUL- ATIONS	$k_s \times 10^{10}$	131		131		129		129	
	ME ppm CaCO_3	161		161		147		147	
	DFI	262		262		249		249	
M D I C R O S I O C P A T T I O N G		Anode	Cath.	Anode	Cath.	Anode	Cath.	Anode	Cath.
	Color	M	M	M	RM	LM	LM	M	M
	Amount Rust	L ⁻	L ⁻	L	L ⁺	M ⁻	M ⁻	M	M
	Type Holes	FP,M	FP,M	M	M	TT	TT	TT	TT
	Desc. of Crystal	FDG	FDG	FDG	FD	FT	FT	FT	FT
	General Quality	E ⁻	E	G ⁺	G ⁻	F	F	F	F
RUSTING TEST	Test Rating	6	7		2**	19	19		6**
POLAR. TESTS	ΔZ	+0.18		+0.03		+0.08		+0.01	

Table 2 - Cont.

	Test No.	45		45			
	Specimen	C.I. Plates		Pipe Nipples			
	Run Time Hrs.	1.0		1.0			
	Water Vel. fps	7.1		5.6			
C H E M I C A L I S	Water Temp °C	13		13			
	pH	9.70		9.70			
	Tot. Alk. ppm CaCO ₃	457		457			
	Ca ⁺⁺ ppm CaCO ₃	210		210			
	CO ₃ ⁼ ppm CaCO ₃	149		149			
	T.D. Solids ppm	462		462			
EQUILI- BRIUM CALCUL- LATIONS	k _s x 10 ¹⁰	129		129			
	ME ppm CaCO ₃	147		147			
	DFI	242		242			
M D I E C S R C O R S I C P O T P I I O C N		Anode	Cath.	Anode	Cath.		
	Color	M	M	M	M		
	Amount Rust	L	L	L	L ⁺		
	Type Holes	FP,M	SP,M	TT	TT		
	Desc. of Crystal	FD	FD	FDT	FT		
	General Quality	G	G	G	G ⁻		
RUSTING TEST	Test Rating	4	6		5 ^{**}		
POLAR. TESTS	ΔZ	+0.23		+0.03			

B. Remarks on Polarization Curve Notation

1. For the sake of completeness and to provide an example, a few polarization curves have been included that are erratic in nature and of otherwise doubtful value. Further elaboration on these tests will be found in the Discussion of Results.
2. After cathodic polarization was shown to be the primary phenomenon, measurement of the anode polarization was no longer made.
3. For clarity only the 0, 60 and 120 minute polarization curves were drawn for most of the tests leaving out the 30 and 90 minute measurements. However when the tests were of shorter duration or irregular polarization took place, the appropriate time curves are shown to indicate these conditions.
4. The following notation was used to designate the polarization curves obtained at different time intervals:

Time	Symbol
0	○
30	●
60	◇
90	◆
120	◊
150	◈

5. The specimen number is located in a small circle in the upper left hand corner of each set of polarization curves.

6. The notation and effect of deleting the 30 and 90 minute polarization curves can be seen by comparing Figure 23 which shows all the polarization curves for specimen 18 with the reduce set of curves shown in Figure 24 (p. 114).

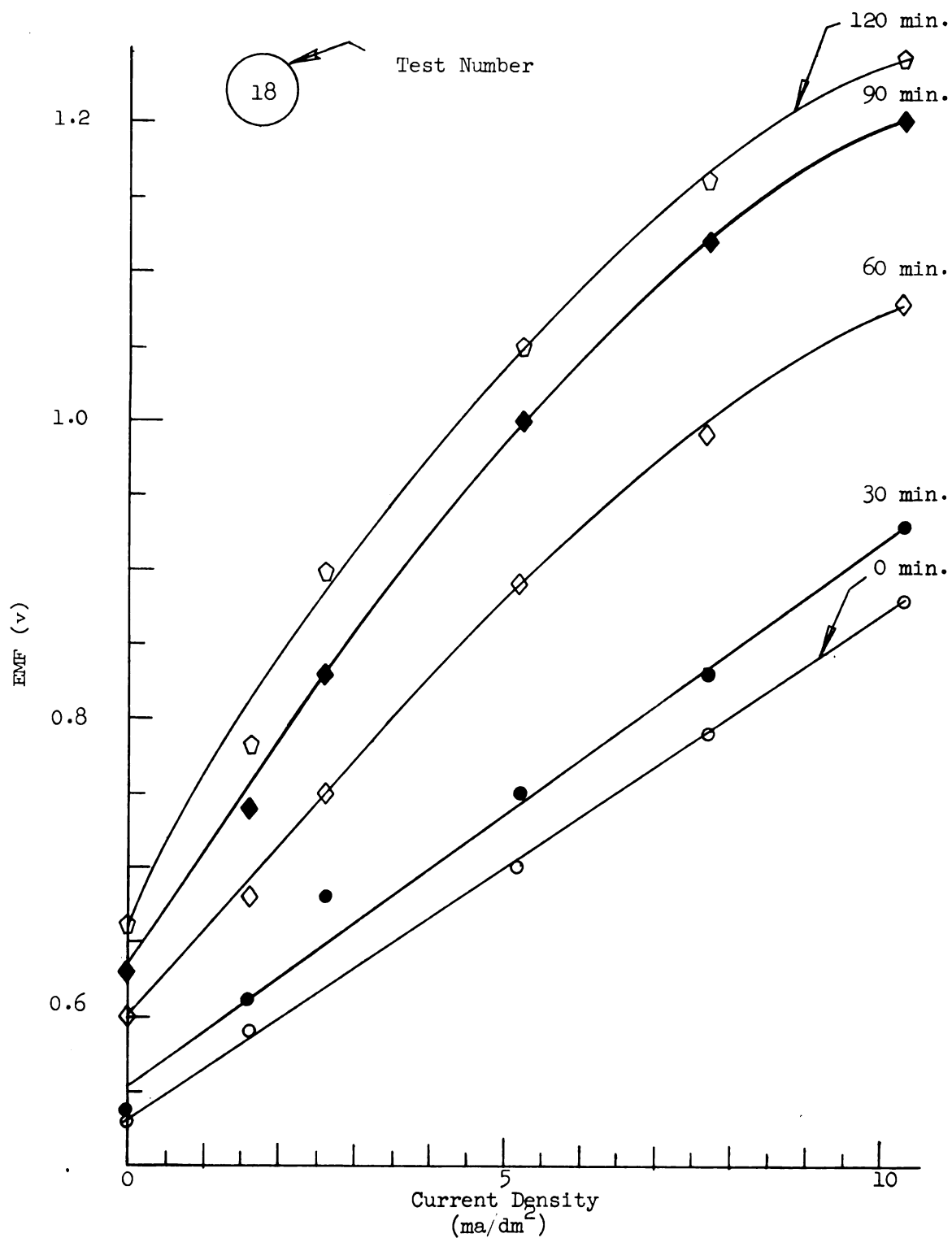


Figure 23. Illustration of Polarization Curve Notation.

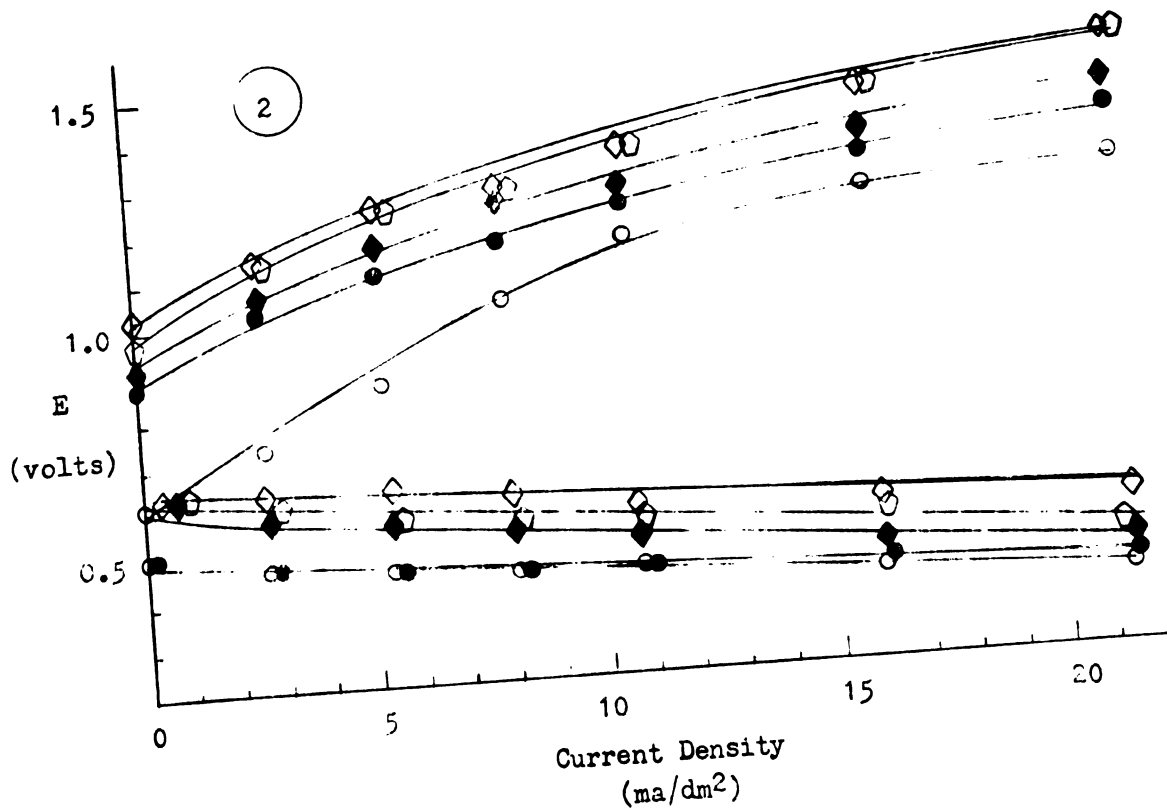
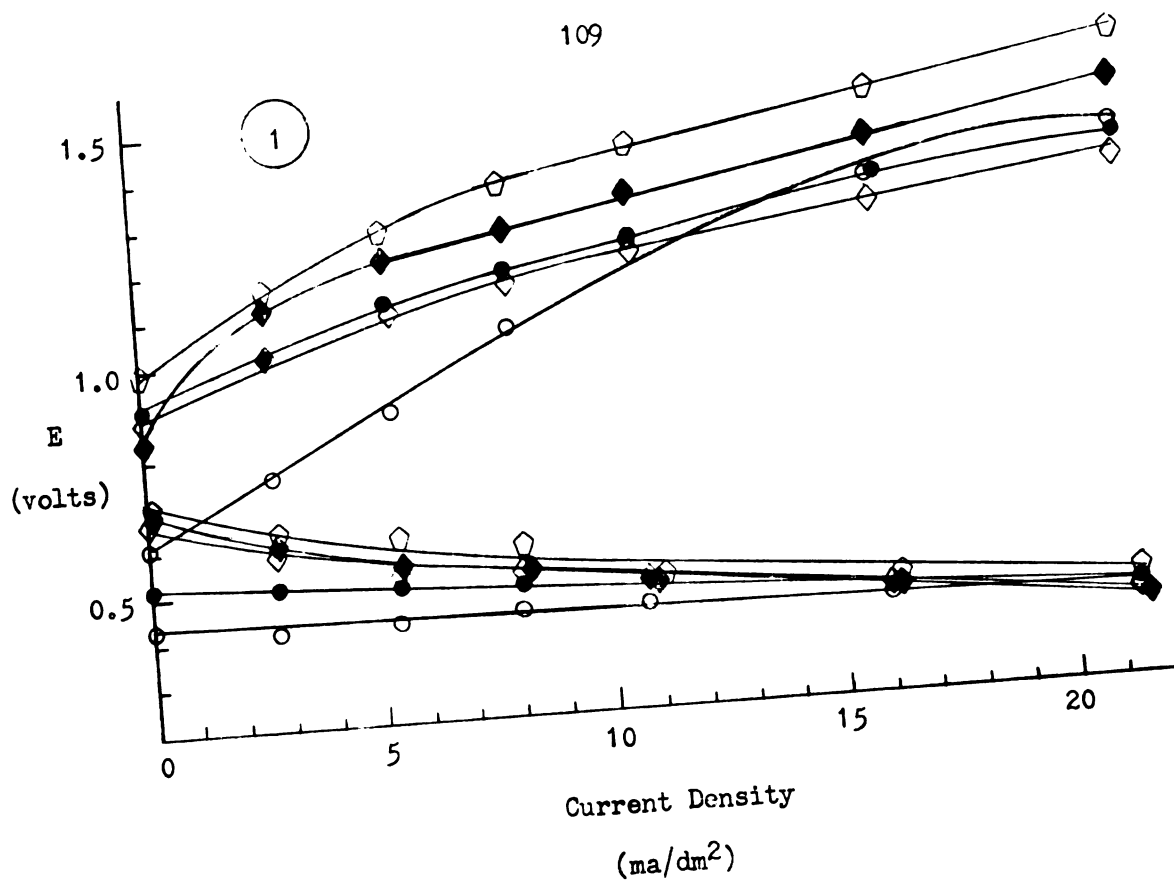


Figure 24. Polarization Curves.

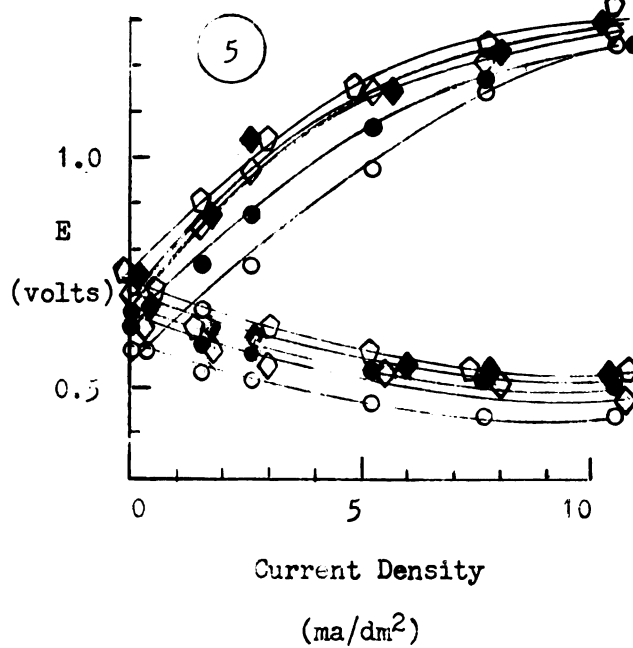
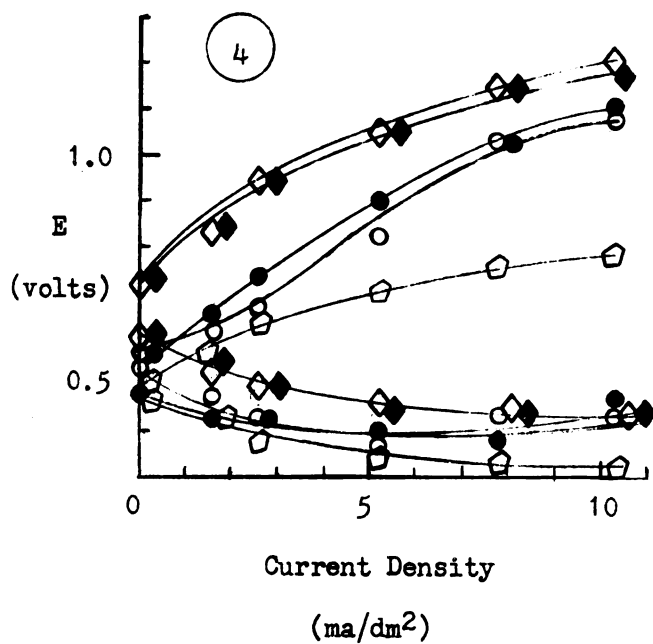
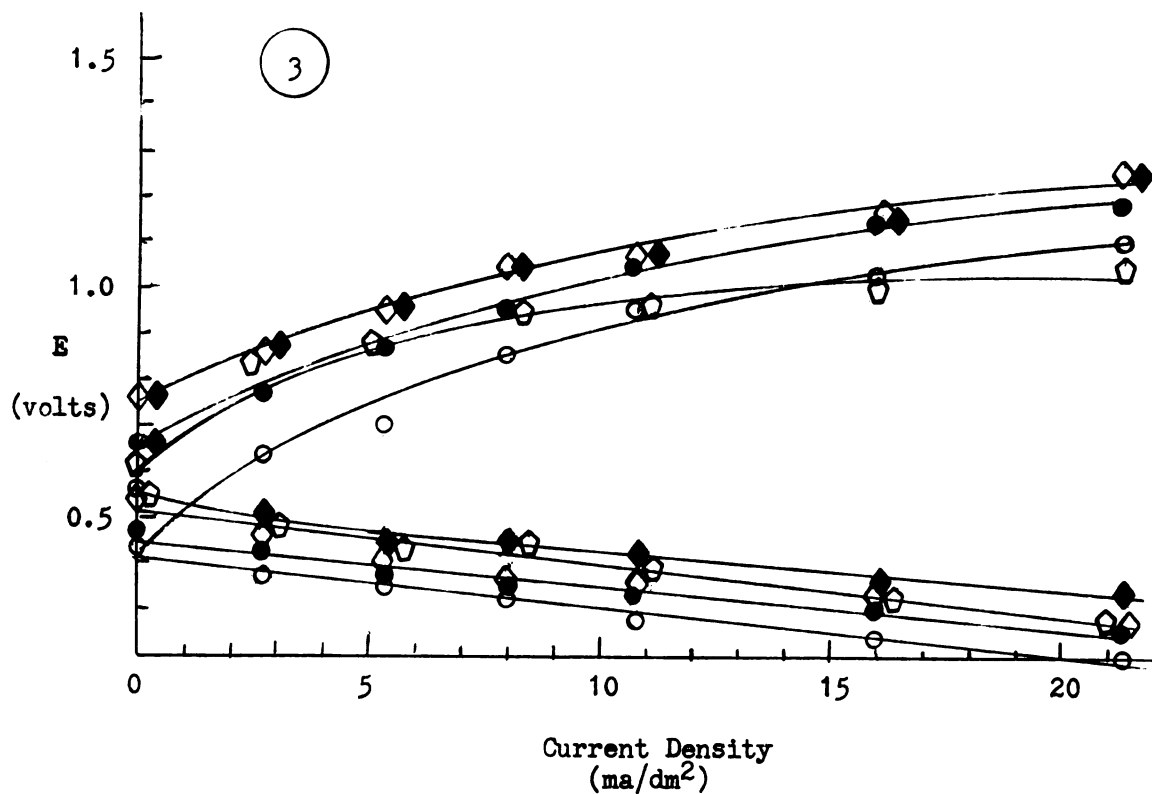


Figure 24 - Cont.

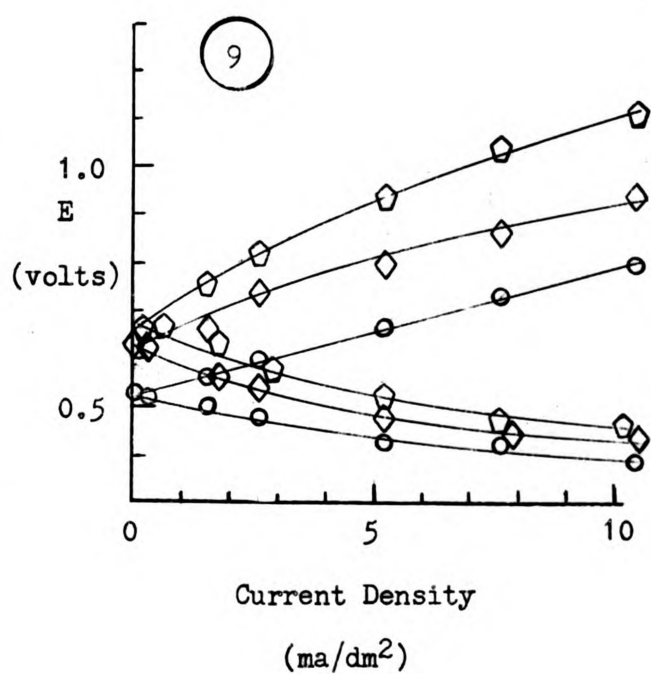
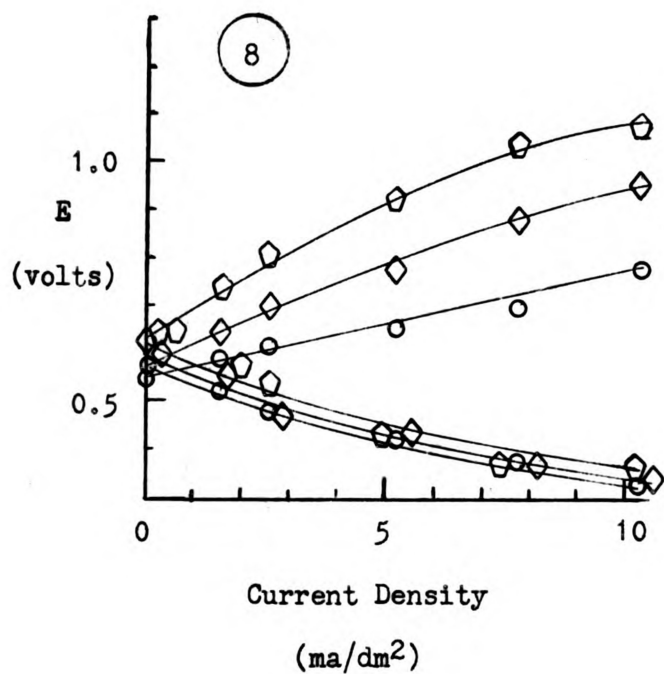
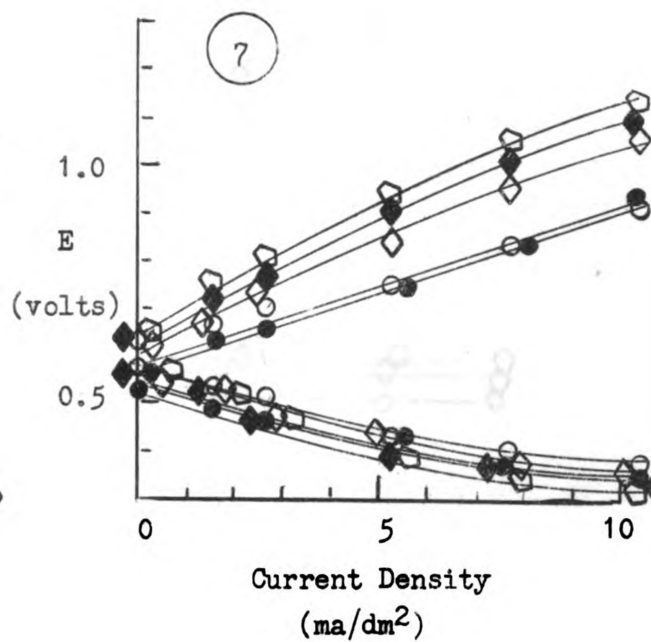
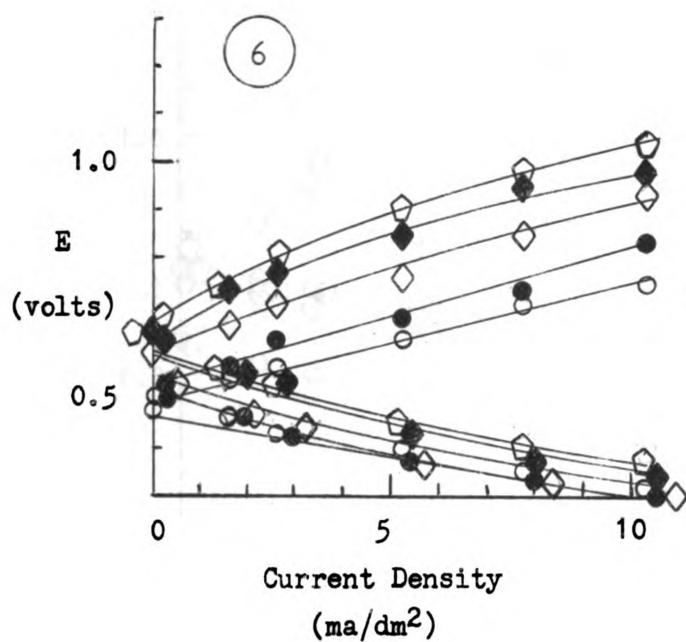


Figure 24 - Cont.

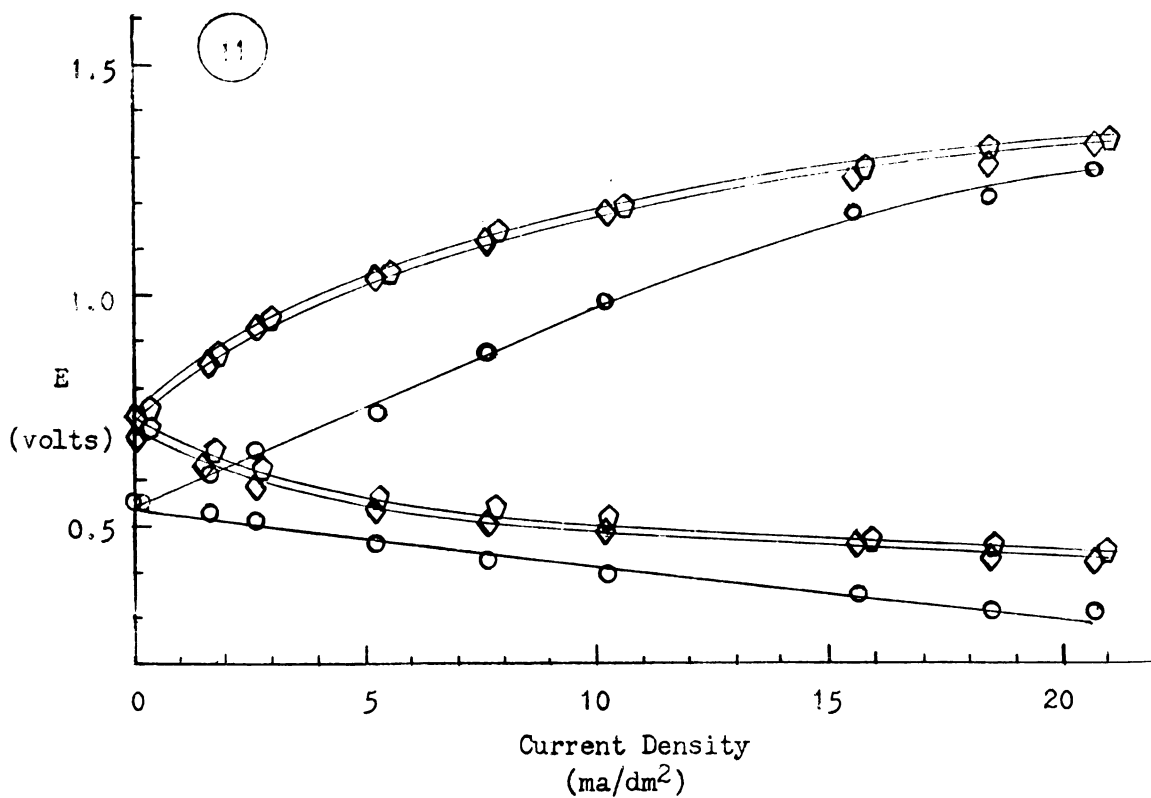
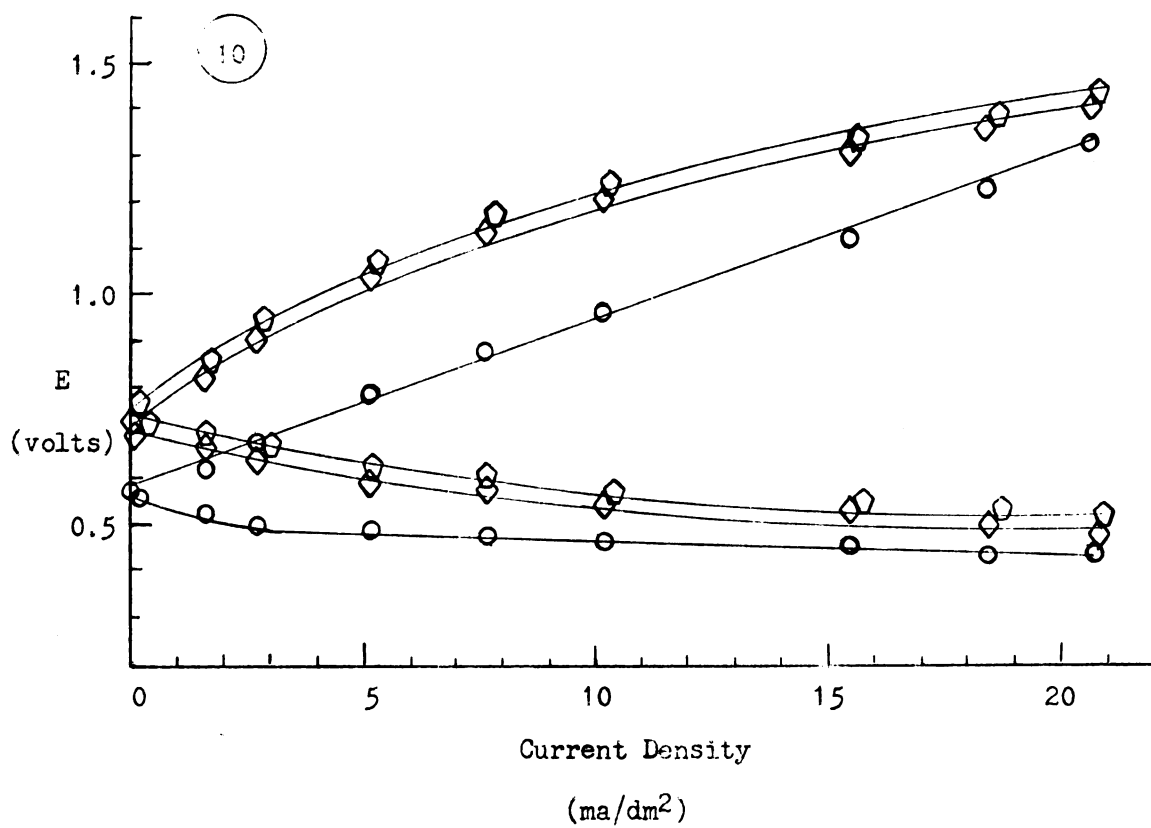


Figure 24 - Cont.

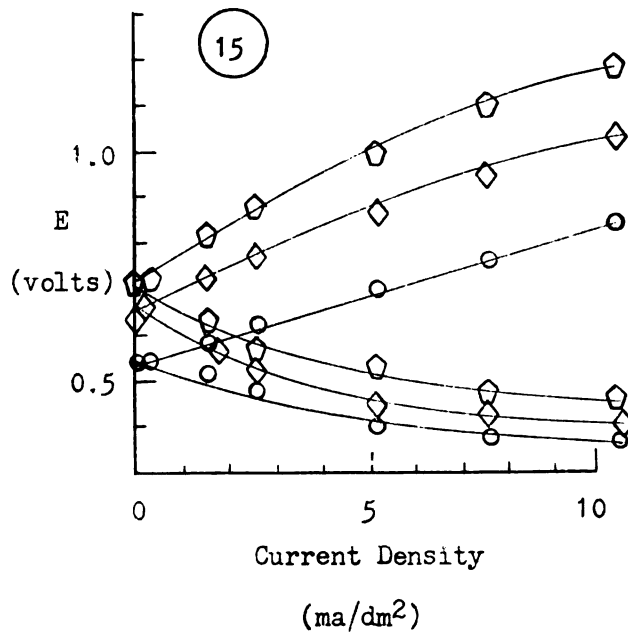
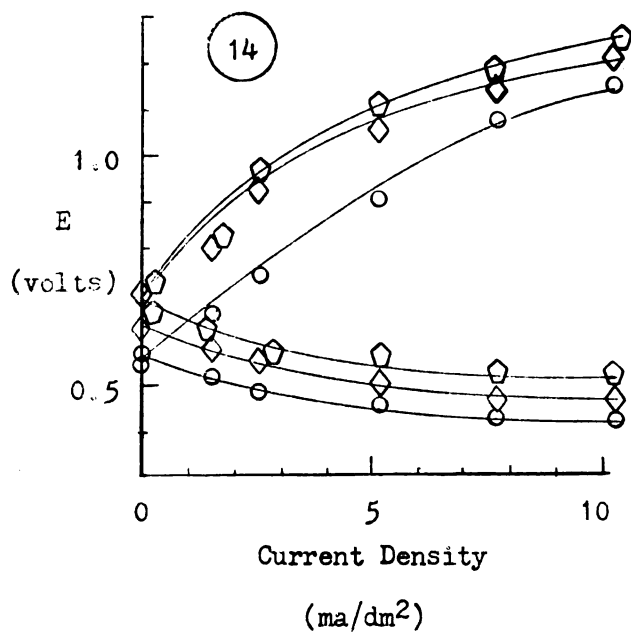
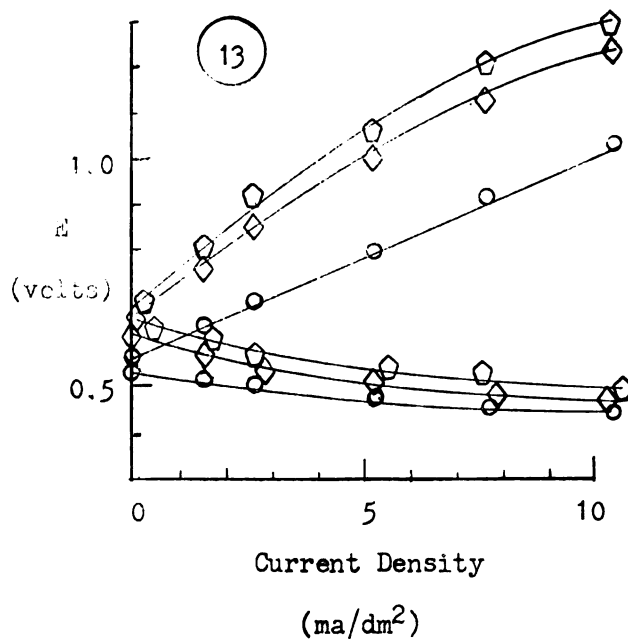
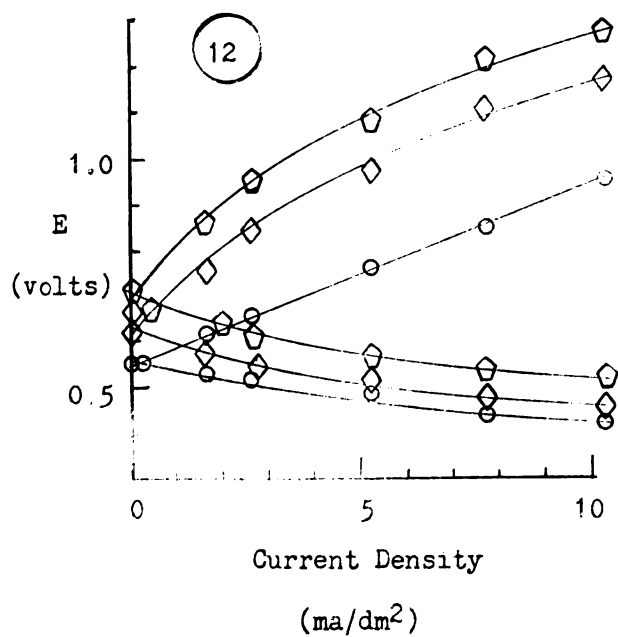


Figure 24 - Cont.

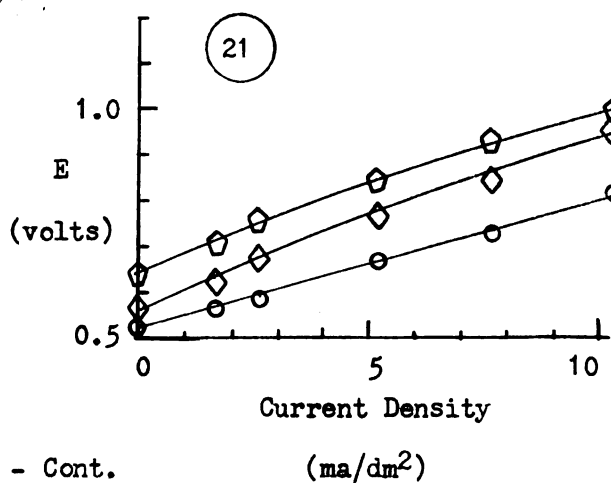
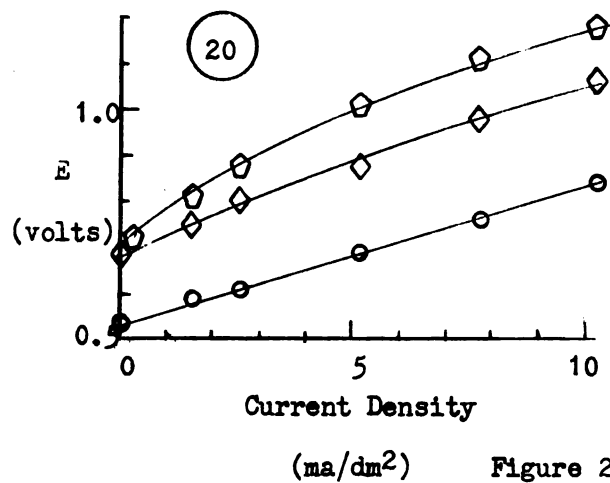
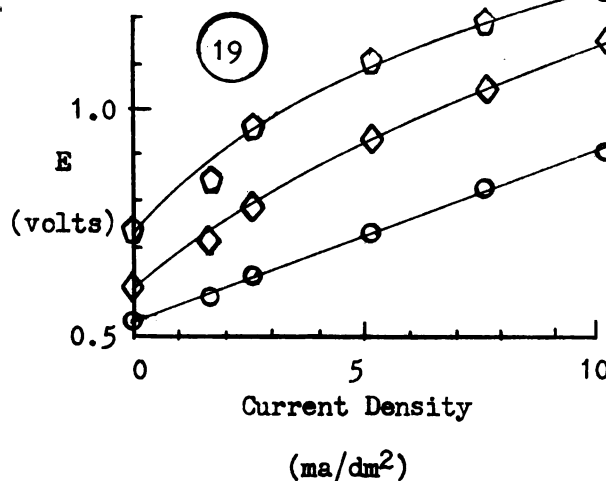
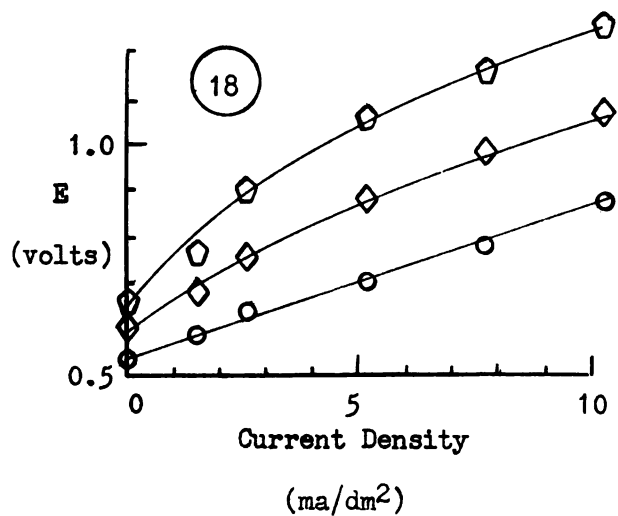
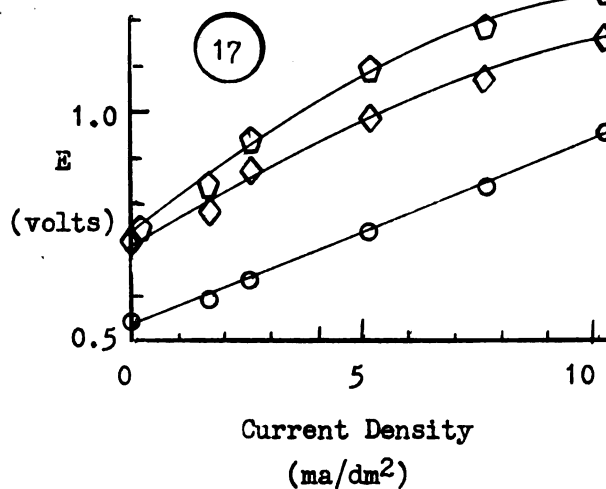
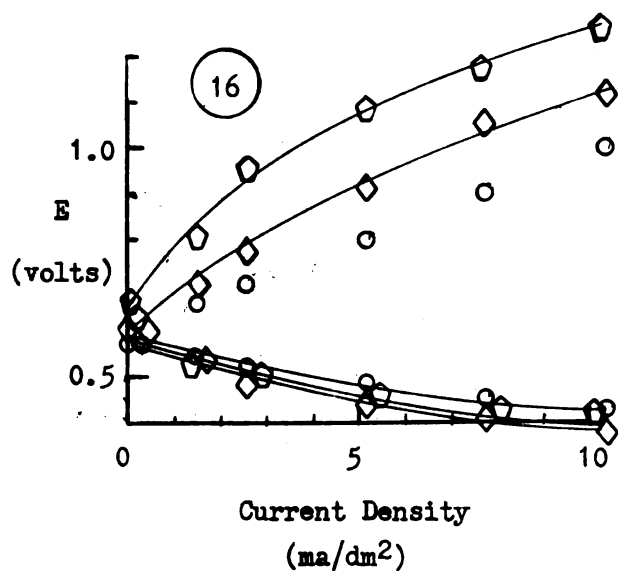


Figure 24 - Cont.

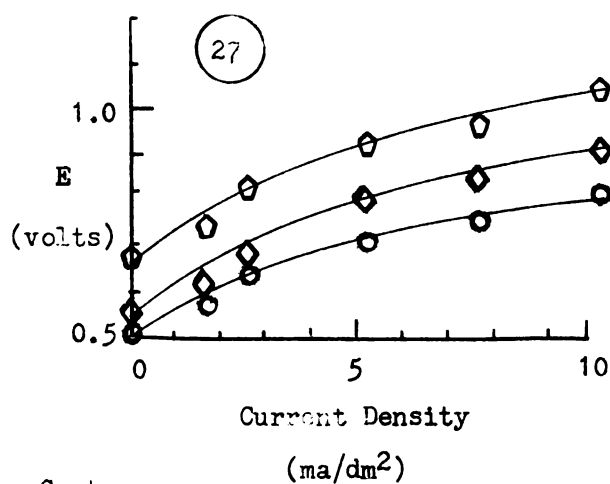
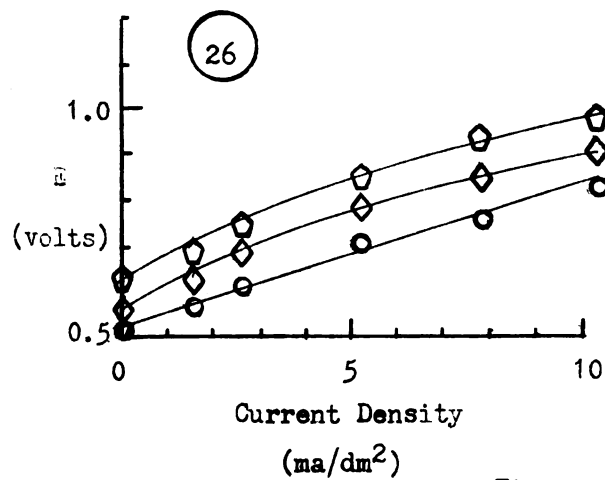
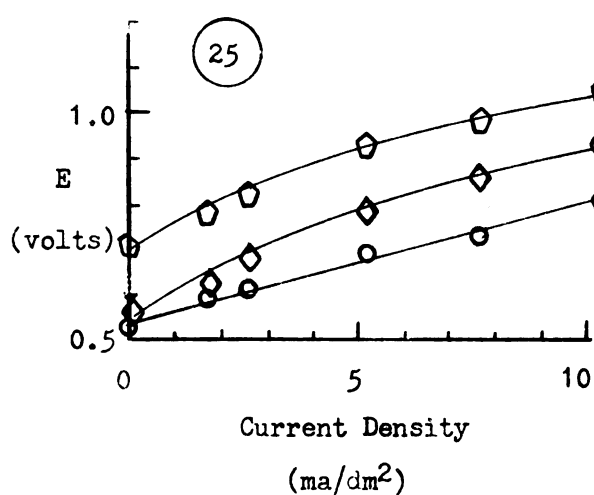
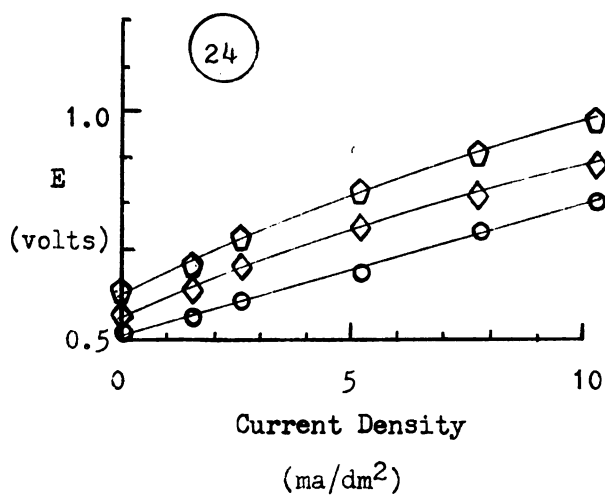
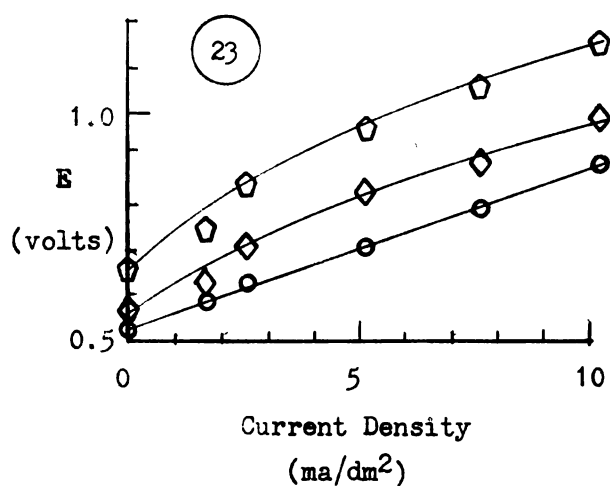
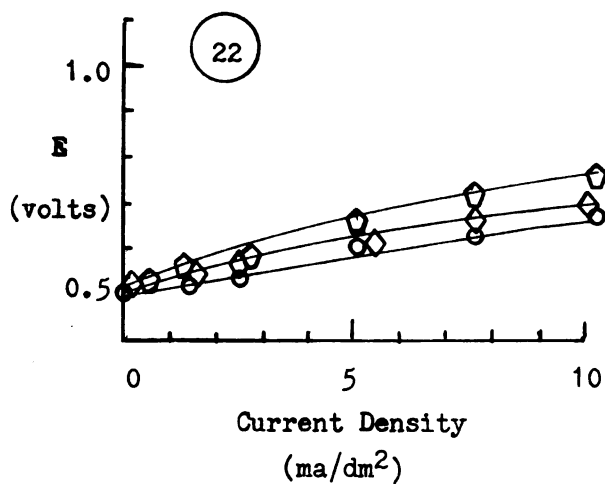


Figure 24 - Cont.

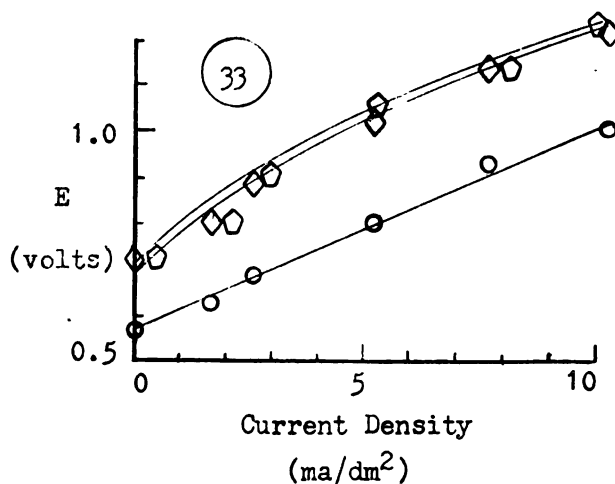
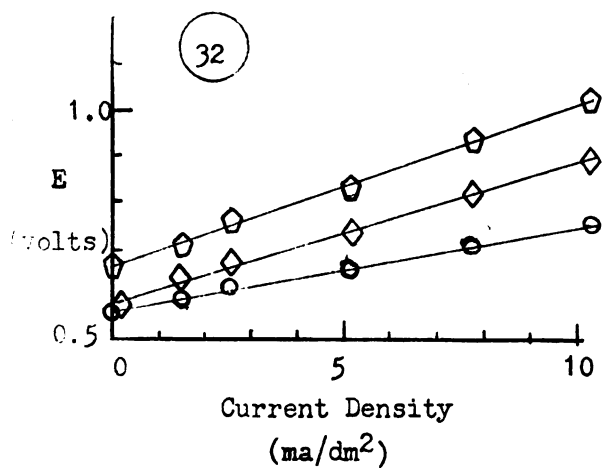
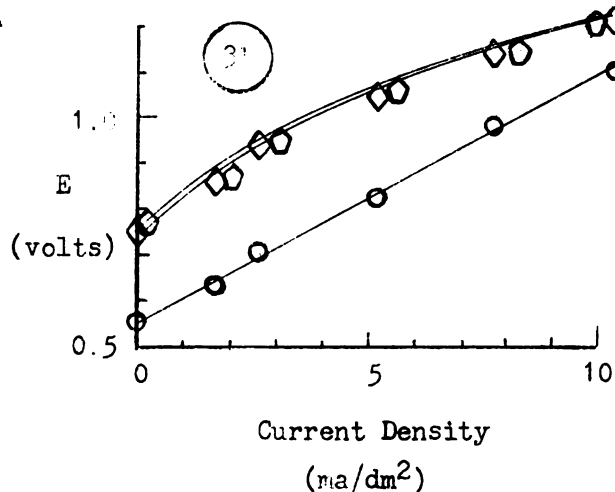
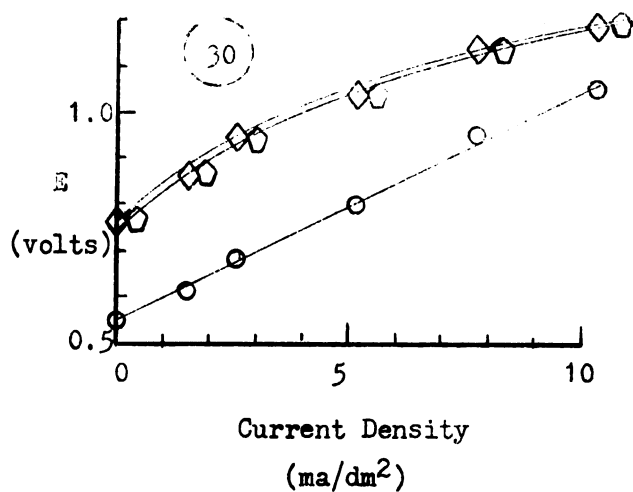
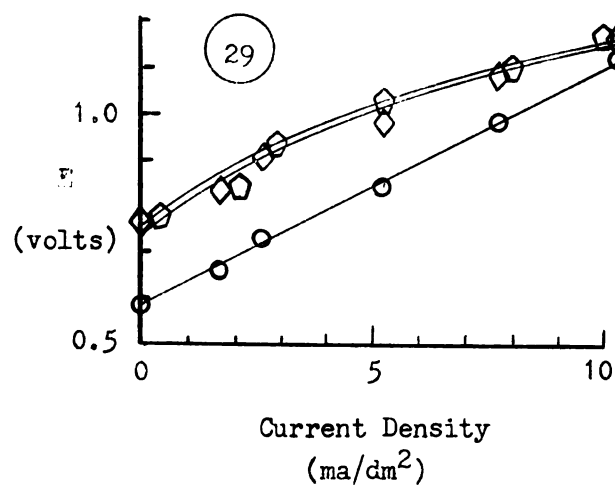
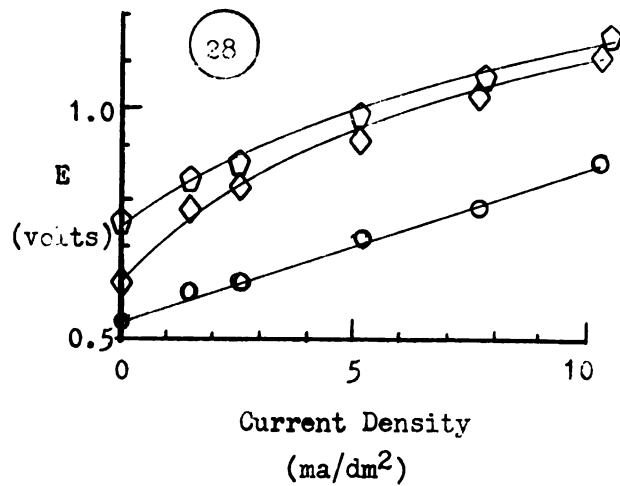


Figure 24 - Cont.

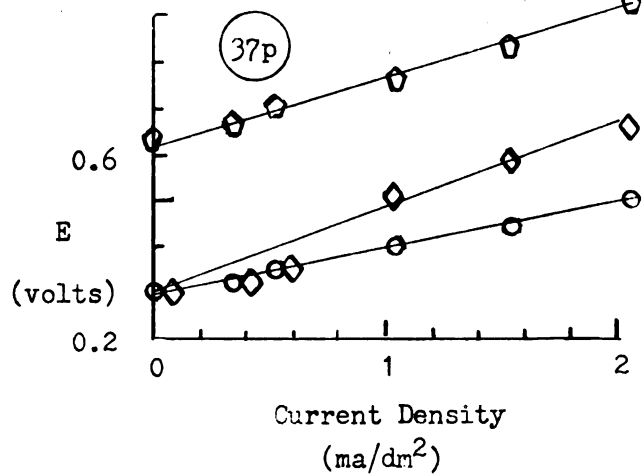
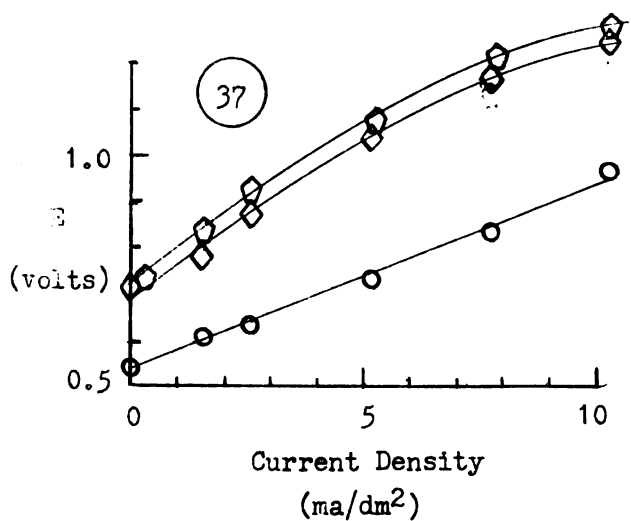
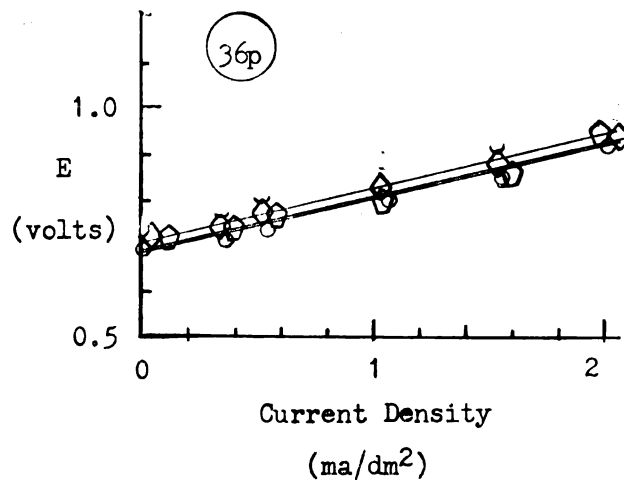
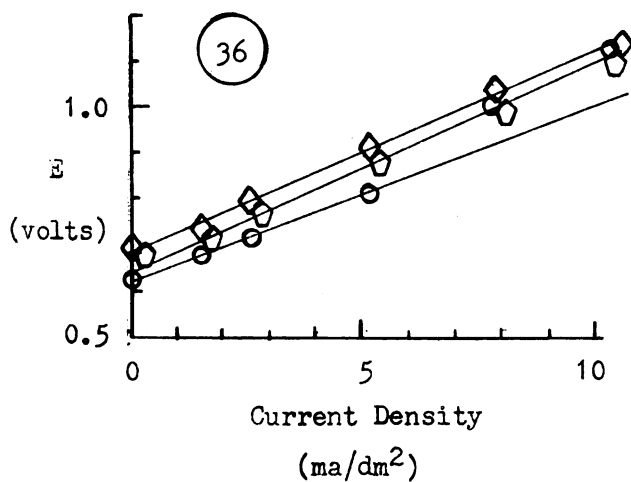
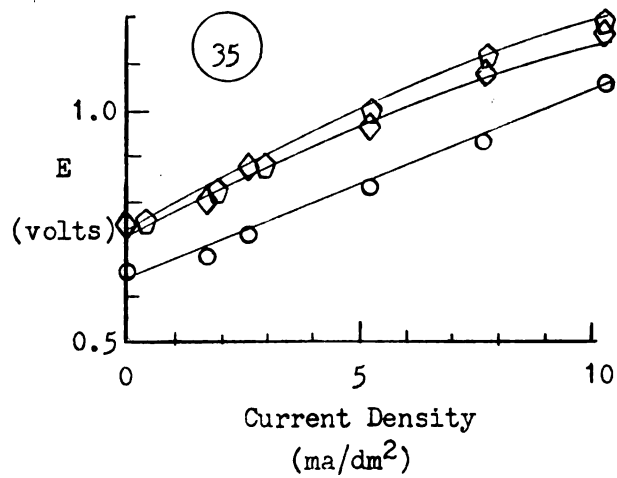
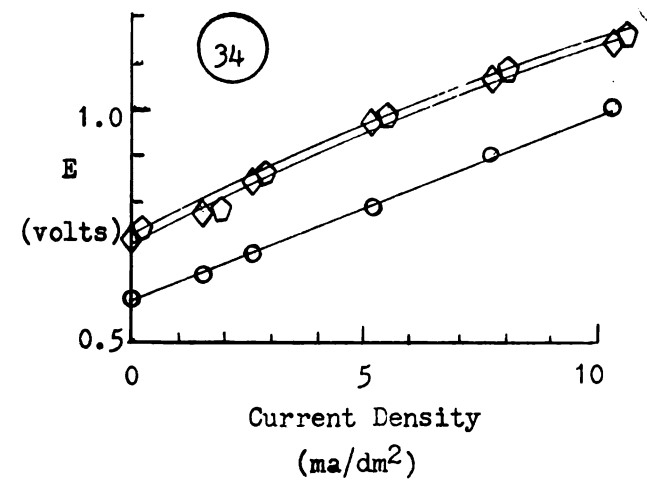


Figure 24 - Cont.

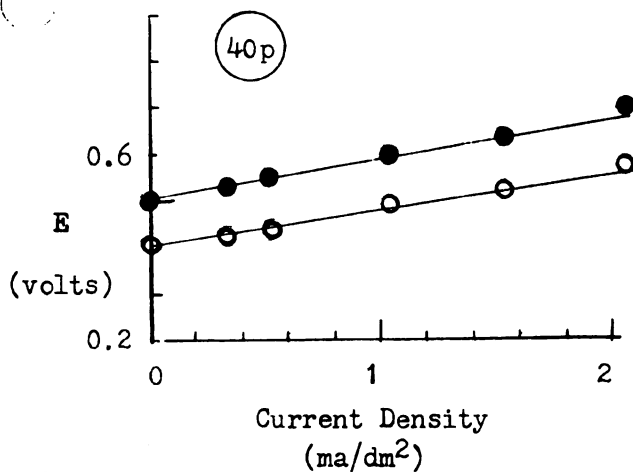
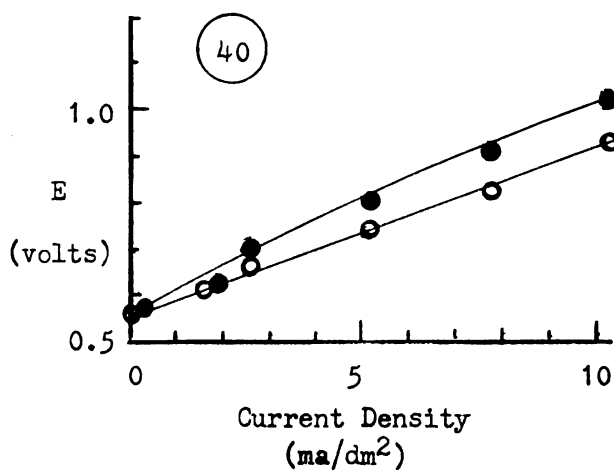
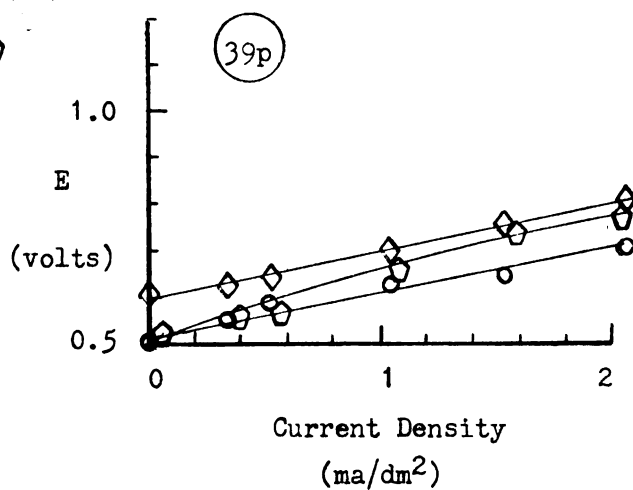
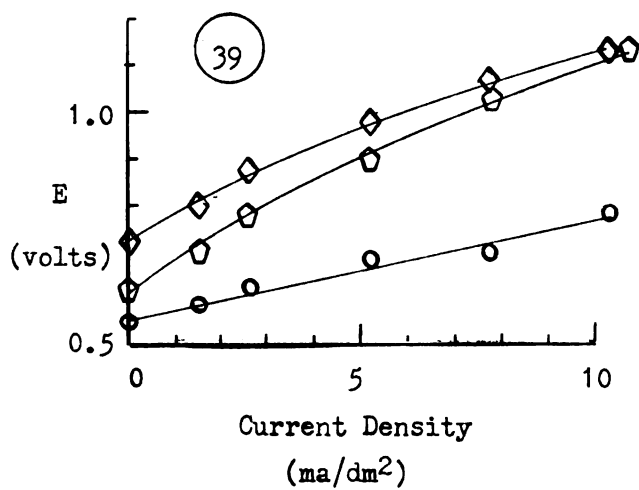
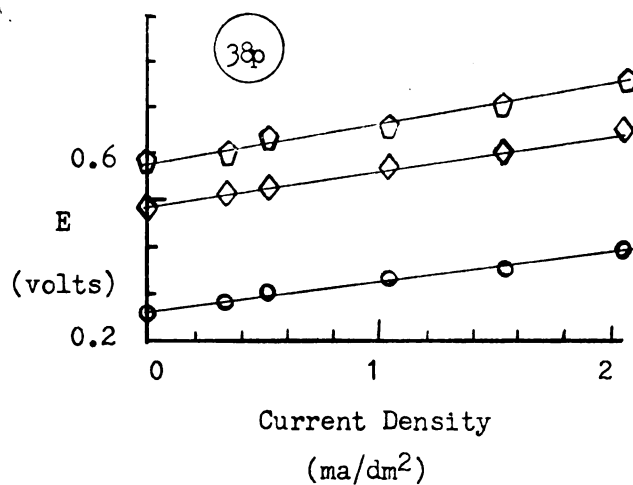
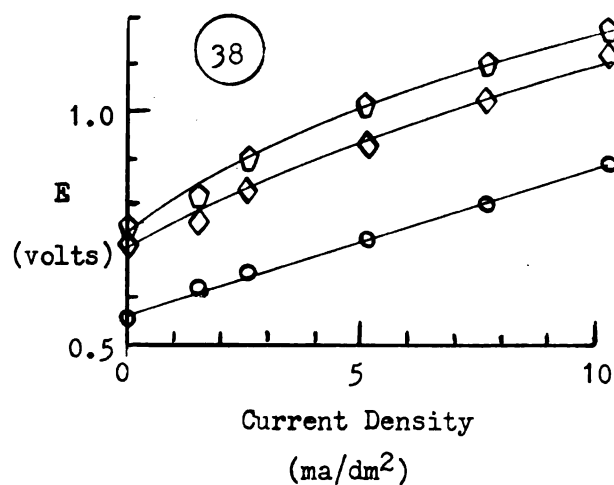


Figure 24 - Cont.

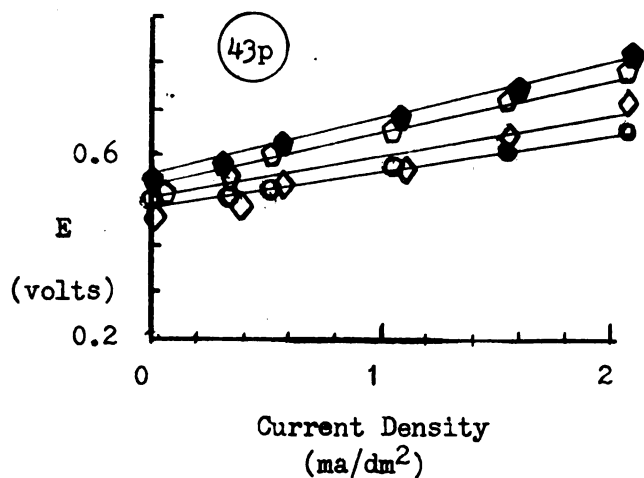
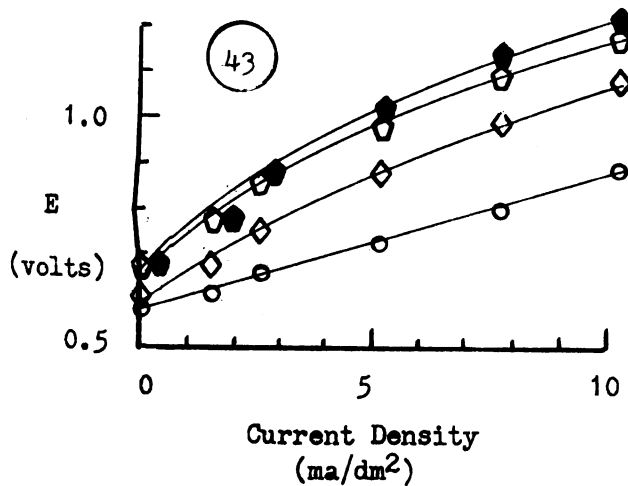
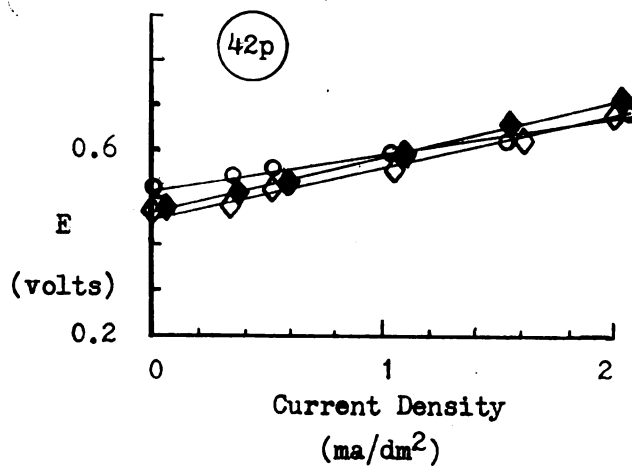
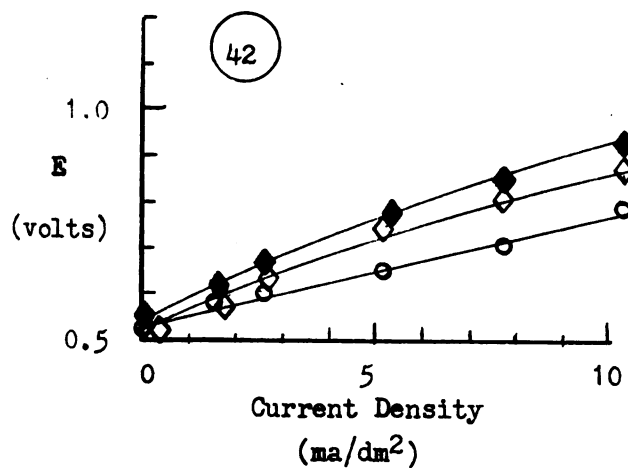
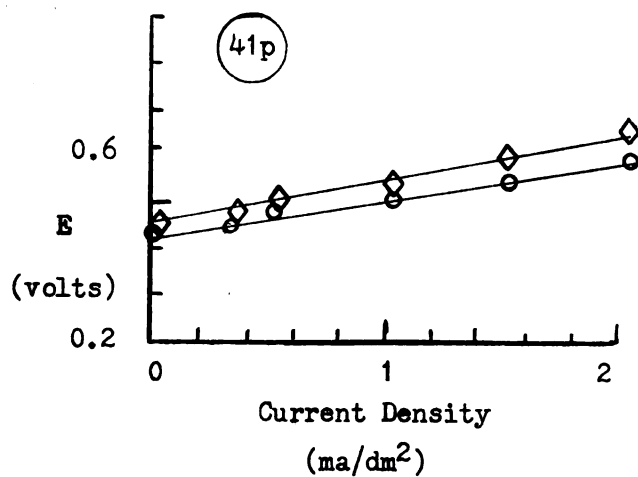
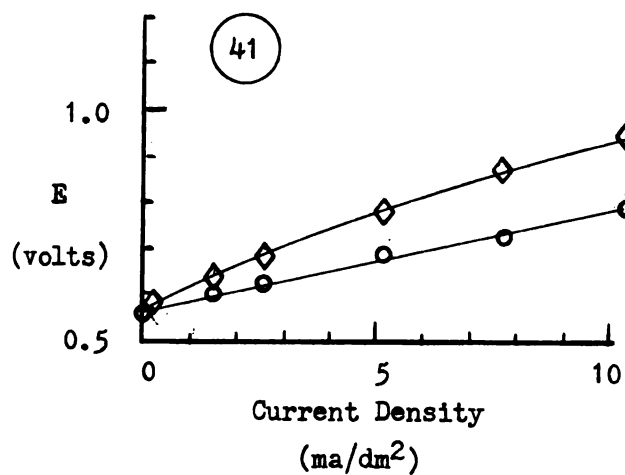


Figure 24 - Cont.

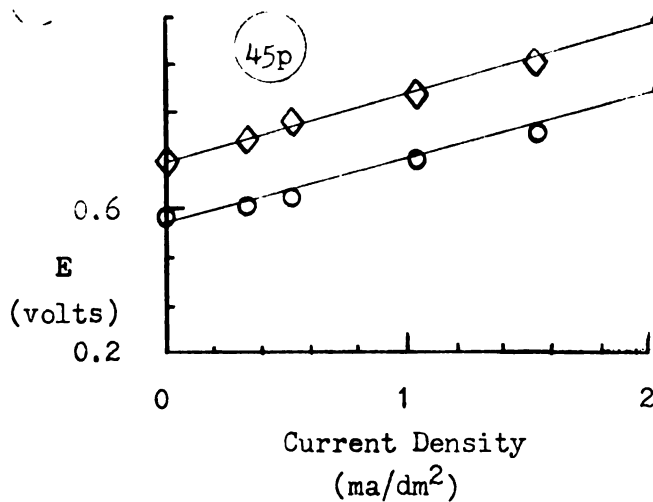
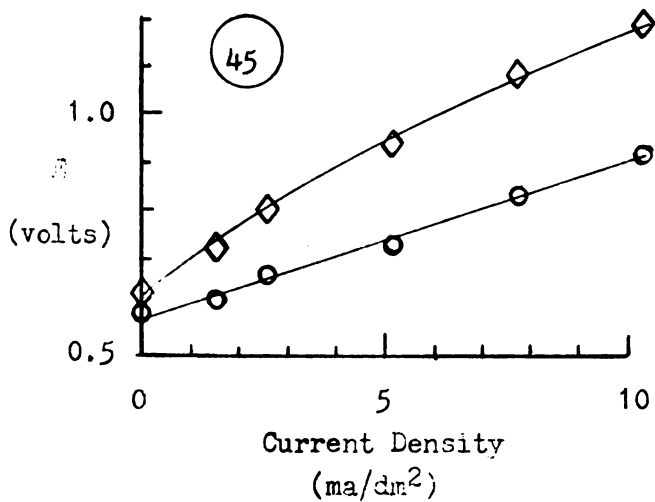
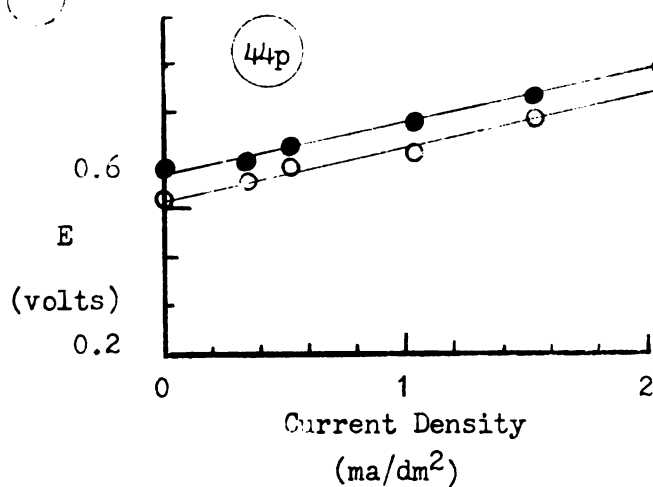
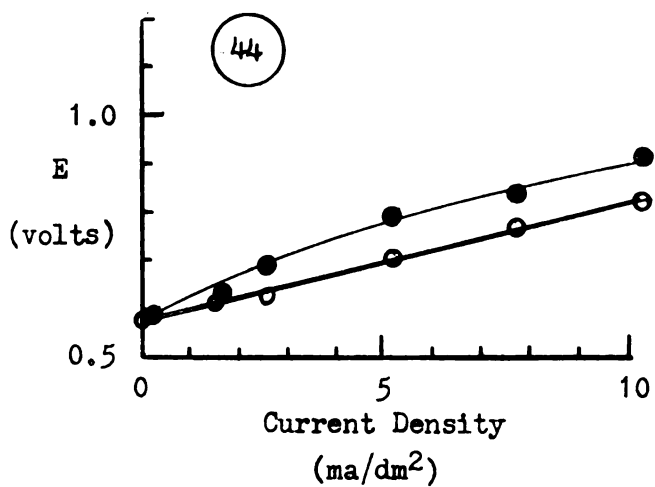


Figure 24 - Cont.

Table 3

Chemical Analysis of Rusting-Test Water *

Date	Alkalinity**			pH	Hardness*		Diss. O ₂	Res. Cl
	total	carb.	bicarb.		total	noncarb.		
9-22	37	18	19	9.88	85	48	3.6	0.3
9-23	37	20	17	9.95	85	48	3.4	0.3
9-24	35	22	13	10.05	84	49	3.5	0.3
9-25	41	22	19	9.98	84	43	3.4	0.3
9-26	45	16	29	9.70	84	39	3.0	0.3
9-27	37	20	17	9.95	84	47	3.6	0.3
9-28	33	20	13	10.02	83	50	3.0	0.3
9-29	35	20	15	9.98	84	49	3.0	0.3
9-30	36	18	18	9.89	85	49	2.5	0.3
10-1	35	22	13	10.05	83	48	2.8	0.3
10-2	39	26	13	10.14	81	42	3.0	0.3
10-3	40	26	14	10.12	81	41	4.1	0.3
10-4	36	20	16	9.98	84	48	2.6	0.3
10-5	36	20	16	9.98	87	51	3.2	0.3
10-6	35	28	7	10.26	87	52	2.0	0.3
10-7	35	30	5	10.35	81	46	1.6	0.3
10-8	35	28	7	10.26	84	49	2.0	0.3
10-9	40	24	16	10.05	84	44	2.5	0.3
10-10	42	24	18	10.01	81	39	2.1	0.3
Ave.	37.3	22.3	15	10.03	83.7	46.4	2.86	0.3
Median	36	22	16	10.01	84	48	3.0	0.3

*0.25 ppm polyphosphate is added to the treated water

**ppm as CaCO₃

Table 4

Analysis of Corrosion Equilibrium Parameters for Rusting-Test Water

Date	pH	Tot. Alk.*	Ca ⁺⁺ *	CO ₃ ⁼ *	DFI **	ME**	LI
9-22	9.88	37	41.5	13.7	5.36	10.3	1.03
9-23	9.95	37	40.0	15.1	5.70	11.4	1.08
9-24	10.05	35	39.7	16.1	6.03	12.2	1.10
9-25	9.98	41	37.5	17.5	6.21	13.2	1.12
9-26	9.70	45	39.5	13.3	4.95	9.7	0.90
9-27	9.95	37	41.0	15.1	5.84	11.5	1.10
9-28	10.02	33	38.7	14.7	5.36	10.9	1.07
9-29	9.98	35	38.7	15.0	5.46	11.1	1.07
9-30	9.89	36	41.3	13.9	5.41	10.5	1.02
10-1	10.05	35	38.7	16.1	5.88	12.1	1.09
10-2	10.14	39	38.7	19.2	7.00	14.7	1.17
10-3	10.12	40	38.2	19.6	7.06	15.0	1.14
10-4	9.98	36	44.0	15.5	6.44	12.1	1.13
10-5	9.98	36	43.2	15.5	6.31	12.1	1.13
10-6	10.26	35	45.2	18.6	7.94	15.0	1.16
10-7	10.35	35	43.0	19.9	8.06	15.9	1.13
10-8	10.26	35	40.7	18.6	7.15	14.5	1.12
10-9	10.05	40	39.2	18.0	6.65	13.8	1.15
10-10	10.01	42	38.0	18.5	6.65	14.1	1.16
Ave.	10.03	37.3	40.4	16.5	6.29	12.6	1.10
Median	10.01	36	39.7	16.1	6.21	12.1	1.12

* ppm as CaCO₃** temp. = 13°C, tot, dissolved solids = 180 ppm, K_S¹ = 106

DISCUSSION OF RESULTS

A. Discussion of Calcite Coating Developed

The protective coatings from this work are quite different in appearance from calcium carbonate based deposits which have been described in the literature. These differences are primarily due to the constant polyphosphate feed of 0.5 ppm which was maintained throughout all the coating development tests and to the low 1 - 2 ppm dissolved oxygen concentration of the test water.

1. Macroscopic Description of the Calcite Coatings

The calcite coatings developed in these experiments are translucent and crystalline in structure. The material is hard and is not easily scratched with a knife point. The crystal structure of the coating is tightly bonded to the metal surface, and in most cases the coating is continuous over the surface of the specimen. The deposition appears to be homogeneous in nature.

With the exception of coatings described by McCauley (25), (26), (27), the calcite deposits just described are in sharp contrast to the natural coatings of calcium carbonate-corrosion products reported by other workers. The coatings also differ in structure from the metaphosphate--corrosion product coating developed by Eliassen and Lamb (8), (9).

2. Microscopic Description of the Calcite Coatings

The range of crystal size may be seen in Figure 25, which shows 100x microphotographs of various quality coatings. The appropriate test number is indicated below each photograph of this figure. The anode and cathode are distinguishable by the A and C respectively which follows the test number.

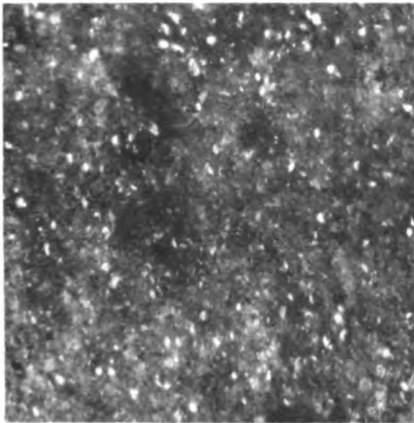
The effect of displacement velocity and calcium carbonate supersaturation on the coating appearance may be seen by comparison of microphotographs.

a) Velocity Effects

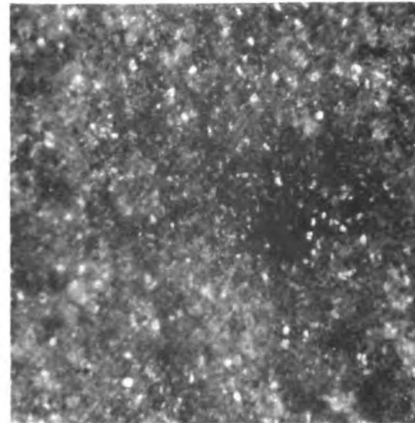
Velocity effect is shown by comparing the coating of specimen 35-C, Figure 25 page 127 (for which the velocity was 4.5 fps) with the coating of specimen 18-C, Figure 25 page 125 (7.5 fps velocity). The coating developed at the lower velocity is noted to be uneven and extensive uncoated (rusted) areas are evident at low points on the surface of the specimen. The coating developed at the higher velocity is smooth and uniform in appearance with only a few holes of 20 micron or less diameter.

b) Effects of Calcium Carbonate Supersaturation

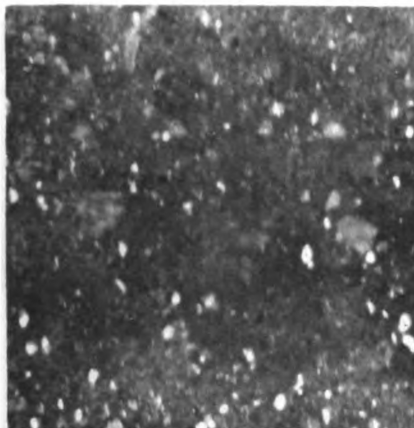
If specimens 21-C, 27-A, 18-C, and 28-C of Figure 25 page 126, 125, and 127 are compared, the effect of the degree of calcium carbonate supersaturation can be seen by the variation in the quantity and size of calcite crystals. At very high supersaturations ($DFI > 450$) the crystals become very large and distorted as pictures for specimens 21-C and 27-A. At lower supersaturations (DFI of 250), a much finer crystal growth is evident as pictured for specimen 18-C. At still lower



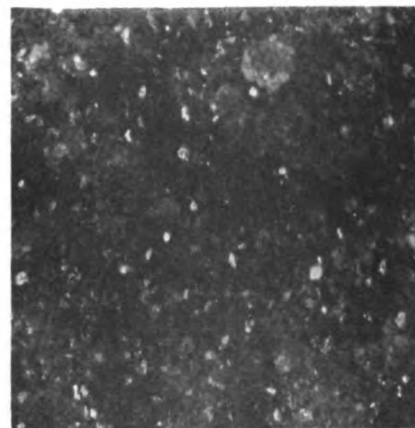
18-C (1)



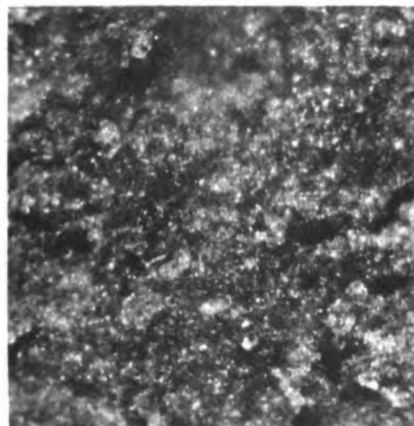
18-A (1)



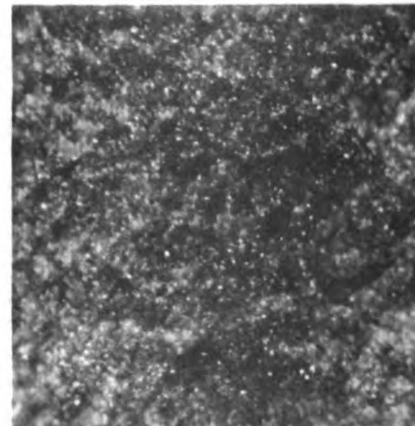
43-C (7)



43-A (6)

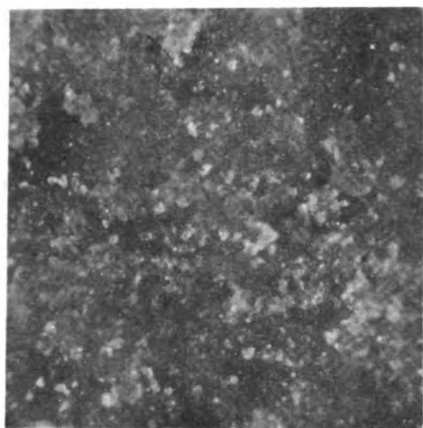


40-C (13)

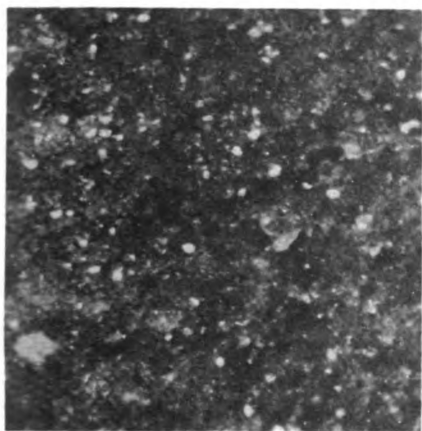


40-A (10)

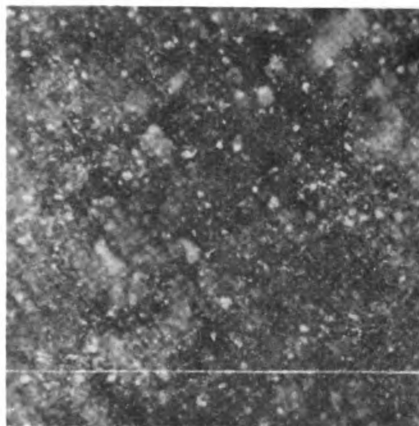
Figure 25. Microphotographs (100x) of Calcite Coatings on Cast Iron Specimens



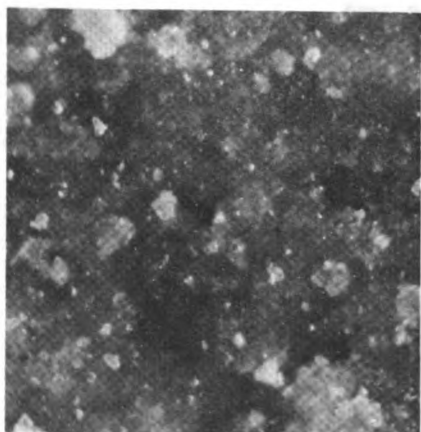
27-A (13)



38-C (16)

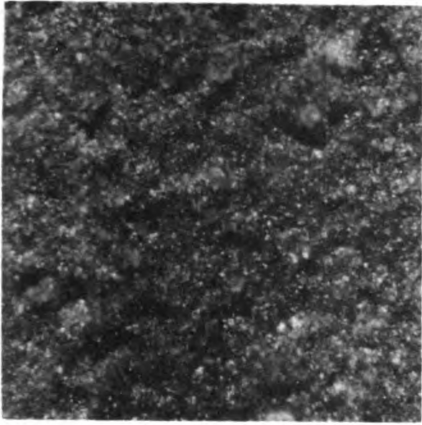


38-A (17)

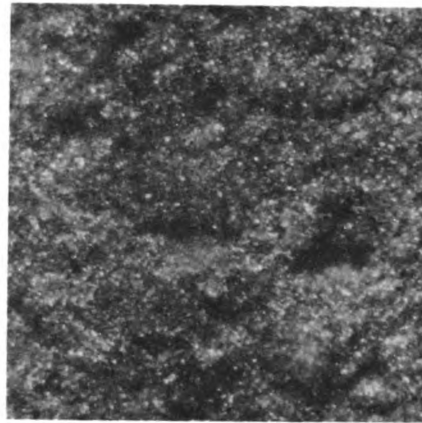


21-C (17)

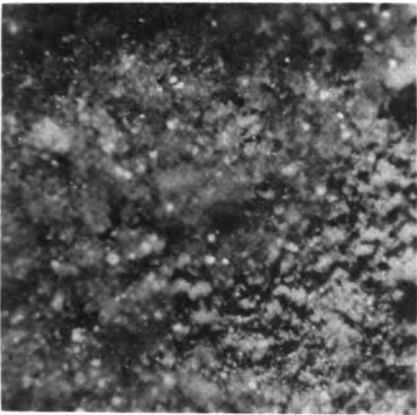
Figure 25 (cont.)



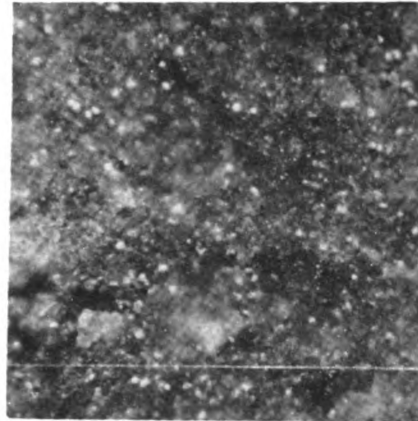
44-C (19)



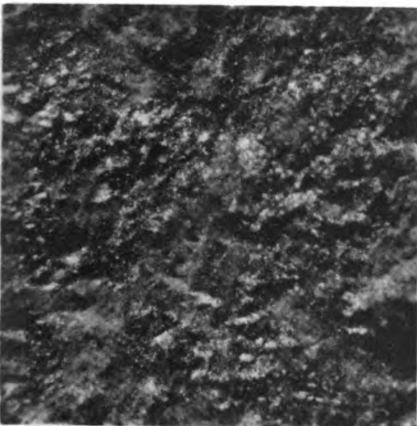
44-A (19)



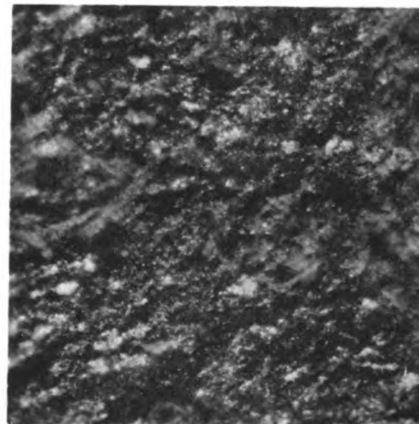
35-C (20)



35-A (20)



28-C (23)



28-A (23)

Figure 25 (cont.)

supersaturations (DFI<120) the crystal size is even finer but very little development takes place. This last condition is shown on specimen 28-C.

The observed growth of large distorted crystals with large supersaturations of calcium carbonate is similar to that reported by Reitemeier and Buehrer (34). These workers found that increasing concentrations of metaphosphate (up to 0.9 ppm) under static conditions effected an increase in crystal size and distorted the normal rhombic shape of the calcite structure.

From studies on the variation in crystal size and shape for various magnitudes of calcium carbonate supersaturation, it appears that distortion and size of crystal formation is a function of CaCO_3 supersaturation as well as polyphosphate concentration. This result would be predicted if the inhibitive crystallization mechanism involves adsorption of the phosphate on the faces of growing crystals as reported by Reitemeier and Buehrer (34) and Rice and Hatch (35). With large CaCO_3 supersaturations crystal nuclei form at a fast rate, providing large surface areas to adsorb the phosphate. The large number of crystal nuclei then agglomerate and grow into large crystals with distorted shapes.

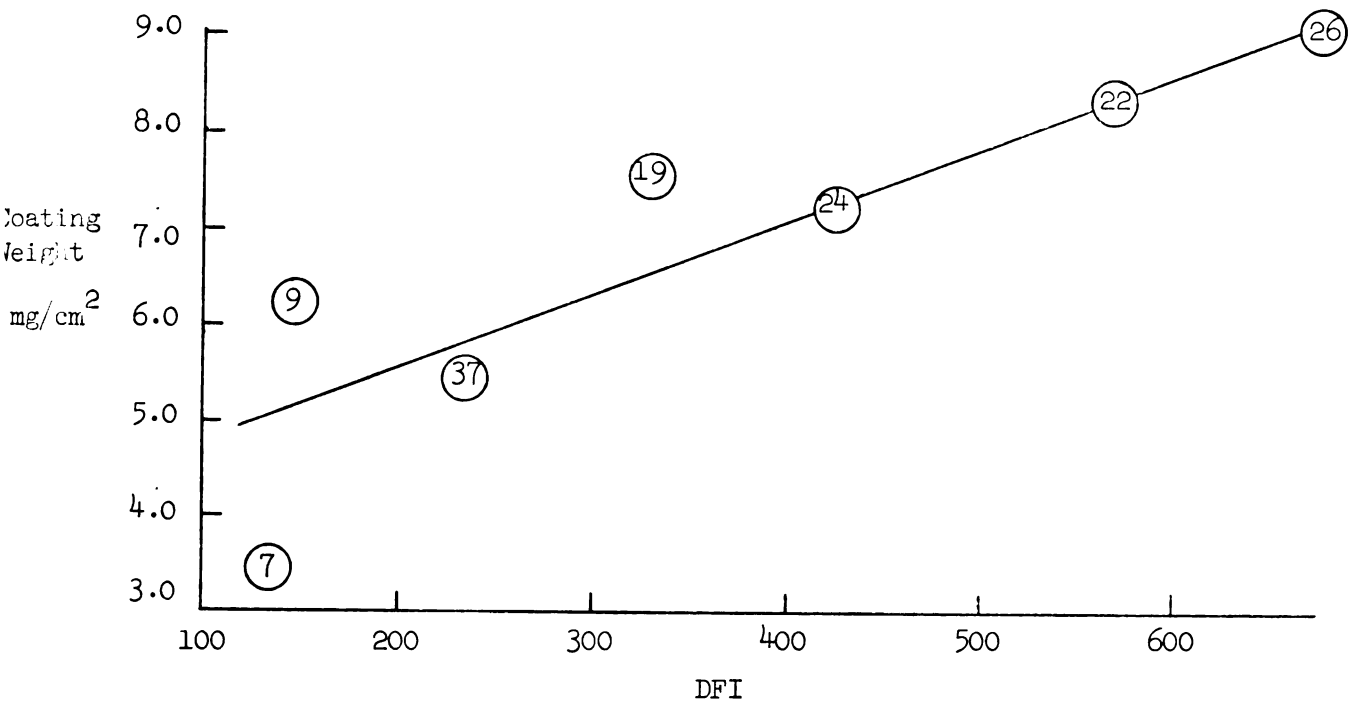
3. Effect of the Driving Force Index and Momentary Excess on the Weight of Calcite Coating Developed

Several indexes based on calcium carbonate supersaturation have been reported for use as indicators of calcium carbonate deposition in water distribution systems. The Langelier "saturation index" (17), Ryznar "stability index" (38), and "saturation excess" (48) have all proven to be nonquantitative in

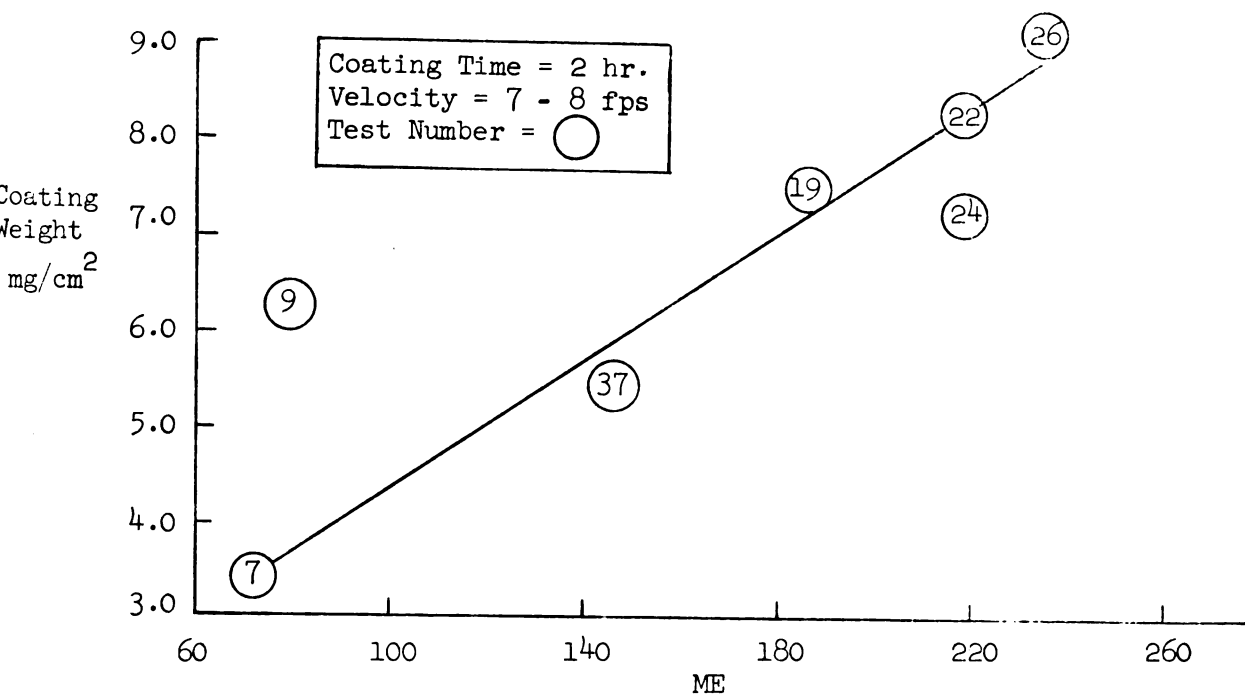
nature. However, two more recent indexes, Dye's "momentary excess" (6) and McCauley's (25) "driving force index," both of which are based on principles of physical chemistry, appear to be quantitative. Figure 26 shows the weight of calcium carbonate deposited on test specimen in two hours with a displacement velocity of 7-8 fps. For this figure, the deposition weight is plotted as a function of (a) the driving force index and (b) the momentary excess. It is seen that a nearly linear relationship exists in both cases. The relationship is strongest for large magnitudes of DFI.

It is important to note that the linearity shown in Figure 26 was established with data from a single type water where the calcium concentration was relatively constant at a high value of 200-230 ppm as CaCO_3 . The variation in DFI and ME for this ground water was obtained by pH adjustment; the range of carbonate ion concentration was from 80 to 375 ppm as CaCO_3 .

Both the ME and the DFI concepts are based on established principles of physical chemistry and have been formulated in equations 36 and 37 respectively in the Theoretical Considerations Section. From these equations it appears that the linear relationships shown in Figure 26 should hold regardless of whether the carbonate or the calcium is the variable. However, there is no experimental evidence at this time with waters of differing calcium concentrations to prove or disprove this presumption.



a) Driving Force Index



b) Momentary Excess Index

Figure 26. Weight of CaCO₃ Coating as a Function of Equilibrium Indexes.

B. Inhibitive Action of Calcite Coatings as Determined by Polarization Tests

1. Iron--Iron Galvanic Cell Polarization

It has been clearly established by other workers (7), (11), (13), (28), (39), (40), (44), and (46) that a bare iron galvanic cell is under cathodic control. That is, the cathodic electron transfer mechanism is the slower of the two electrode reactions and must be "coaxed" with a higher potential to maintain the reaction.

In the Theoretical Consideration Section polarization was shown to result from thermodynamically irreversible electrode reactions and to be a function of current density. Polarization may be further defined as the change in electrode potential, ΔE , with the flow of current.

Figure 27 shows a typical set of polarization curves from the data of one test in which a useful anti-corrosion CaCO_3 coating was developed. The initial cathodic control is evidenced in Figure 27 by the large, initial polarization ΔE_{C-0} of the bare iron cathode, in comparison with the initial polarization ΔE_{A-0} of the bare iron anode. The initial, zero-coating-time, polarization curves are straight lines, indicating the polarization to be ohmic in character and, according to Evans (12), probably due to approach-resistance polarization.

The initial difference in potential between the bare iron anode and cathode is probably due to a small flow of current through the experimental test cell. That is, the potential of the specimen electrodes was measured, as previously described, with a vacuum tube voltmeter, with some very small current flowing at

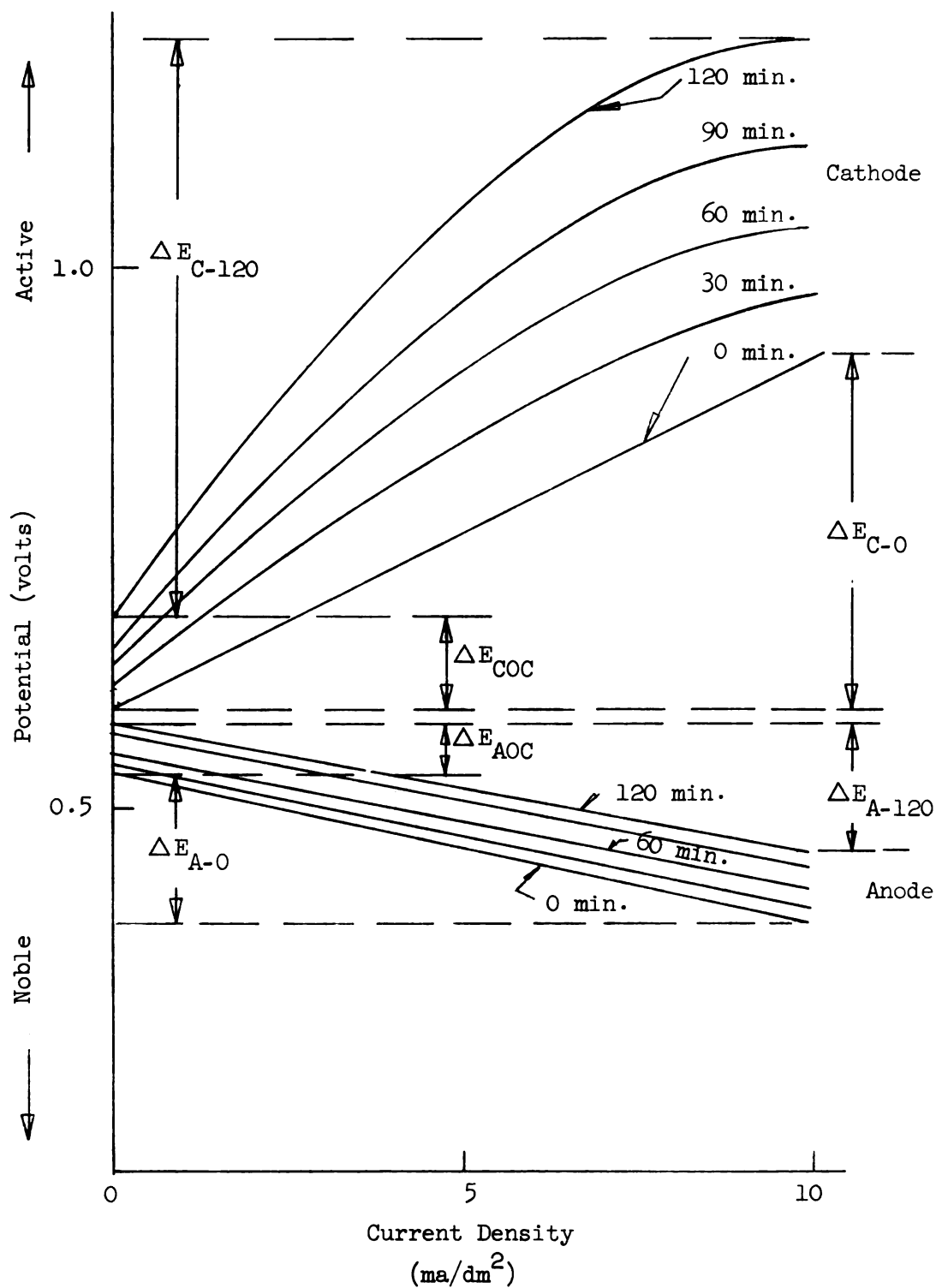


Figure 27. Typical Plate Specimen Polarization Curves During the Development of a Good Coating.

the supposedly open circuit reading. The potential difference at open circuit was then due to polarization from the small current density flowing when the initial measurement was taken.

The initial EMF is a function of: (1) The concentration of ferrous iron in the water, (2) The temperature of the water, (3) The distance between the metal specimen and the standard calomel reference electrode, (4) The purity of the iron, (5) The surface condition of the metal, (6) The concentration of other ions, and (7) The degree of prewetting and air entrainment. The first six variables are nearly constant for all tests. Therefore the slight variation in initial EMF of the electrodes is most probably due to the air entrainment and prewetting.

2. Effect of Calcite Coating on Polarization of Iron Electrodes

a) Calcite Coatings shown to be Cathodic Inhibitors

The effectiveness of some inhibitors has been shown to be related to the increased polarization brought about by their presence. For this reason it seems logical to devise a notation which indicates the degree of polarization change caused by the calcite coating.

Since polarization is defined as the change in electrode potential with current flow, an appropriate notation is signified by ΔZ , as defined in the Data Section. It will be recalled that ΔZ is (the polarization of the coated iron specimen) minus (the polarization of the bare iron) when the impressed current density is 10 ma/dm^2 . Thus, ΔZ is a measure of the increased polarization (positive change in potential) of the electrode due to the calcite coating.

As can be seen from an inspection of the polarization curves in the Data Section, the cathodes become increasingly polarized as the calcite coating builds on the specimens. Figure 27 shows typical polarization curves during coating build up. The polarization effect of Figure 27 is shown by the change in potential ΔE with impressed current density. For clarity, the subscript A and C followed by a number indicates the anode and cathode electrodes respectively at the end of an indicated coating time.

From Figure 27 it is evident that the thermodynamic effect of the calcite coating increases the cathode polarization. This change in cathode potential is designated as ΔE_C (or increased polarization) with coating time. Thus, for 120 minutes, and with a given increase in impressed current density, ΔE_{C-120} is a much greater value than ΔE_{C-0} for all impressed current densities. From this, it is concluded that the calcite coatings of these tests are cathodic inhibitors.

Eliassen and Lamb (10), McCauley and Abdullah (28), Rabald (33), and Evans (12) have reported similar but less pronounced findings for polarization due to calcium carbonate--corrosion product coatings. The previously reported work usually presented the polarization shift over a much longer period of time, indicating a more inefficient coating development. Stumm (39) would appear to be the only investigator to recently report calcium carbonate--corrosion product coatings as anodic inhibitors.

Eliassen and Lamb (8) showed that when metaphosphate alone was adsorbed on iron cathodes no increase in polarization was observed. However, the calcite coating is a very effective

cathodic polarizer, probably due to the uniform crystal structure which develops in a short time. This concept is in agreement of that of Potter (31) who stated: "The crystal form of the deposited calcium carbonate has an important bearing on its efficiency as a cathodic inhibitor, and it appears that certain phosphates, e.g., calgon, improve the inhibiting properties of the carbonate by causing it to deposit in regular tabular array."

It is fair to note that although the coating has been shown to be thermodynamically a cathodic inhibitor, it also acts as a protective coating to the anodes, according to Potter's (31) definition. That is, the coating covers the entire metal surface, reducing the contact between the anodic areas and the water, thereby stifling the anodic reaction. A possible danger of pitting attack due to intensification of corrosion may therefore exist if and when a local failure in the coating occurs. This type of attack was noted in the rusting test herein reported. As was mentioned previously, dynamic conditions and the presence of a slight supersaturation of calcium carbonate appear to make these local coating "faults" self-healing.

Returning to Figure 27, it will be noticed that the calcite coating causes a shift of both anode and cathode open circuit potentials in the more active direction. The open circuit shift ΔE_{ACC} and ΔE_{COC} for the anode and cathode, respectively, are of the same magnitude and direction. This shift indicates that the tight knit coating makes contact with the electrolyte more difficult; hence the effect is the same as that for an increase in potential due to a decreased concentration of the electron-transferring-ions in the vicinity of the electrode. Such

observation is in keeping with that of other investigators who have reported a shift in potential in the active direction with film formation.

b) Probable Polarization Mechanism

It is not the purpose of this thesis to define the mechanism which causes polarization of the calcite coated cathode specimens. However, it is interesting to speculate on the specific cause of cathode polarization.

As was discussed earlier, Evans (12) has defined the four types of polarization mechanisms to be: (1) Ohmic drop, (2) Approach resistance, (3) Concentration difference, and (4) Activation energy. Each of these types will be considered and by the process of elimination an attempt made to pinpoint the correct mechanism.

In such an evaluation, it is important to recall that each polarization mechanism is an independent function of the current density. Therefore all mechanisms are probably acting at a given value of current density but one is probably dominant.

The approach-resistance and ohmic drop polarization mechanisms must be eliminated as the primary polarization mechanisms due to the nonlinear shape of the polarization curves during coating development at current densities above approximately 2 ma/dm². Moreover, if the mechanism were primarily one of coating resistance to electron passage, both electrodes should be affected equally, which is obviously not the case.

According to Potter (31), concentration polarization causes the polarization potential to become increasingly larger with

increased current density. Therefore, concentration polarization must also be eliminated, because the data show the change in polarization of the coated cathodes to decrease with increasing current density.

Upon the basis of this reasoning, the primary mechanism of cathodic polarization of the coated specimens appears to be one of activation polarization, with varying contributions from the other three mechanisms at different current densities.

When other conditions are constant, current density may determine the primary polarization mechanism. Such effect is shown by considering the polarization test on the coated pipe specimens. The pipe polarization tests usually show a linear relationship between electrode overpotential and impressed current density. This relationship indicates the principal mechanism to be approach-resistance polarization. Activation polarization was not of importance in these tests due to the very small impressed current densities (one fifth of that employed for the plate specimens).

For the high alkalinities of this experimental work it is doubtful that current passage was due to the classical hydrogen ion discharge at the cathode. More likely, the dipole water molecule carried current through the solution in the manner suggested by Potter (31). (See page 30 in the Theoretical Considerations Section).

c) Erratic Polarization Curves

The number of tests were sufficient to establish the shape for a set of normal polarization curves. Of the total 45 tests

of this experimental work on polarization techniques 35 sets are normal and 10 sets of curves are found to be unusual or faulty. These tests (1, 2, 3, 4, 5, 14, 29, 30, 31, 39) have been included for completeness and because they illustrate improper techniques and equipment failure. In all the above faulty tests the polarization parameter ΔZ was negative, indicating some improper procedure or equipment malfunction. The above specimens were not used in the rusting tests and therefore have been eliminated from the analysis in the following sections.

In general, the unusual aspects exhibited in the polarization tests were either (1) a very high initial polarization curve of the bare metal or (2) a sudden drop in the polarization curves during the latter part of an experiment to a position below that noted earlier in the experiment.

As an example of the type (1), high initial polarization phenomenon, consider test 1 and 2 of Figure 24 page 109. Curves from these two tests, made at a time during which experimental procedures were being established, show the effect of leaving plates in the cell an appreciable time before the first potential measurements are made. The technique allows time for the formation of a slight coating of rust or calcium carbonate, either of which causes the initial curves to be higher than is anticipated.

There seems to be two reasonable explanations for type (2) deviation. One explanation appears to be related to the handling of plates before insertion into the test cell. Test 4 in Figure 24 page 110 illustrates a test during which one polarization curve drops below previous positions. Fingerprints can be clearly seen

on the coated specimen due to shadings of different colored coatings, indicating that some oil from the fingers is transferred to the specimen. Coating development for the oil-coated points is poor for the low CaCO_3 supersaturation of this test.

In a few other instances where later polarization curves are irregular with respect to the initial curve position, material or equipment failure appears to be at fault. In a few of the early tests the EPOXY paint used for coating the back surfaces of the specimens is observed to have sloughed off. The loss of the nonelectrolytic paint increases the effective area of the plates making the apparent current density for each potential measurement erroneously high, thus causing the curves to be plotted incorrectly. Test 39 in Figure 24 page 118 illustrates a test where the calomel electrode used as a reference became erratic before the last 120 minute measurements could be made.

C. Results of Polarization Measurements of Anti-Corrosion Quality

1. Rusting Tests on Calcite Coated Cast Iron Specimens

In general, the coatings provided good protection for the iron specimens in both the static and dynamic tests. After 17 days exposure to the test water, described in the Procedure Section, the specimens have been ranked by comparison with each other in such a fashion as to assign a rating to each plate specimen signifying its relative position among the other specimens subjected to the same test conditions. Thus, a rating of 4 indicates that three plates show signs of less corrosion.

a) Plate Specimens

Table 5 summarizes the data for the specimens subjected to the 17 day rusting test. The data are arranged in order of decreasing anti-corrosion value. The order or rating of the static (cathode specimens) appears on the left side of the table. The corresponding dynamic test rating for the anode of the specimen pair is found in the right-hand column.

Figure 28 shows four specimen pairs after exposure in the rusting tests. The specimen's relative rating is given in parenthesis under each picture. The photographs of this figure show that test specimen 32, which was ranked a low 18 of 23, offers a considerable degree of protection.

Dynamic conditions appear to lessen the corrosive attack as compared to that experienced during static tests. This fact suggests that a film is built over the local active anodes on the surface of the coated plates, and that dynamic conditions tend to make corroding areas to be self-healing.

The development of the local anodes is apparent from dark areas on the coating at the end on the 17 day test period. Microscopic inspection reveals that anodic points tend to develop in two ways: (1) At a hole in the coating or (2) at weak points such as found over large depressions and along the longitudinal edges of the plates which are not coated with calcite due to placement in the test cell. The bare plate edges are covered with fingernail polish before exposure in the rusting test, but in some cases the fingernail polish bonds poorly or does not completely cover the edges.

Table 5

Results of Static and Dynamic Rusting Tests

Spec. No.	Static Rust Rank	ΔZ	DFI	ME	Ave. Vel. (fps)	Coat. Time (hrs)	Micr. Rating (cath)	Micr. Rating (anode)	Dyn. Rust Rank
18	1	.24	235	127	7.5	2	G	E ⁻	1
17	2	.16	212	110	7.6	2	G ⁺	E	2
15	3	.14	195	107	7.6	2	E	G ⁺	14
23	4	.14	412	211	7.6	2	G	E	3
20	5	.16	305	181	7.5	2	G	G	7
45	6	.23	242	147	7.1	1	G	G	4
43	7	.18	262	161	7.1	2.5	E	E ⁻	6
16	8	.16	185	105	7.6	2	G ⁺	G	11
41	9	.11	226	137	7.1	1	G	G	5
42	10	.11	274	162	7.1	1.5	G	G ⁺	9
12	11	.20	166	91	7.8	2	G	G ⁺	8
13	12	.17	156	85	7.6	2	G	G	15
40	13	.08	250	158	7.1	0.5	G ⁻	G	10
27	14	.05	681	215	7.6	2	F ⁺	F	13
8	15	.22	169	89	8.0	2	G	G	16
38	16	.10	249	156	4.5	2	G ⁻	G ⁻	17
21	17	.06	550	213	7.5	2	F	F ⁺	12
32	18	.16	155	85	7.9	2	F ⁺	F ⁺	18
44	19	.08	249	147	7.1	0.5	F	F	19
35	20	.06	180	118	4.5	2	F ⁻	F	20
36	21	.05	115	75	4.5	2	P	P	21
34	22	.02	141	107	2.8	2	P ⁺	P	22
28	23	.04	67	36	7.7	2	NC	NC	23



(C-1)

Test 18



(A-1)

Figure 28. Photographs of Coated Plate Specimens (2X) After Exposure to the Rusting Tests.



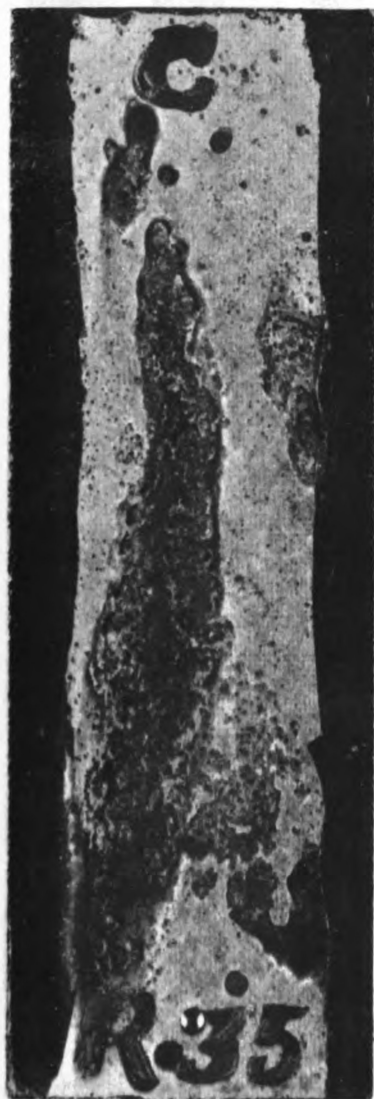
(C-9)

Test 42



(A-10)

Figure 28 - (cont.)



(C-18)

Test 32



(A-18)

Figure 28 - (cont.)



(C-23)

Test 28



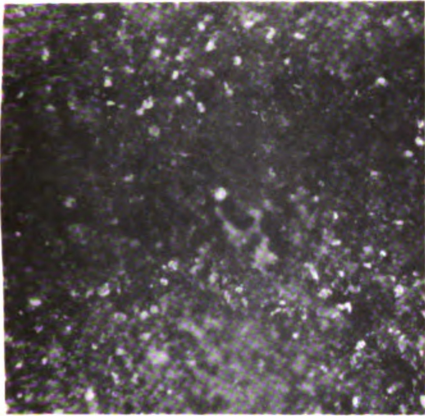
(A-23)

Figure 28 - (cont.)

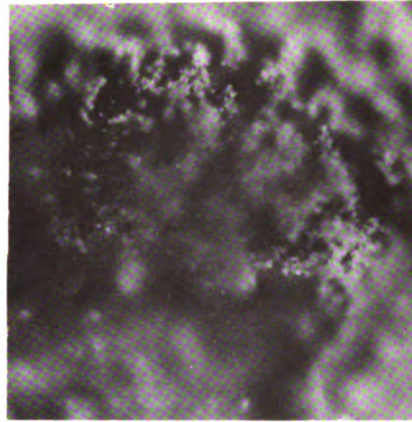
To illustrate the development of local corrosion cells on the coated plates, consider Figure 29 which shows 100X microphotographs of a representative example of the effectiveness of the calcite coating in inhibiting corrosion. Figure 29 (b) shows a hole in the coating where corrosion is starting, probably at a depressed point in the metal which was developed during sandblasting. Another spot on the same specimen is noted in Figure 29 (a).

The effectiveness of calcite coating is shown in Figure 29 (e) and (f), representing "before" and "after" pictures of one of the best coatings (specimen 18-A). On the other hand, Figure 29 (c) and (d) show the different forms of the extensive corrosive attack exhibited on the anode and cathode respectively, of a specimen pair (test number 28) which has developed only a trace coating. In the case of specimen 18-A, which is coated with a hard, uniform deposit, no difference in the crystal structure can be observed after the 17 day exposure period. The attack on specimen 28 is evident from comparison of the "before" microphotographs found in Figure 25, page 127 with the "after" pictures shown in Figure 29.

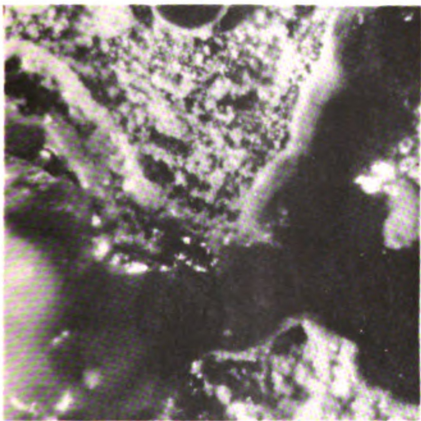
Figure 30 shows an enlarged sketch of a local anode on a plate such as test 32 in Figure 28 page 144. A small hole through the coating is apparent in this photograph. It may be presumed that the coating imperfection results from an initial pot hole in the metal. Coating development is made difficult by the low flow velocity at the bottom of this depressed area in the metal. Coating developed at this spot is superficial in



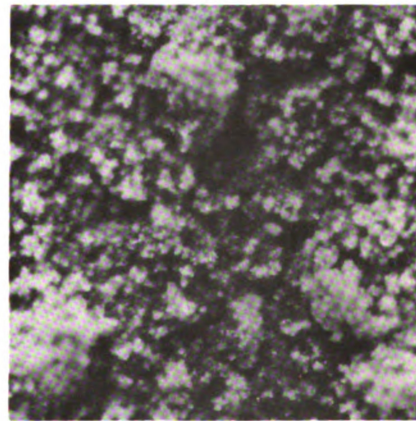
8-C
(a)



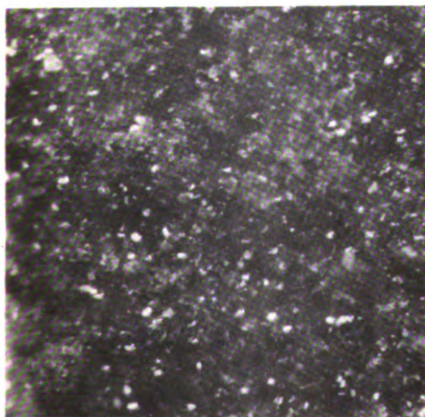
8-C
(b)



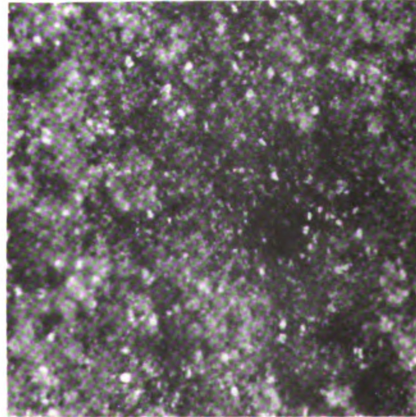
28-C
(c)



28-A
(d)



18-A
(e)



18-A
(f)

Figure 29. Microphotographs (100X) of Coated Iron Plates Showing the Effects of Exposure to the Rusting Tests.



18-A
(a)



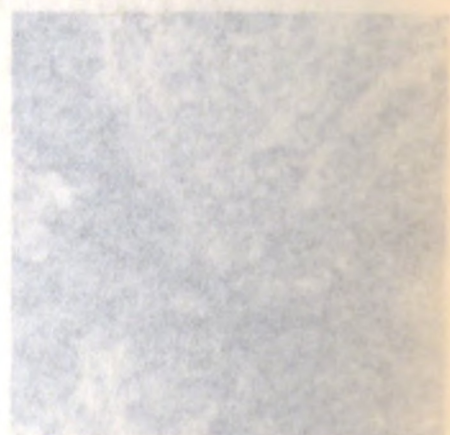
18-A
(b)



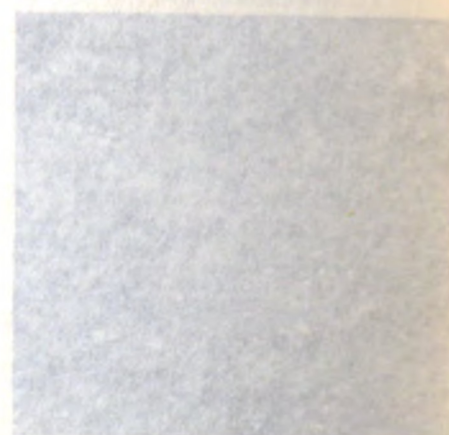
18-A
(c)



18-B
(a)



18-B
(b)



18-B
(c)

Figure 29. Microphotographs (100X) of Coated Iron Plates Showing the Effects of Exposure to the Rusting Tests.

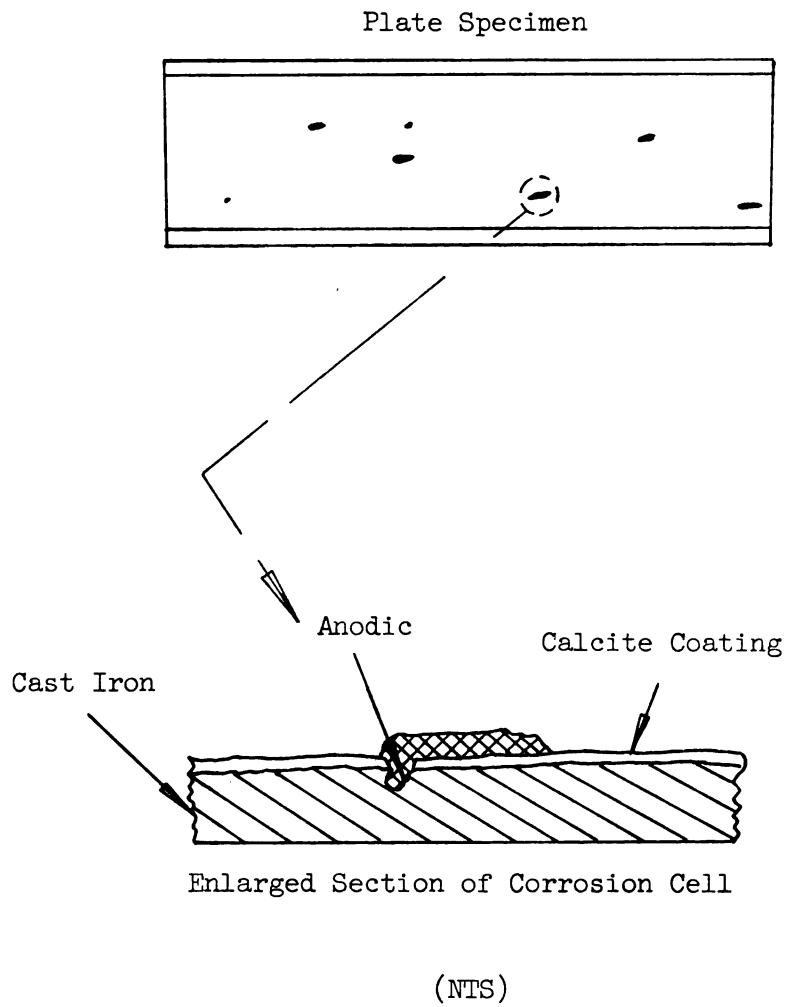


Figure 30. Typical Corrosion Cell.

nature and did not fill the hole. Under these conditions, establishment of a concentration cell is to be anticipated with the resulting corrosion at the weak point. The material around the pit shows no effect from the dynamic test and the anodic oxidation products form a layer over the top of the adjacent coating.

b) Pipe Specimens

Due to limitations in the test apparatus, the pipe specimens were coated at water velocities of 5.6 fps and less. Static test with the pipe specimens reveals little difference in the corrosion patterns of pipes and plates. The six pipe specimens are ranked separately and the resulting order is summarized in Table 6.

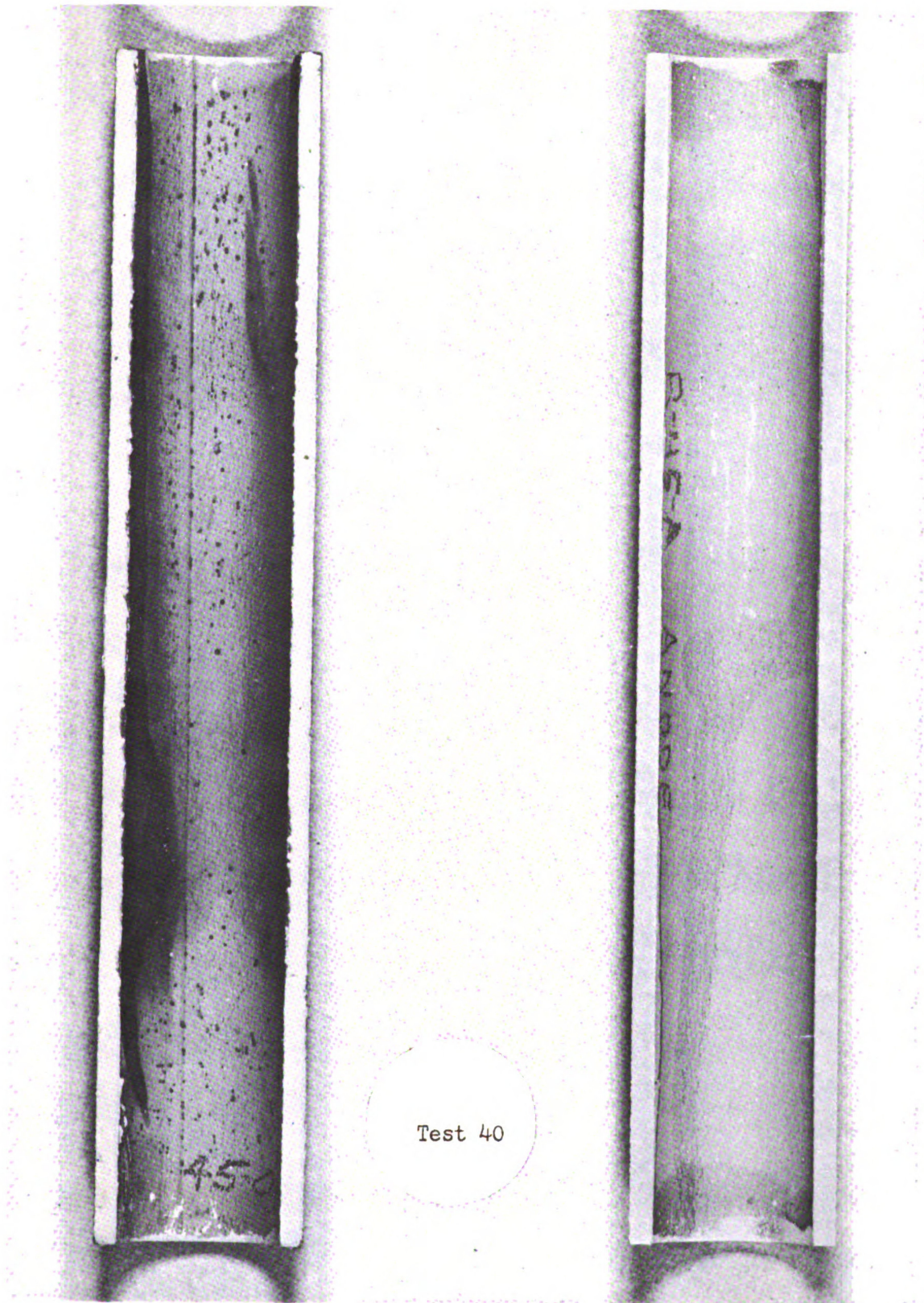
Figure 31 illustrates the anti-corrosion quality exhibited by the pipe specimens. The right-hand pipe-half of Figure 31 is the unexposed cathode of the test pair. A careful examination of the photograph shows a shadow running longitudinally down the cathode pipe-half. This shadow resulted from rusting which took place before the experiment was begun, due to a leaky valve in the apparatus. The rust has been subsequently covered over with a calcite coating.

The range of the variables (time, velocity, and calcium carbonate supersaturation) explored with pipe test cells was limited, since only 10 pipe cell experiments were made. Moreover, polarization curves with pipe cells are inconclusive. For these cells, only generalized statements concerning coating development can be made upon the basis of physical appearance and microscopic examination. Upon such basis, it would appear that the hydraulic

Table 6

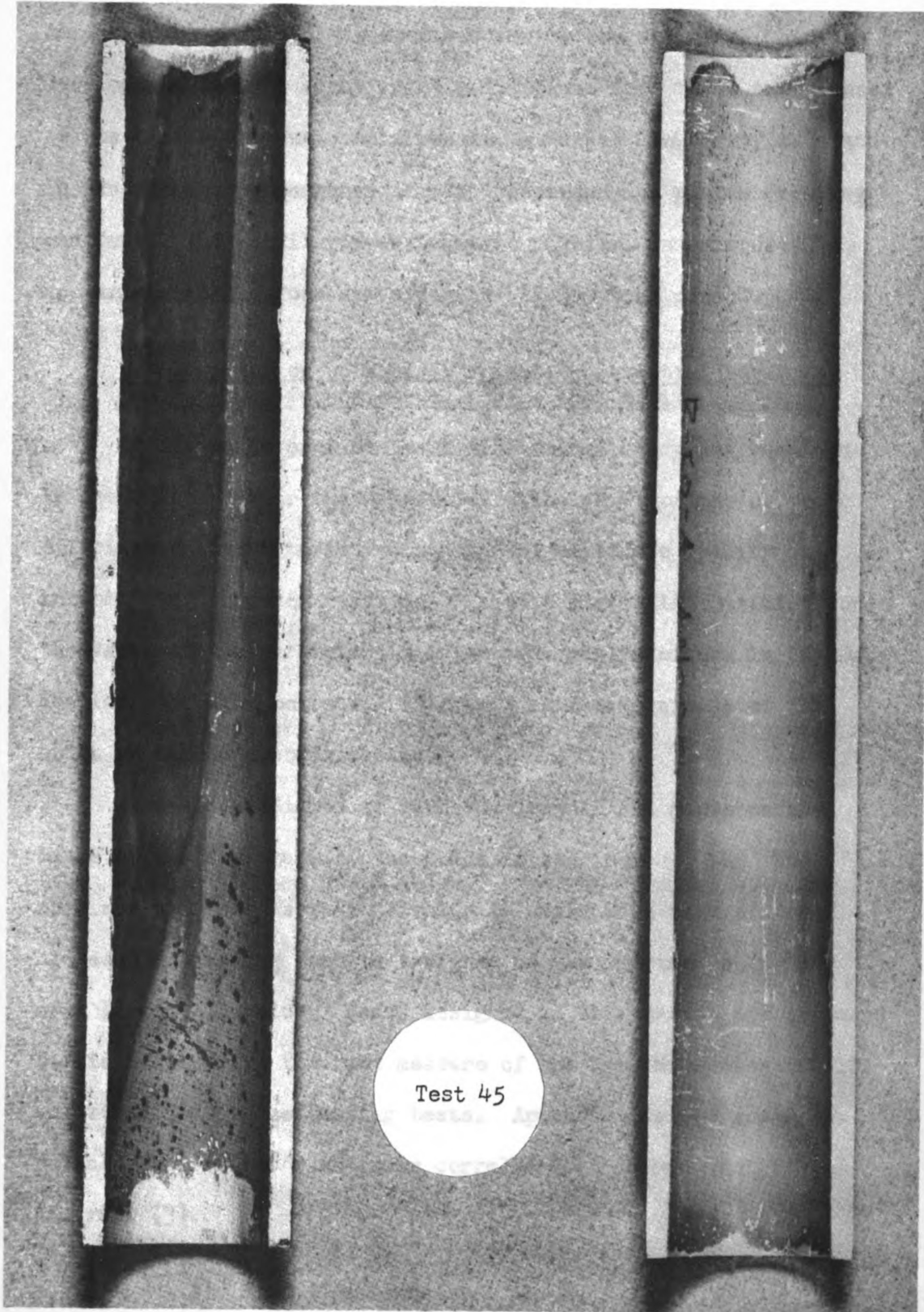
Results of Static Rusting Test on Cathode Pipe Specimens

Spec. No.	Static Rusting Rank	ΔZ	DFI	ME	Vel. (fps)	Coat. Time (hrs)	Micr. Rat.
40	1	.04	250	158	5.6	0.5	G
43	2	.03	262	161	5.6	2.5	G ⁺
41	3	.02	226	137	5.6	1	G ⁻
38	4	.01	249	156	5.6	2	G
45	5	.03	242	147	5.6	1	G
44	6	.01	249	147	5.6	0.5	F



(1)

Figure 31. Photographs of Coated Pipe Specimens (2X) Before and After Exposure to Static Rusting Test.



Test 45

As a result of the correlation studies of the test data with
a fairly strong relation Figure 31 - (cont.)

conditions over the plate specimen during the period of coating development are not significantly different from those experienced by the pipe specimens. As a result, a marked similarity is noted in the physical appearance of pipe specimens and plates from any one test. This similarity extends to physical and microscopic appearance both before and after the 17 day test period.

2. Correlation between Polarization Potential Parameter and Anti-Corrosion Quality of the Calcite Coatings

As discussed previously, a statistical study has been made to determine whether the magnitude of the shift of the cathodic polarization curve is indicative of the coating's ability to inhibit the corrosion reaction. In this statistical examination, the value of the parameter ΔZ is as previously defined in the Data Section. It will be recalled that ΔZ is the magnitude of the shift in cathodic polarization.

A rank is assigned to each specimen of the group on the basis of the magnitude of the polarization increase ΔZ . The specimen with the largest ΔZ value is assigned a rank of "one" and each succeeding rank is assigned to the specimen with the next largest ΔZ value. Ranks assigned in this manner are compared statistically with the rank measure of the anti-corrosion quality as determined by the rusting tests. Appendix C gives a sample calculation for the rank-order correlation employed in this analysis (3).

a) Plate Specimens

As a result of the correlation analysis it is evident that a fairly strong relationship does exist between ranks assigned

from polarization curves and ranks assigned from rusting tests. The correlation coefficient is 0.69 for the static rusting test and 0.64 for the dynamic test. This correlation shows conclusively that the probability of a coating exhibiting good anti-corrosion qualities increases with increasing ΔZ .

The relationship between the increase in polarization ΔZ , with the anti-corrosion qualities of the specimens can be seen graphically in Figure 32. The calculations for the regression line in the static rusting test - ΔZ plot are given in Appendix D. It will be noted that, in general, the microscopic ratings agree with the anti-corrosion quality rating.

b) Pipe Specimens

Figure 33 shows that the anti-corrosion quality of the calcite coating on the pipe specimens is also a function of ΔZ . The magnitude of ΔZ is less than in Figure 32 because the impressed current density is only about a fifth that employed on the plate specimens. The number of pipe specimens is not sufficient to make a statistical correlation meaningful. However, the data suggests that a correlation similar to that for plate specimens can be established when additional data are available.

c) Correlation between the Dynamic and Static Rusting Tests

Since the parameter ΔZ is a function of cathode polarization, some doubt exists as to the applicability of this parameter for evaluation of the quality of the anode specimens. For comparison, microscopic inspection was made of anode and cathode plates for estimating differing degrees of anti-corrosion quality. For most

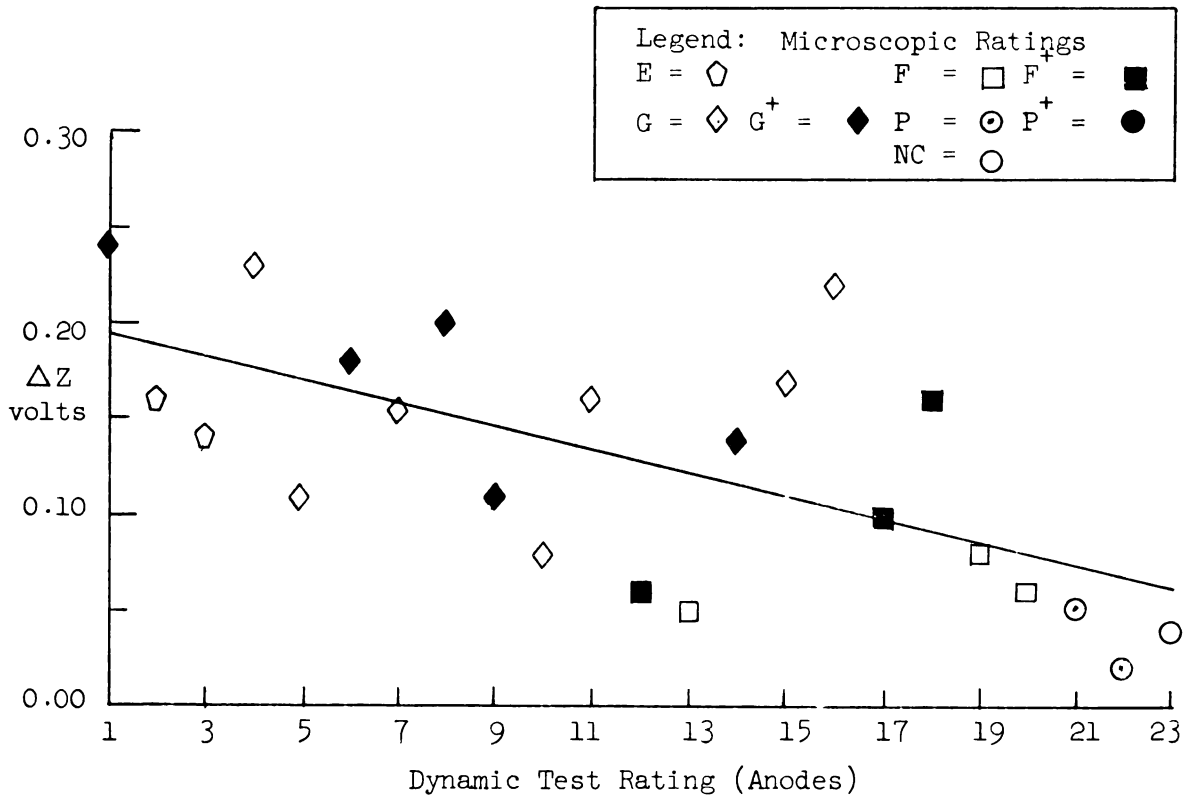
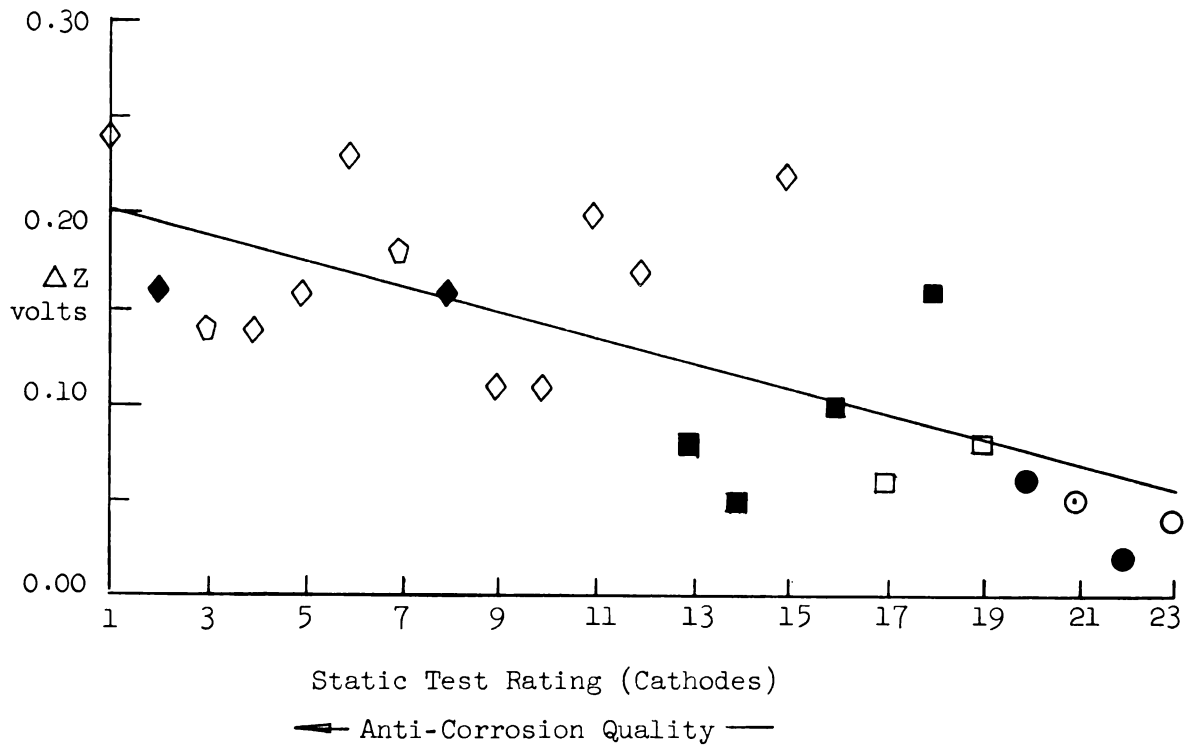


Figure 32. Anti-Corrosion Quality Related to Polarization Parameter.

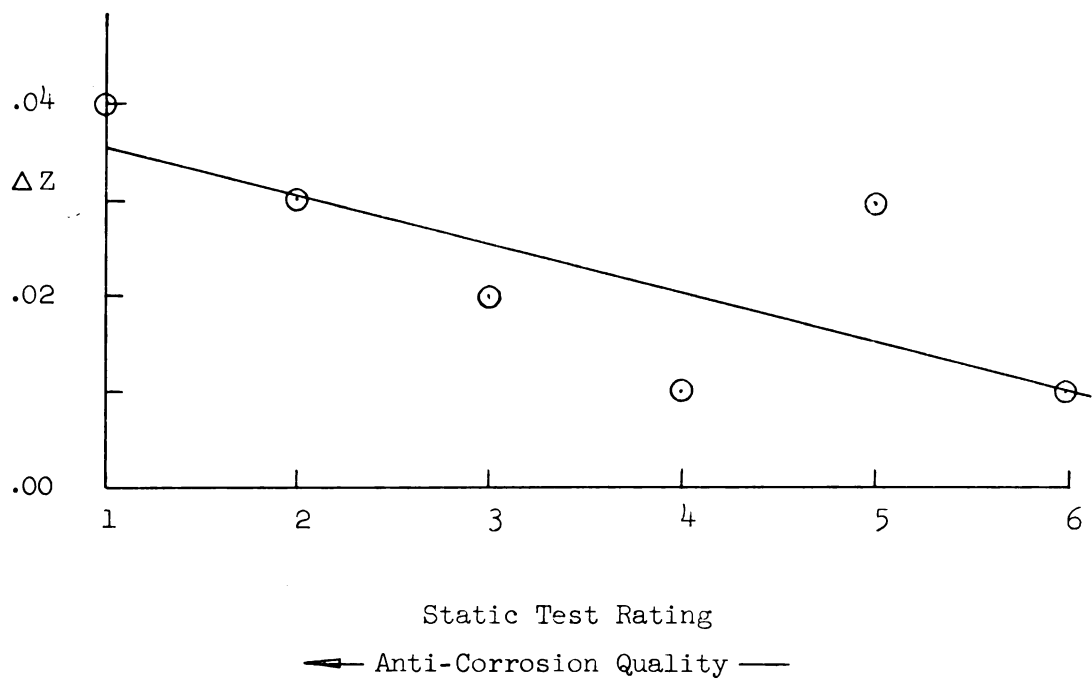


Figure 33. Anti-Corrosion Quality of Pipe Specimens Related to Polarization Parameter.

specimen pairs no apparent difference can be noted. In a few cases, some difference in quality in the crystal structure of the coatings is observed. Differences are probably due to unequal roughness of the two electrode specimens.

In order to evaluate the variation, if any, of the anti-corrosion quality of specimen pairs, the dynamic rating of the anode is plotted versus the static rating of the cathode. The resulting plot of these data is shown in Figure 34, and it is noted that the correspondence is nearly one to one. The major exception is test specimen 15 where the anode rating is much poorer than that for the cathode, probably due to a large local failure on the anode. The rank-order correlation coefficient for the anode-cathode ratings of Figure 34 is 0.90 with the chance occurrence being much less than one in one thousand.

From this evaluation it may be concluded that the magnitude of the cathode polarization ΔZ predicts anti-corrosion qualities with about equal validity when used for anode and cathode specimens.

D. Effect of Driving Force Index and Momentary Excess on the Anti-Corrosion Quality of the Calcite Coatings

Data from rusting tests establish an optimum range of calcium carbonate supersaturation as expressed by the DFI and ME. Figure 35 shows a plot of DFI values versus ratings assigned specimens from the rusting tests. From this figure an optimum DFI value of 175 to 450 is suggested.

Figure 36 shows a similar plot of ME values versus specimen ratings. Here, the relationship is not so clear cut because both

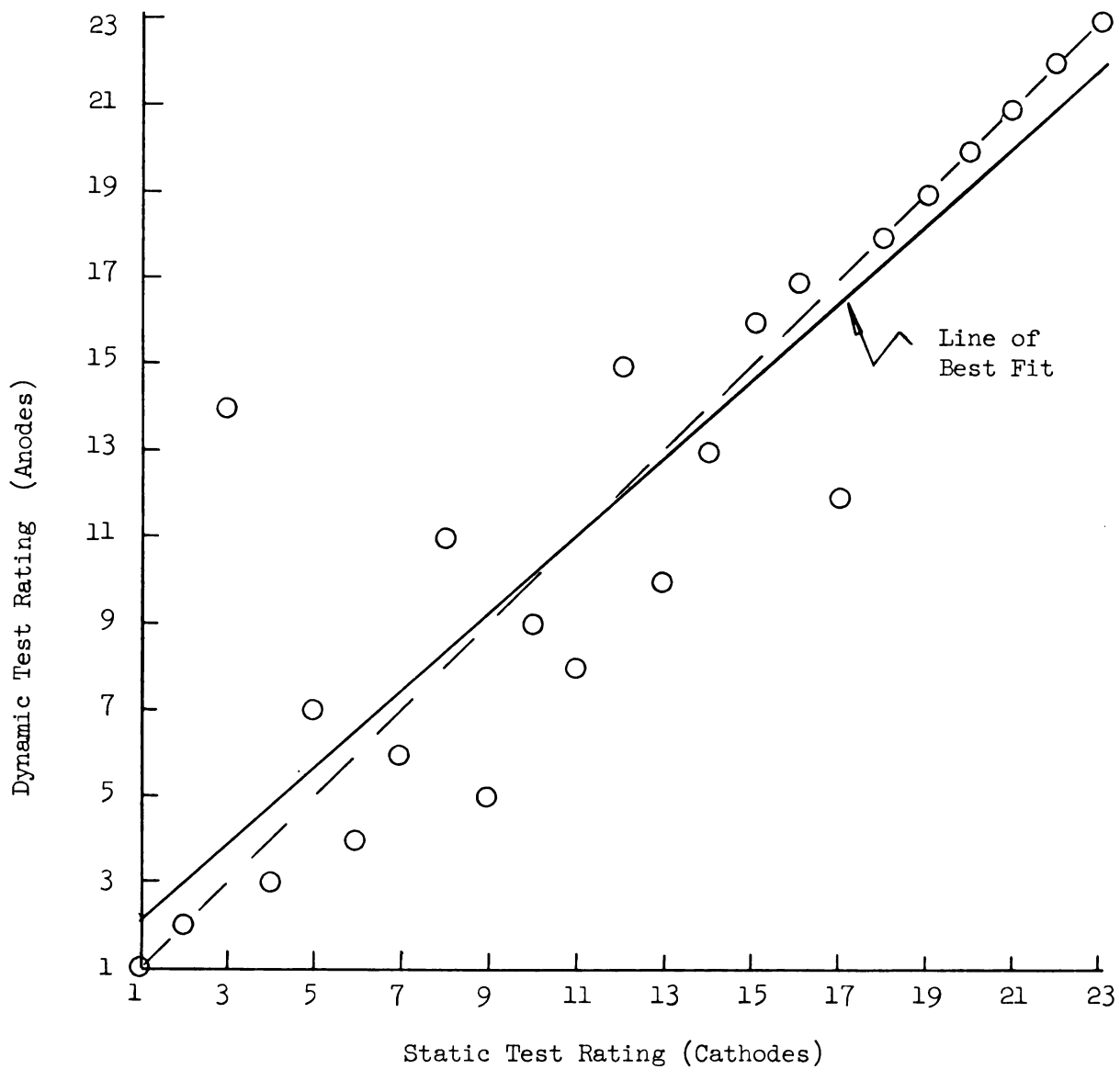


Figure 34. Cathode--Anode Anti-Corrosion Quality Ratings Compared.

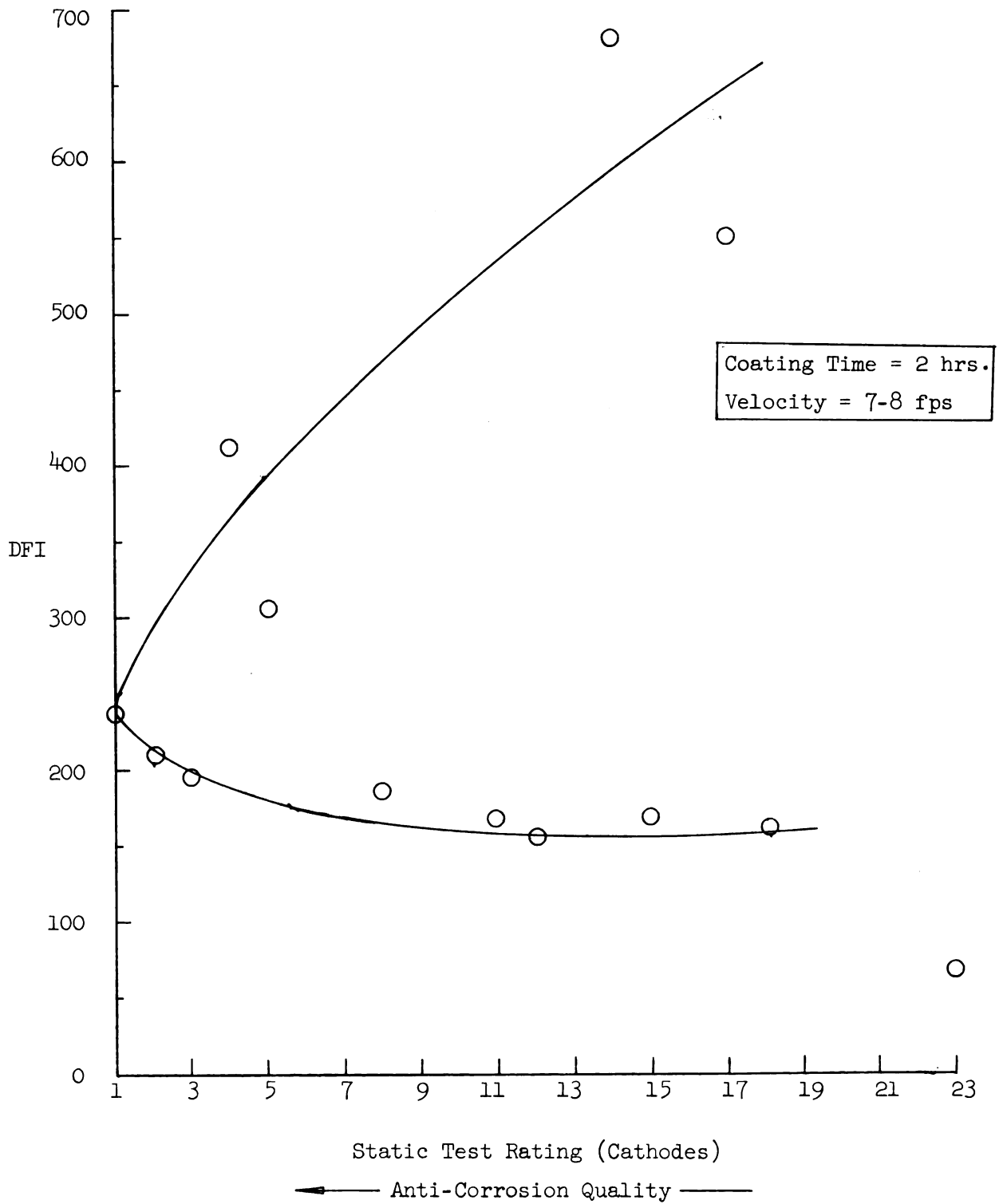


Figure 35. Coating Effectiveness as a Function of the DFI.

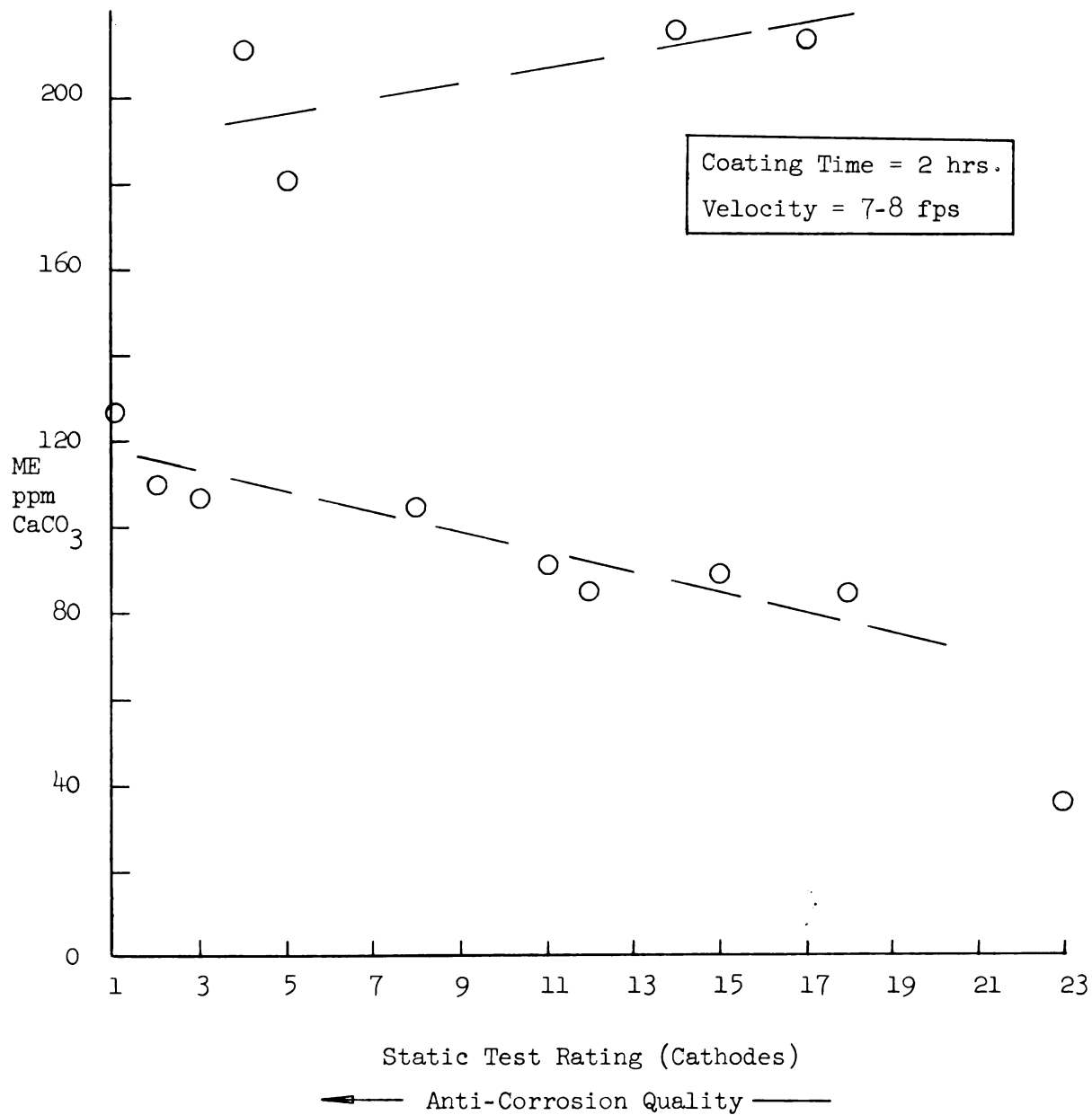


Figure 36. Coating Effectiveness as a Function of the ME.

high quality and inferior coatings were developed at ME levels greater than 180 ppm.

The very high 550 and 675 DFI values of Figure 35 do not have correspondingly high ME values in Figure 36 because the magnitude of the ME is limited by the lesser of the calcium or the carbonate concentration. Thus, the carbonate concentration may be the limiting influence on the magnitude of the ME in some tests, the calcium level in others. The weakness of the ME index is its failure to reflect the magnitude of the concentrations of both the calcium and carbonate ions which are present in a solution.

Figure 37 summarizes the relationship between the DFI, the polarization parameter ΔZ , and the resulting degree of protection for coatings developed under various levels of supersaturation. The optimum DFI range appears to be between 175 and 450. Coatings developed under these conditions for at least an hour with a displacement velocity of 7-8 fps result in very high quality coatings. The polarization parameter ΔZ for such coatings is in the order of 0.8 volts or greater.

McCauley (25) has reported the development of calcite coatings in two hours at a velocity of 3 fps and a DFI between 135 and 245. The work reported in this thesis has definitely established that coatings developed at the lower end of this range are inferior in quality.

The weight of coating deposited is not a determining factor for anti-corrosion value. As was shown earlier, the weight of coating deposited increases linearly with the DFI. However, Figure 37 indicates that high coating weights at high DFI levels yield inferior coatings.

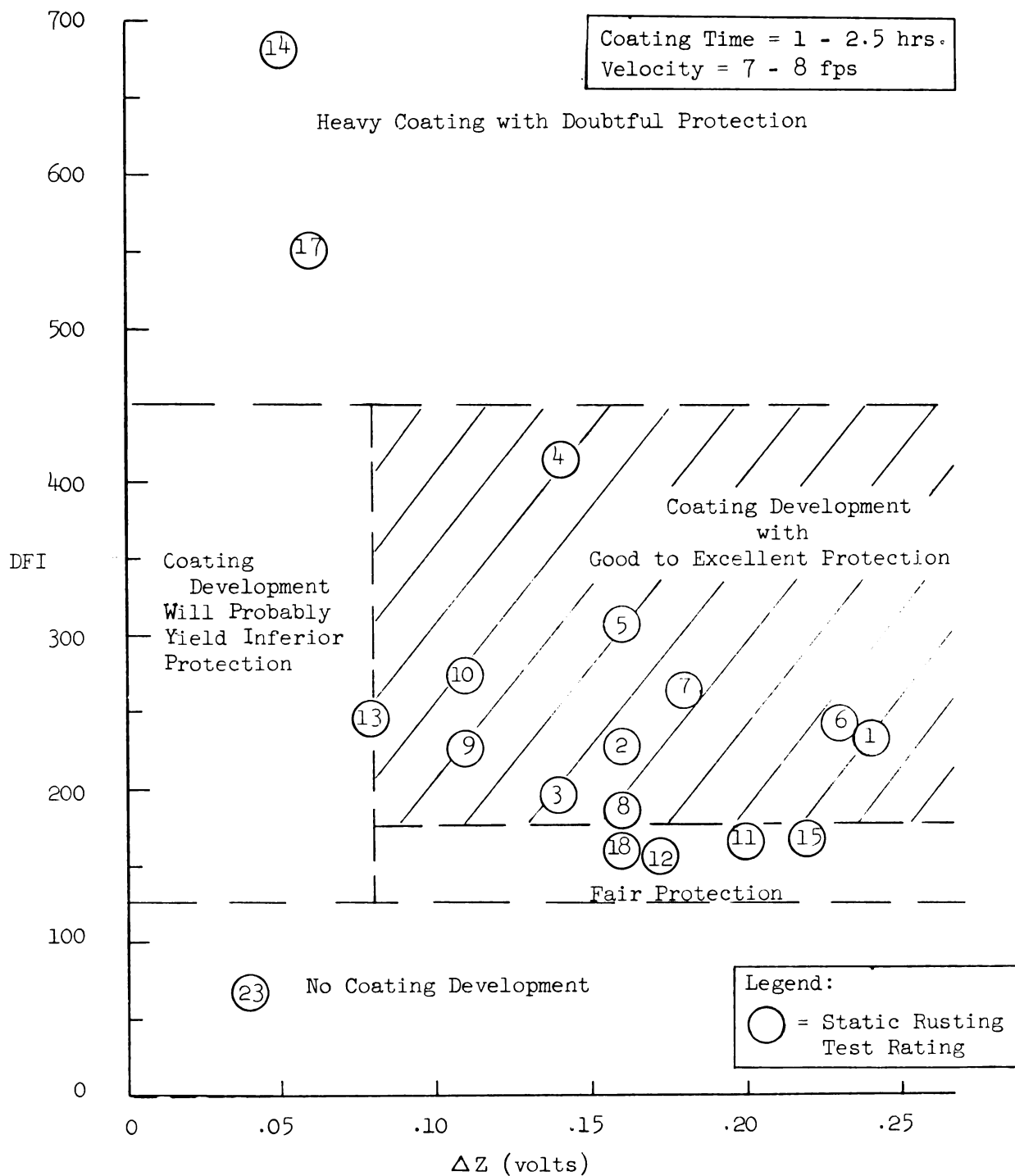
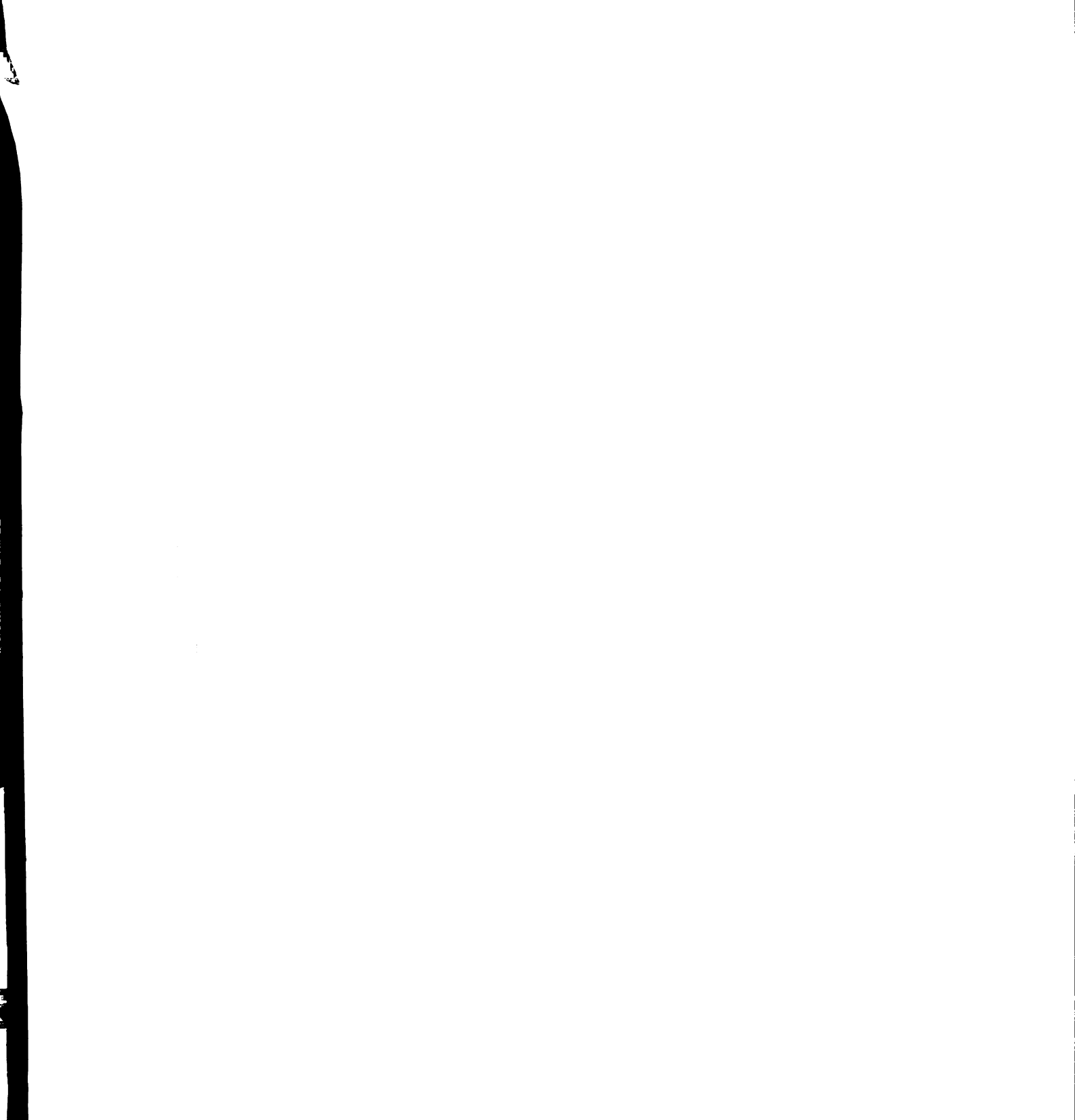


Figure 37. Coating Anti-Corrosion Quality as a Function of DFI and Polarization Parameter ΔZ .



E. Effect of Development Flow Velocity on the Anti-Corrosion Qualities of the Calcite Coatings

As outlined in the Literature Review, previous workers have reported that both pure calcite and mixed iron - CaCO_3 coatings develop faster and have greater protective power when the coating is deposited in flows of higher velocity than are commonly found in water main service. McCauley (25) has calculated the marginal velocity for establishing hydraulic roughness to be 3-4 fps. However McCauley's studies have also shown much better coatings to be developed at 8 fps than at 3 fps.

The majority of the coatings reported here were developed at velocities of between 7 and 8 fps. Table 7 summarizes the anti-corrosion ratings of four specimens developed at lower flow velocities. The anti-corrosion value of the coatings listed in this table are definitely inferior to those developed at higher velocity. The coating from the condition of lowest flow velocity (specimen 34) was the poorest coating tested. It will be noted that specimen 36 with 4.5 fps displacement velocity is superior to specimen 34 (with 2.8 fps velocity) even though the DFI of specimen 36 was in the doubtful threshold range.

As can be seen in Table 7, the polarization parameter ΔZ predicts the relative rankings of the calcite coatings developed under low velocity conditions.

F. Effect of Length of Coating Development Period on the Anti-Corrosion Value of the Calcite Coatings

The results of the rusting test indicate that a coating offering superior protection against corrosion may be developed in as little as thirty minutes time. Table 8 summarizes the

Table 7

Effect of Coating Development Velocity on
Anti-Corrosion Quality of Specimens

Spec. No.	Ave. Vel. (fps)	<u>Rusting Test</u> <u>Rating</u>		Micr. Rating A C	ΔZ	DFI	ME	Coating Time
		Dynamic (Anodes)	Static (Cath.)					
38	4.5	16	16	G ⁻ G ⁻	.10	249	156	2
35	4.5	20	20	F F ⁻	.06	180	118	2
36	4.5	21	21	P P	.05	115	75	2
34	2.8	22	22	P P ⁺	.02	141	107	2



Table 8

Effect of Time of Coating Development
on Anti-Corrosion Quality of Specimens

Spec. No.	Coating Time (hrs)	Static Rust Rating	Dynamic Rust Rating	ΔZ	Micr. Rating C A	DFI	ME	Ave. Vel. (fps)
45	1.0	6	4	.23	G G	242	147	7.1
43	2.5	7	6	.18	E E ⁻	262	161	7.1
41	1.0	9	5	.11	G G	226	137	7.1
42	1.5	10	9	.11	G G ⁺	274	162	7.1
40	0.5	13	10	.08	G ⁻ G	250	158	7.1
44	0.5	19	19	.08	F F	249	147	7.1

effects of varying periods of coating development.

When other conditions are constant, surface conditions cause some variation in the rate of crystal development. Therefore, the time-coating rate is not always constant. However, when conditions are optimum adequate coating development takes place within an hour to an hour-an-a-half, and the two hour periods used in most of these experiments is quite conservative.

The magnitude of the polarization parameter ΔZ has been found to be of more importance in determining anti-corrosion value than the time period of coating development.

G. Practical Application of the Polarization Technique to Measure Anti-Corrosion Quality of Calcite Coatings

These experiments have shown calcite coatings to offer good protection for cast iron exposed to water. The coatings can be established in distribution mains by straight forward techniques similar to that suggested by McCauley (27).

It would now appear that a much needed measuring device is available for determining the quality of corrosion protection provided by the newly developed calcite coatings. A portable apparatus is easily constructed which incorporates a test cell and polarization measuring equipment. By tapping a water main at a convenient location, small amount of treated water can be circulated through the test cell and polarization measurements made on a test specimen as a coating is built up. The point at which an adequate coating is developed can then be determined by the point at which the ΔZ of the polarization measurements reaches a significant magnitude.

CONCLUSIONS

The following conclusions are drawn from the investigations undertaken in this thesis:

1. With proper chemical and velocity controls, hard, firmly bonded, glass like calcite coatings were developed on cast iron specimens. Coatings developed on small flat plates were found to be representative of those developed in 3/4 inch test nipples.
2. The driving force index (DFI) and the momentary excess (ME) were found to be linearly related to the weight of coating deposited on the specimens, other conditions being constant.
3. The driving force index was shown to have a parabolic relationship to coating quality. The optimum range of DFI for coating development was between 175 and 450.
4. The ME value was shown to be of less value than the DFI for predicting the quality of coating developed.
5. Above a DFI level of 125, the size and distortion of the rhombic calcite crystal increased with increasing DFI.
6. Polarization tests showed calcite coatings to be cathodic inhibitors.

7. The overpotential exhibited by the cathode specimens was probably due primarily to activation polarization.
8. Rusting tests showed the calcite coatings to offer effective protection against corrosion. Local anodic areas, developed due to small imperfections in the coating during dynamic rusting conditions, tended to be self healing.
9. The magnitude of cathode polarization (ΔZ) was shown to be useful for predicting the anti-corrosion quality of the calcite coatings. A correlation coefficient of 0.69 for the static rusting test and 0.64 for the dynamic test was found for the ΔZ -relative-position relationship.
10. A correlation coefficient of 0.90 between the relative resistance ratings of the cathode-anode specimen pairs showed the cathode and anode coatings to be of equal quality.
11. Better coatings were developed at velocities of 7 to 8 fps than at 2.8 and 4.5 fps.
12. The length of coating development time appeared to be of much less importance than the degree of polarization established in a given coating time. However under optimum conditions, an hour to an hour-and-a-half appears to be required to develop a protective coating with high anti-corrosion value.

RECOMMENDATIONS

A fairly good understanding of the optimum conditions for development of calcite coatings has been achieved but the minimum flow velocity for adequate protection needs to be better defined. The high velocity necessary for coating development is one of the major drawbacks of these techniques.

It would be helpful to know more about the actual mechanism causing deposition and crystal growth in order to evaluate the effects of other ionic constituents on coating development.

Further polarization studies on different types of water would prove useful in determining the significant polarization change which must occur before a protective coating is established.

For long term corrosion protection with calcite coatings, the minimum ratio of metaphosphate--calcium carbonate excess required in the water to maintain the protective coating must be established.

APPENDIX A

Some Calculations of Chemical Feed and Hydraulic Conditions
of Rusting Apparatus

1. Calculation of Polyphosphate Feed

- a) Desired a concentration in test water of 0.5 ppm
- b) Pump delivered 350 gpm
- c) Calculation of the required feed rate:

assume 0.5 pounds of phosphate mixed with 50 gallons
water - resulting concentration of phosphate;

$$\text{concentration} = \frac{0.5 \# \text{ phos.}}{50 \text{ gal. water}} \times \frac{1}{8.33 \#/\text{gal.}} = \frac{0.0012 \# \text{ phos.}}{\# \text{ water}}$$

concentration = 1200 ppm, a reasonable value

$$\text{required flow rate} = \frac{350 \text{ gpm} \times 0.5 \text{ ppm} \times 60 \text{ min/hr}}{1200 \text{ ppm}} = 8.75 \text{ gph}$$

$$\text{required flow rate} = 8.75 \text{ gph}$$

2. Calculation of Flow Parameters for Dynamic Rusting Apparatus.

- a) Calculation of the velocity over the cast iron plates.

$$\text{Flow through the box} = Q = 12 \text{ gpm} = 0.0268 \text{ cfs}$$

$$Q = AV$$

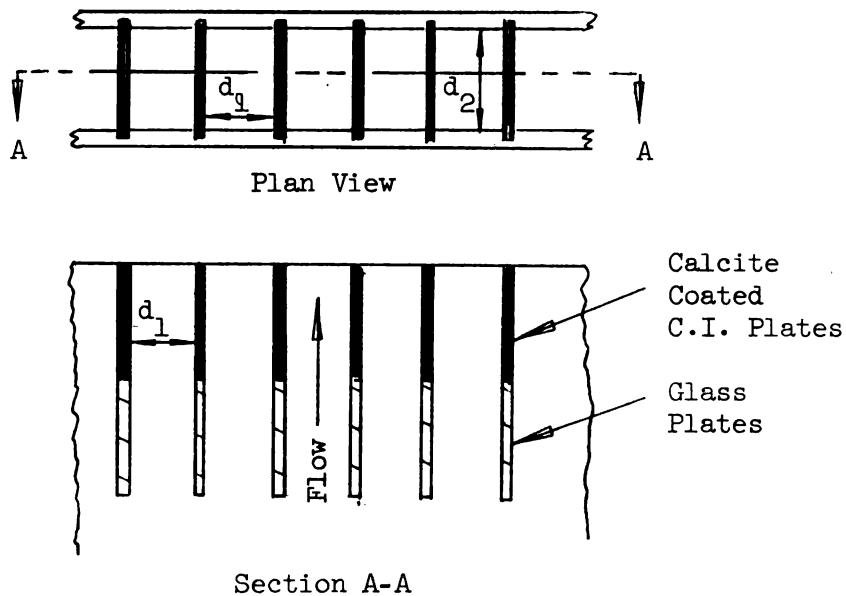
There were 41 openings 0.60 inches in width with 0.375
inch spacing between plates.

Therefore, the effective cross sectional area, A

$$A = 41 \times 0.375 \times 0.60 = 9.21 \text{ inches}^2 = 0.064 \text{ sq. ft.}$$

$$\text{Velocity, } V = Q/A = 0.0268 \text{ cfs}/0.064 \text{ sq. ft.} = 0.419 \text{ fps}$$

b) Calculation of Reynolds Number



Dynamic Rusting Apparatus

$$N_R = \frac{V \times R}{r}, \text{ where}$$

N_R = Reynolds Number

V = Velocity in fps

R = Hydraulic radius in feet

r = Kinematic Viscosity

$$R = 4 \text{ (area) / (perimeter)} = 4 (d_1 \times d_2) / (2d_1 + 2d_2)$$

$$d_1 = 0.375 \text{ inches} = .0312 \text{ feet}$$

$$d_2 = 0.600 \text{ inches} = .0500 \text{ feet}$$

$$R = 0.0385$$

$$N_R = (0.419 \text{ fps} \times 0.0385 \text{ feet}) / (1.41 \times 10^{-5} \text{ sq. ft. sec.}^{-1})$$

$$N_R = 1140, \text{ laminar flow}$$

APPENDIX B

Calculation of the Driving Force Index and Momentary Excess

Item (Test 23)	Mg/liter
Calcium (as calcium carbonate)	214
Alkalinity (as calcium carbonate)	516
Total dissolved solids	537
Temperature (degrees C)	14
pH	10.00
$K_s \times (10)^{10}$ (as calcium carbonate) See (6), page 800.	130
Hydroxide (OH^- as calcium carbonate) See (41), pages 54-55.	2
Carbonate (CO_3^{--} as calcium carbonate) See (41), pages 54-55.	250
DFI	412
ME	211

$$\text{DFI} = \frac{\text{Ca}^{++} \text{ (as CaCO}_3\text{)} \times \text{CO}_3^{--} \text{ (as CaCO}_3\text{)}}{K_s (10)^{10} \text{ (as CaCO}_3\text{)}} = \frac{214 \times 250}{130} = 412$$

$$\text{ME} = \frac{\text{Ca}^{++} + \text{CO}_3^{--}}{2} - \sqrt{\left(\frac{\text{Ca}^{++} + \text{CO}_3^{--}}{2}\right)^2 - (\text{Ca}^{++} \times \text{CO}_3^{--} - K_s (10)^{10})}$$

$$= \frac{214 + 250}{2} - \sqrt{\left(\frac{214 + 250}{2}\right)^2 - (214 \times 250 - 130)}$$

$$= 232 - \sqrt{(232)^2 - 53,370}$$

$$= 211 \text{ ppm as CaCO}_3$$

APPENDIX C

Rank Correlation Coefficient for Static Rusting Test Rating
vs Polarization Parameter (ΔZ) Rating

Specimen No.	Static Test Rating (x)	Polar Rating (y)	D (x-y)	D ² (x-y) ²
18	1	1	0	0
17	2	8.5	-6.5	42.25
15	3	11.5	-8.5	72.25
23	4	11.5	-7.5	56.25
20	5	8.5	-3.5	12.25
45	6	2	4	16
43	7	5	2	4
16	8	8.5	-0.5	.25
41	9	13.5	-4.5	20.25
42	10	13.5	-3.5	12.25
12	11	4	7	49
13	12	6	6	36
40	13	16.5	-3.5	12.25
27	14	20.5	-6.5	42.25
8	15	3	12	144
38	16	15	1	1
21	17	18.5	-1.5	2.25
32	18	8.5	9.5	90.25
44	19	16.5	2.5	6.25
35	20	18.5	1.5	2.25
36	21	20.5	0.5	.25
34	22	23	-1	1
28	23	22	1	1
				<hr/> 623.50

$$r_s = 1 - 6\sum D^2 / N(N^2 - 1) = 1 - 6(623.5) / 23(23^2 - 1)$$

$$r_s = 0.69$$

$$t = r_s \sqrt{(N-2)/(1-r_s^2)} = .69 \sqrt{(23-2)/(1-.69^2)}$$

$$t = 4.36 \quad \text{therefore} \quad p < .001$$

APPENDIX D

Calculation of Regression Line for Static
Test Rating vs ΔZ

Specimen No.	Static Test Rating (x)	ΔZ (y)	(xy)	(x ²)	(y ²)
18	1	.24	.24	2	.0576
17	2	.16	.32	4	.0256
15	3	.14	.42	9	.0196
23	4	.14	.56	16	.0196
20	5	.16	.80	25	.0256
45	6	.23	1.38	36	.0529
43	7	.18	1.26	49	.0324
16	8	.16	1.28	64	.0256
41	9	.11	.99	81	.0121
42	10	.11	1.10	100	.0121
12	11	.20	2.20	121	.0400
13	12	.17	2.04	144	.0289
40	13	.08	1.04	169	.0064
27	14	.05	.70	196	.0025
8	15	.22	3.30	225	.0484
38	16	.10	1.60	256	.0100
21	17	.06	1.02	289	.0036
32	18	.16	2.88	324	.0256
44	19	.08	1.52	361	.0064
35	20	.06	1.20	400	.0036
36	21	.05	1.05	441	.0025
34	22	.02	.44	484	.0004
28	23	.04	.92	529	.0016
	<hr/>	<hr/>	<hr/>	<hr/>	<hr/>
	276	2.92	28.26	4324	.4630

Regression line of best fit

$$\bar{y}_x = \bar{y} + b(x - \bar{x})$$

$$\bar{y} = \Sigma y / n \quad \bar{x} = \Sigma x / n$$

$$b = \frac{S_{y \cdot x}}{S_x^2}$$

$$\bar{y} = \frac{2.92}{23} = 0.127 \quad \bar{x} = \frac{276}{23} = 12$$

$$S_{y \cdot x} = \frac{n \Sigma xy - (\Sigma x)(\Sigma y)}{n(n-1)} = \frac{23(28.26) - (276)(2.92)}{23(23-1)}$$

$$S_{y \cdot x} = -0.308$$

$$S_x^2 = \frac{n \Sigma x^2 - (\Sigma x)^2}{n(n-1)} = \frac{23(4324) - (276)^2}{23(23-1)} = 46.0$$

$$b = \frac{-0.308}{46.0} = -0.0067$$

$$\bar{y}_x = 0.13 - 0.0067(x-12)$$

BIBLIOGRAPHY

1. Byrns, H. F., and Kretschmer, W. J. "Demonstration of the Theory of Cathodic Protection," Proceedings of the Fourth Annual Underground Corrosion Short Course; Technical Bulletin No. 56. West Virginia University: Engineering Experiment Station. 1959.
2. Camp, T. R. "Corrosiveness of Water to Metals," J. New Eng. Water Works Assoc. 60. June, 1946. 188-216, 282-93.
3. Dixon, W. J., and Massey, F. J., Jr. Introduction to Statistical Analysis. New York: McGraw-Hill Book Company, Inc. 1957.
4. Dye, J. F. "The Calculation of Alkalinities and Free Carbon Dioxide in Water by the Use of Nomographs," J. Am. Water Works Assoc. 36. August, 1944. 895-900.
5. _____. "Calculation of Effect of Temperature on pH, Free Carbon Dioxide, and the Three Forms of Alkalinity," J. Am. Water Works Assoc. 44. April, 1952. 356-72.
6. _____. "Correlation of the Two Principle Methods of Calculating the Three Kinds of Alkalinity," J. Am. Water Works Assoc. 50. June, 1958. 800-20.
7. Eliassen, R., and Lamb, J. L., III. "Mechanism of the Internal Corrosion of Water Pipes," J. Am. Water Works Assoc. 45. December, 1953. 1821-94.
8. _____. "Mechanism of Corrosion Inhibition by Sodium Metaphosphate Glass," J. Am. Water Works Assoc. 46. May, 1954. 445-60.
9. _____. "Corrosion Control with Metaphosphate Glass," J. New Eng. Water Works Assoc. 44. March, 1955. 31-68.
10. Eliassen, R., and Skrinde, R. T. Research Request to the National Science Foundation. 1955.
11. Evans, U. R. Metallic Corrosion, Passivity, and Protection. Edward Arnold & Co. 1937.
12. _____. The Corrosion and Oxidation of Metals. New York: St Martin's Press. 1960.

13. Gatty, O., and Spooner, E. C. R. The Electrode Potential Behavior of Corroding Metals in Aqueous Solutions. London: Oxford University Press. 1938.
14. Glasstone, S., and Lewis, D. Elements of Physical Chemistry. 2d ed. Princeton, N. J.: D. Van Nostrand Comp., Inc. 1960.
15. Hach Ver Catalog. Hach Chemical Co. Ames, Iowa. Catalog No. 3.
16. Illig, G. L., Jr. "Glassy Phosphates in Water Treatment," J. Am. Water Works Assoc. 49. June, 1957. 805.
17. Kortüm, G., and Bockris, J. O'M. Textbook of Electrochemistry. Elsevier Publishing Company, Inc. 1951.
18. Langelier, W. F. "The Analytical Control of Anti-Corrosion Water Treatment," J. Am. Water Works Assoc. 28. 1936. 1500.
19. _____. "Effect of Temperature on the pH of Natural Waters," J. Am. Water Works Assoc. 38. Feb., 1946. 179-85.
20. _____. "Chemical Equilibria in Water Treatment," J. Am. Water Works Assoc. 38. Feb., 1946. 169-78.
21. Larson, T. E. "Evaluation of the Use of Polyphosphates in the Water Industry," J. Am. Water Works Assoc. 49. Dec., 1957. 1581.
22. Larson, T. E., and Buswell, A. M. "Calculation of Calcium Carbonate Saturation Index and Alkalinity Interpretations," J. Am. Water Works Assoc. 34. 1942. 1667.
23. Leighou, R. B., and Warner, J. C. Chemistry of Engineering Materials. 4th ed. New York: McGraw-Hill Book Co., Inc. 1942.
24. McCauley, R. F. "Protective Coatings for Water Distribution Systems," J. Am. Water Works Assoc. 49. October, 1957. 1303-1309.
25. _____. "Use of Polyphosphates for Developing Protective Calcite Coatings," J. Am. Water Works Assoc. 52. June, 1960. 721-34.
26. _____. "Calcite Coating Protects Water Pipes," Water and Sewage Works. 107. July, 1960. 276-81.
27. _____. "Controlled Deposition of Protective Calcite Coatings in Water Mains," J. Am. Water Works Assoc. 52. Nov., 1960. 1386-96.
28. McCauley, R. F., and Abdullah, M. O. "Carbonate Deposits for Pipe Protection," J. Am. Water Works Assoc. 50. Nov., 1958. 1419-28.

29. Monie, W. D., and Scales, H. B. "Maintaining Pipeline Coefficient "C" After Water-Main Cleaning," J. New Eng. Water Works Assoc. 46. Sept., 1957. 203-33.
30. Moore, E. W. "Calculation of Chemical Dosages Required for the Prevention of Corrosion," J. New Eng. Water Works Assoc. 52. Sept. 1938. 311-17.
31. Potter, E. L. Electrochemistry, Principles and Applications. London: Cleaver-Hume Press Ltd. 1956.
32. Powell, S. T. "Cold Water Vacuum Dearthation," Water & Sewage Works. 93. March, 1946. 93-97.
33. Rabald, Erich. Corrosion Guide. London: Elsevier Publishing Co., Inc. 1951.
34. Reitemeier, R. and Buehrer, T. "The Inhibiting Action of Minute Amounts of Sodium Hexametaphosphate on the Precipitation of Calcium Carbonate Solutions," J. Physical Chemistry. 44. 1940. 535.
35. Rice, O., and Hatch, G. B. "Threshold Treatment of Municipal Water Supplies," J. Am. Water Works Assoc. 31. July, 1939. 1171-85.
36. Romeo, A. J., Skrinde, R. T., and Eliassen, R. "Effects of Mechanics of Flow on Corrosion," J. San. Eng. Div., Proc. Am. Soc. of Civil Eng. 84. July, 1958. 1702-1-30.
37. Rosenstein, L. U. S. Patent 2,038,316 (1936); reissue 20,360 (1937); reissue 20,754 (1938).
38. Ryzner, J. W. "A New Index for Determining Amount of Calcium Carbonate Scale Formed by a Water," J. Am. Water Works Assoc. 36. 1944. 472.
39. Skold, R. V., and Larson, T. E. "Measurement of the Instantaneous Corrosion Rate By Means of Polarization Data," Corrosion. 13. Feb. 1957. 139-42.
40. Speller, F. N. Corrosion, Causes, and Prevention. New York: McGraw-Hill Book Co. 1951.
41. Standard Methods for the Examination of Water, Sewage and Industrial Wastes. Public Health Assoc., Inc., and Am. Water Works Assoc. 10th ed. 1955.
42. Stericker, William. "Sodium Silicates in Water to Prevent Corrosion," Ind. and Eng. Chemistry. 30. March, 1938. 348-58.
43. Stumm, Werner. "Investigation on the Corrosive Behavior of Waters," Proc. Am. Soc. of Civil Eng. 86. No. SA6. Nov. 1960. 27-45.

44. Sudrabin, L. P., and Marks, H. C. "Cathodic Protection of Steel in Contact with Water," Ind. and Eng. Chem. 44. Aug. 1952. 1786-91.
45. Tillmans, J. Die Chemische Untersuchung von Wasser und Abwasser. Germany: Wilhelm Knapp, Saale. 1932.
46. Uhlig, H. (ed.) The Corrosion Handbook. New York: John Wiley & Sons, Inc. 1948.
47. _____. "The Cost of Corrosion to the United States," Chem. & Eng. News. 27. Sept. 26, 1949. 2764-67.
48. Water Quality and Treatment. The American Water Works Assoc., Inc. New York. 1950.
49. Whitney, W. R. "The Corrosion of Iron," J. Am. Chem. Soc. 25. 1903. 394.

ROOM USE ONLY.



